STAY ON TARGET: MECHANISMS OF CASEIN KINASE 1 TARGETING TO CONTROL MITOTIC CHECKPOINT FUNCTION

By

Zachary Cole Elmore

Dissertation

Submitted to the Faculty of the

Graduate School of Vanderbilt University

in partial fulfillment of the requirements for

the degree of

DOCTOR OF PHILOSOPHY

in

Cell and Developmental Biology

May 11, 2018

Nashville, TN

Approved:

Kathleen L. Gould, Ph.D.

Ethan Lee, M.D., Ph.D.

Todd Graham, Ph.D.

David Cortez, Ph.D.

ACKNOWLEDGEMENTS

Without the love and support of my family, none of this would be possible. I would like to thank my mother who always created an atmosphere of learning and encouraged me to pursue my interests no matter what they may be. My mother always had books for me to read and never hesitated to take me to the library so that I could indulge my love of knowledge.

I would like to thank my high school chemistry teacher Kara Becker for igniting my love of science and pushing me to be a better student. Without her wonderful teaching and encouragement, I know I would not be involved in science. I would also like to thank the late Johnny Mathias who pushed me as a student and human being and taught me the value of hard work. He is sorely missed.

I would like to thank my mentor Dr. Kathy Gould who taught me how to think about scientific problems and gave me encouragement and direction when experiments weren't working. I would also like to thank the Gould lab for all of the wonderful discussions about science and for our fun beer Fridays where we talked about everything under the sun. All of you gave me great advice and were amazing sources of inspiration.

Lastly, I would like to thank my fiancé Dana. We have been through so much together and you have always been there through the good times and the bad. I am excited to start our new life together and can't wait to experience the journey that awaits us. I couldn't have picked a better partner.

TABLE OF CONTENTS

Page

LIST OF FIGURES

CHAPTER I

INTRODUCTION

Overview of the eukaryotic cell cycle

The cell is the basic unit of life. Cells are dynamic entities and must grow and divide to propagate life on Earth. Cells undergo coordinated periods of growth and division that collectively are known as the cell division cycle. The primary goal of the cell division cycle is to duplicate the genome and divide the genetic and cytoplasmic material to produce two new cells. The cell division cycle is composed of four phases known as G1, S, G2 and M. Collectively, interphase is composed of three of the phases including G1, S and G2. G1 and G2 are phases of cellular growth with S phase taking place between these two gap phases. S phase is the period when the genomic material of the cell is duplicated so that the cell has two copies of the genome that can be equally distributed between two daughter cells. After interphase, the duplicated genomic material of the cell will be equally distributed to two daughter cells in a phase known as mitosis (Fig. 1-1). Mitosis is a process of nuclear division where the genome of the cell is equally segregated to opposite spindle poles. After this segregation has occurred, the cytoplasm of the cell is physically divided to create two new daughter cells in a process known as cytokinesis (Fig. 1-1).

Faithfully executing the events of the cell division cycle is critical to maintain the genomic integrity of each daughter cell. Defects in the cell division cycle are linked with

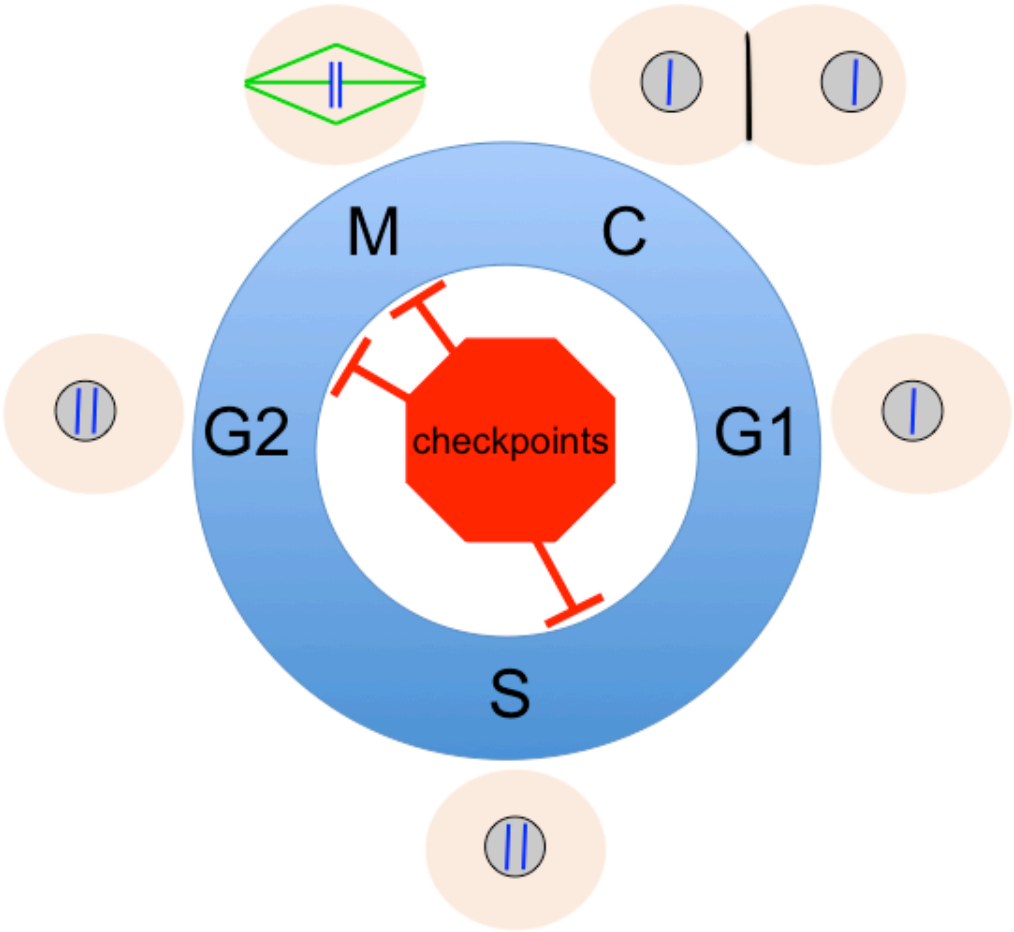

Figure 1-1. The eukaryotic cell division cycle and cell cycle checkpoints
Cell growth occurs in G1 and G2 phases and the genome (blue) is duplicated during S phase. In mitosis, the duplicated genome is segregated by the mitotic spindle (green) to the poles of the dividing cell. After mitosis occurs, the two daughter cells are physically divided in cytokinesis via a cytokinetic ring (black). In animal cells (pictured), the nuclear envelope (black) is disassembled during mitosis but regenerated after cytokinesis. Cell cycle checkpoints delay the cell division cycle to prevent a compromised genome from being distributed into the ensuing progeny. The DNA damage response stalls entry into S phase and M phase when damaged DNA is detected. A spindle checkpoint delays mitotic progression if chromosome segregation errors are detected.

many developmental disorders and neoplasia such as cancer. Therefore, it is critical to understand the basic mechanisms of cell division in order to understand how errors in these processes drive human disease.

Schizosaccharomyces pombe as a model system to study cell division

Much of our current understanding of cell division derives from studies utilizing simpler model organisms such as the "fission yeast" *Schizosaccharomyces pombe*. This unicellular organism is rod shaped due primarily to restriction of growth to cell tips (Mitchison and Nurse, 1985). *S. pombe* is a highly suitable model system for studying the cell cycle because its cell size correlates strongly with cell cycle stage, it is amenable to genetic and biochemical studies, and a comprehensive collection of deletion and temperature-sensitive mutants are readily available (Goyal et al., 2011; Moreno et al., 1991; Wixon, 2002). Because many key genes required for *S. pombe* cell division are conserved in metazoans, studies of the *S. pombe* cell cycle have pioneered many principal discoveries that have shaped our current understanding of cell division in multi-cellular organisms.

While mechanisms regulating cell division are similar between *S. pombe* and mammalian cells, there are some critical differences. One such difference is that *S. pombe* undergo a closed mitosis where the nuclear envelope does not break down during mitosis. This differs in mammalian cells where the nuclear envelope disassembles in early mitosis and re-forms at the end of cell division. Furthermore, while both build an actomyosin-based contractile ring (CR) to complete cytokinesis, they do so during different cell cycle stages (*S. pombe* in early mitosis and human cells in anaphase). In yeasts, cell wall material is deposited behind the constricting CR and ingressing plasma membrane at the division site (Balasubramanian et al., 2012). Despite these differences, *S. pombe* remains an excellent model system to study the molecular mechanisms regulating cell division.

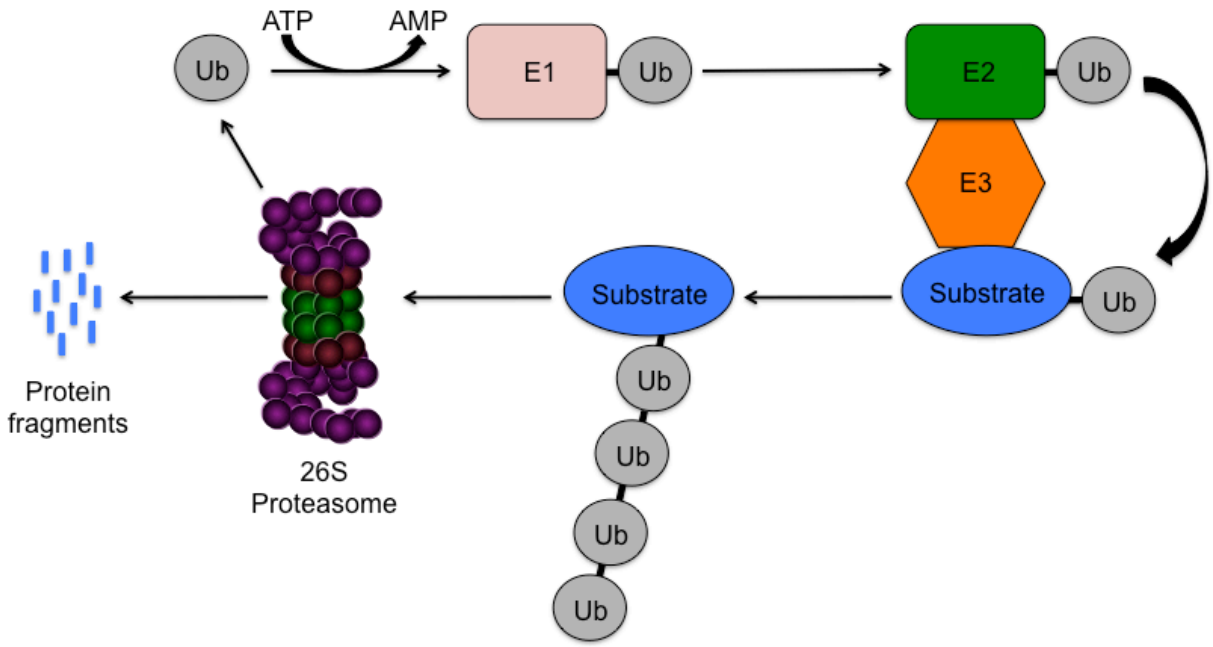

Figure 1-2. The ubiquitin-proteasome system (UPS). Substrate ubiquitination takes place in three general steps. First, ubiquitin is activated in an ATP-dependent process ending in its conjugation to an E1 ubiquitin-activating enzyme by a thioester bond. The charged ubiquitin is then transferred to an E2 ubiquitin-conjugating enzyme via a transthioesterification reaction. Finally, the ubiquitin moiety is transferred to the target protein. This occurs through the activity of an E3 ubiquitin ligase. The ubiquitinated protein is subsequently targeted for degradation by the 26S proteasome.

Cell cycle progression and the ubiquitin-proteasome system (UPS)

To properly coordinate the events of the cell division cycle, each phase must occur sequentially such that one does not begin before the previous phase ends (Nurse, 2000). To ensure the unidirectionality of cell cycle progression, cells rely on the precise degradation of critical cell cycle regulators by the ubiquitin proteasome system (UPS)(Teixeira and Reed, 2013; Wickliffe et al., 2009). For example, at the end of mitosis, the mitotic activator cyclin B is degraded by the ubiquitin proteasome system to allow cells to exit mitosis and ensure that a new mitosis does not occur until the next M phase (Glotzer et al., 1991; Wickliffe et al., 2009). Degradation of cellular proteins by the

UPS is a dynamic and highly regulated process. The targeting of cellular proteins for degradation involves the covalent attachment of ubiquitin to substrate proteins to create a degradation signal that directs tagged proteins for destruction by the 26S proteasome(Hershko and Ciechanover, 1998; Komander and Rape, 2012; Tomko and Hochstrasser, 2013) (Figure 1-2). Ubiquitin is attached to substrates through a tightly coordinated enzyme cascade (E1, E2, E3)(Hershko and Ciechanover, 1998; Komander and Rape, 2012; Tomko and Hochstrasser, 2013) (Figure 1-2). Conversely, ubiquitin is removed from target substrates by deubiquitinating enzymes (DUBs)(Komander et al., 2009; Kouranti et al., 2010; Reyes-Turcu et al., 2009) (Figure 1-3).

Substrate ubiquitination occurs in a variety of forms including mono-ubiquitination through the attachment of a single ubiquitin to a single lysine residue, multi-ubiquitination through the attachment of a single ubiquitin to multiple lysine residues, or poly-ubiquitination though the attachment of a ubiquitin chain to one or more lysine residues. Poly-ubiquitin chains contain multiple ubiquitin moieties connected to each other through one of seven internal lysines (K6, K11, K27, K29, K33, K48, and K63) or the N-terminus, and can be comprised of homogeneous or heterogeneous linkages in either linear or forked arrays. The various forms of ubiquitination impact the modified protein in different ways. For example, K48 linked poly-ubiquitin chains typically mark proteins for degradation through the proteasome system, while K63 linked poly-ubiquitin chains effect checkpoint signaling and protein activation (Heride et al., 2014).

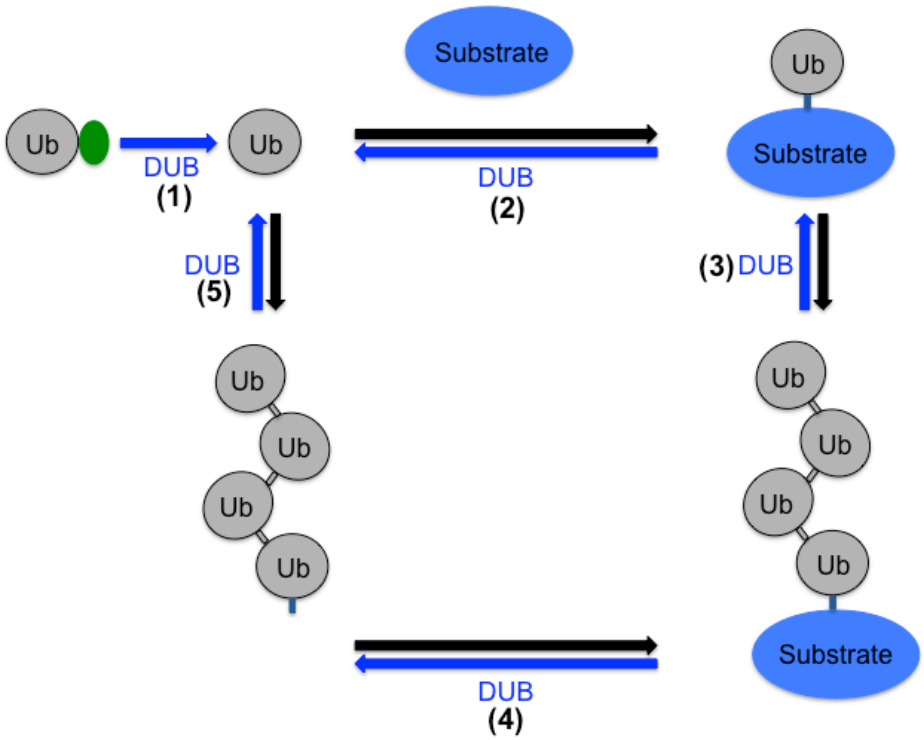

Figure 1-3. General role of deubiquitinases (DUBs)
DUBs are responsible for proteolytically processing precursor ubiquitin (green) into its conjugation competent form (1). DUBs are also responsible for cleavage of monoubiquitin and ubiquitin chains from substrates (2) and (4) respectively. DUBs are also critical in processing ubiquitin chains down to monoubiquitin (3) and replenishing the cellular free ubiquitin pool (5).

DUBs are highly conserved cysteine or metallo-proteases that are classified based on their catalytic domain structure. The 5 DUB families include ubiquitin C-terminal hydrolases (UCHs), ubiquitin-specific proteases (USPs), Machado-Joseph disease proteases, JAB1/MPN/Mov34 metalloenzymes (JAMMs) and ovarian tumor proteases (OTUs) (Kouranti et al., 2010; Nijman et al., 2005). DUBs have many diverse roles in regulating the ubiquitin cycle. DUBs are responsible for processing of ubiquitin precursors into their conjugation competent form, cleavage of ubiquitin from target proteins, processing of ubiquitin chains down to monoubiquitin, and replenishing the

cellular ubiquitin free pool (Komander et al., 2009; Kouranti et al., 2010; Nijman et al., 2005; Reyes-Turcu et al., 2009) (Figure 1-3). In contrast to mammalian cells, which encode approximately 100 DUBs, the *S. pombe* genome encodes only 20 DUBs belonging to 4 of the 5 DUB subfamilies (UCH, USP, OTU and JAMM) (Kouranti et al., 2010). Furthermore, all *S. pombe* DUBs except for the proteasomal DUB Rpn11, are nonessential for viability (Iwaki et al., 2007; Kim et al., 2010; Shimanuki et al., 1995; Stone et al., 2004; Zhou et al., 2003) possibly due to functional redundancy (Beckley et al., 2015).

During mitosis, the metaphase to anaphase transition is controlled by the E3 ubiquitin ligase known as the anaphase-promoting complex (APC/C). The APC/C is a highly conserved E3 ubiquitin ligase composed of 13 subunits (McLean et al., 2011; Primorac and Musacchio, 2013). The APC/C carries out its mitotic function by promoting the degradation of securin and cyclin B through the UPS (McLean et al., 2011; Ohi et al., 2007; Primorac and Musacchio, 2013; Teixeira and Reed, 2013; Wickliffe et al., 2009). The intricate regulation of the APC/C is mediated by the Cdc20 family of activators, pseudosubstrate inhibitors, protein kinases, protein phosphatases and the spindle assembly checkpoint (SAC) (Jia et al., 2013; McLean et al., 2011; Musacchio, 2011; Primorac and Musacchio, 2013). While the mitotic substrates and regulators of the APC/C have been well characterized (McLean et al., 2011; Primorac and Musacchio, 2013; Teixeira and Reed, 2013; Wickliffe et al., 2009), it is not understood whether and how DUBs impact APC/C function and whether this contributes to the regulation of mitotic progression.

Cell cycle checkpoints

Although the process of cell division is highly regulated, mistakes do occur. To deal with these mistakes, the cell utilizes a monitoring system called checkpoints to delay cell cycle progression until the mistakes are corrected (Elledge, 1996; Johnson and Walker, 1999) (Figure 1-1). Checkpoints have two major functions that ensure an accurate cell division cycle. 1) Checkpoints must sense mistakes that occur during the cell division cycle and 2) they must elicit a biochemical response that delays further cell cycle progression. Checkpoints function at multiple points in the cell cycle to ensure the fidelity of genomic duplication and segregation (Figure 1-1). For example, during mitosis, a bipolar mitotic spindle is formed that aligns chromosomes on the metaphase plate before they are segregated to opposite daughter cells during anaphase. To ensure the accuracy of this process, a checkpoint monitors mitotic spindle integrity and spindle attachment to the kinetochores of sister chromatids (Amon, 1999; Musacchio, 2011; Musacchio, 2015). If the cell senses a defect in bipolar spindle attachment to sister chromatids, a series of biochemical events are triggered that inhibit the cell cycle machinery thereby delaying anaphase, mitotic exit and cytokinesis. Because each cell cycle step is activated by distinct signaling events, the cell utilizes multiple mechanisms to simultaneously inhibit each process. For example, the SAC inhibits the APC/C to prevent the degradation of securin and cyclin B thereby preventing anaphase onset and mitotic exit (Amon, 1999; McLean et al., 2011; Musacchio, 2011; Musacchio, 2015; Primorac and Musacchio, 2013). Additionally, studies in yeast demonstrate that another pathway genetically independent of the SAC inhibits cytokinesis during a spindle stress (Beltraminelli et al., 1999; Gardner and Burke, 2000; Johnson et al., 2013). The function

of this checkpoint in *S. pombe* is to inhibit cytokinesis through the silencing of a spindle pole body (SPB) (yeast equivalent of mammalian centrosome) localized kinase cascade termed the septation initiation network (SIN). While much progress has been made in understanding the molecular players utilized in this checkpoint, further work is needed to dissect the signaling event(s) that activate this checkpoint pathway.

The septation initiation network (SIN)

In order to ensure that the duplicated genetic material properly segregated into two daughter cells, mitosis (chromosome segregation) and cytokinesis (division of cytoplasmic material) must be temporally regulated. More specifically, mitosis must precede cytokinesis to ensure that the daughter cells receive an unperturbed genome. During mitotic exit, CDK activity is low due to cyclin B degradation by the APC/C (Teixeira and Reed, 2013; Wickliffe et al., 2009). Because of this occurrence, many organisms use changes in CDK activity as a signal to temporally couple mitosis with cytokinesis. In *S. pombe*, the SIN induces cytokinesis only when CDK activity drops during anaphase (Chang et al., 2001; Guertin et al., 2000; He et al., 1997).

Cellular functions of the SIN

The SIN is a protein kinase cascade essential for CR formation, maintenance, and constriction. The SIN has many functions including temporally regulating cytokinesis with chromosome segregation (reviewed in (Johnson et al., 2012; Krapp et al., 2004; Simanis, 2015), blocking polarized growth during mitosis (Gupta and McCollum, 2011), and promoting mitotic spindle elongation during anaphase (Mana-Capelli et al., 2012). The SIN includes three conserved protein kinase complexes regulated by a Ras-like GTPase that are localized to SPBs via interaction with a bipartite scaffold complex,

Cdc11-Sid4 (Morrell et al., 2004). A pathway homologous to the SIN, termed the mitotic exit network (MEN), exists in the budding yeast *S. cerevisiae* (Bardin and Amon, 2001; Seshan and Amon, 2004). Furthermore, a SIN/MEN homologous pathway exists in metazoans termed the Hippo pathway (Avruch et al., 2012; Hergovich and Hemmings, 2012; Zhao et al., 2011). However, the role of Hippo signaling in metazoan cell division is not well understood. Therefore, gaining a strong understanding of SIN/MEN signaling in yeast could aid our understanding of Hippo signaling during cell division in metazoans.

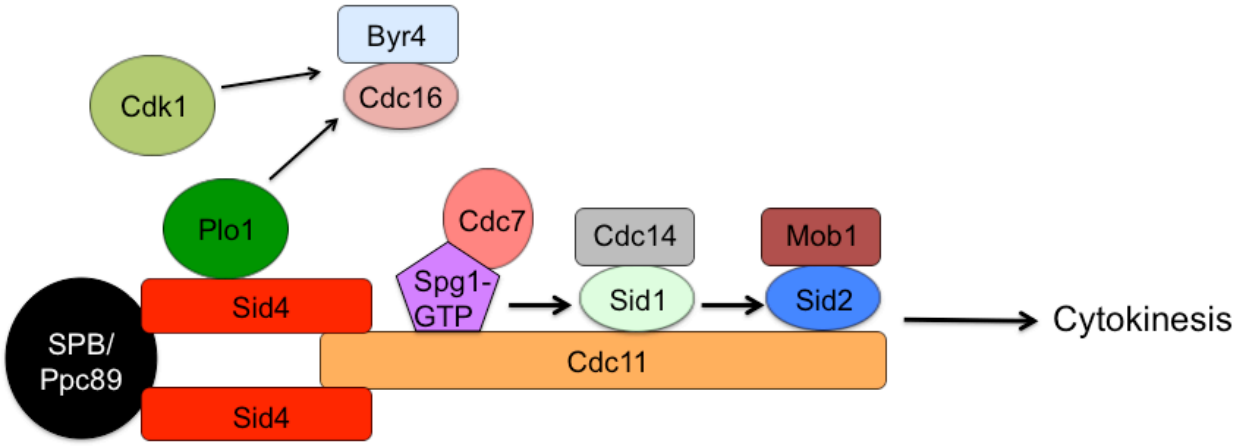

Figure 1-4. The Septation Initiation Network (SIN) is a SPB localized kinase signaling cascade that promotes cytokinesis
In *S. pombe*, the SIN is anchored to the major SPB protein Ppc89 via an interaction with the bipartite scaffold Sid4-Cdc11. Upon mitotic entry, Cdk1 and the Polo-like kinase Plo1 activate the GTPase Spg1 by removing the Cdc16-Byr4 GAP complex from SPBs. Removal of the Cdc16-Byr4 GAP complex allows Spg1 to switch to its active GTP-bound form and bind its effector kinase Cdc7. The Spg1-Cdc7 complex is then able to activate the downstream SIN kinases Sid1-Cdc14 and Sid2-Mob1. Once activated, the Sid2-Mob1 complex translocates to the division site and promotes the formation and constriction of the CR.

The SIN signaling hub is anchored at SPBs

Previous work demonstrated that mitotic SPBs are critical for cytokinesis (Magidson et al., 2006). Accordingly, SIN components assemble at SPBs via an interaction with the Sid4-Cdc11 bipartite scaffold (Figure 1-4) (Chang and Gould, 2000; Krapp et al., 2001; Morrell et al., 2004; Tomlin et al., 2002). Sid4-Cdc11 localizes to SPBs throughout the cell cycle via interaction with the SPB scaffold Ppc89 (Morrell et al., 2004; Rosenberg et al., 2006a). More specifically, Ppc89 anchors the Cdc11-Sid4 complex to SPBs through a direct interaction with the C-terminus of Sid4 (Rosenberg et al., 2006). Taken together, anchoring of Sid4-Cdc11 to Ppc89 institutes a platform that allows for the assembly of SIN components at the SPB (Morrell et al., 2004(Feoktistova et al., 2012)).

Mechanism of SIN activation

A major upstream regulator of the SIN is the Polo-like kinase Plo1. Early in mitosis, Plo1 concentrates at SPBs, the mitotic spindle and the CR (Bahler et al., 1998). Plo1 interacts directly with the scaffold Sid4 and activates the SIN when over-expressed (Morrell et al., 2004; Mulvihill et al., 1999; Ohkura et al., 1995; Tanaka et al., 2001). To activate the SIN, Plo1 along with Cdk1, phosphorylates Byr4, a component of a bipartite GTPase-activating protein (GAP) complex. Phosphorylation of Byr4 facilitates its removal from metaphase SPBs allowing for SIN activation (Rachfall et al., 2014). During mitosis, the consequence of Byr4 removal from SPBs is activation of the Ras super-family GTPase Spg1 and its downstream effectors. Spg1 localizes constitutively to SPBs through an interaction with Cdc11 (Morrell et al., 2004). During interphase, Spg1 binds to the bipartite GAP Byr4-Cdc16 keeping Spg1 in its GDP bound inactive state

(Furge et al., 1999; Furge et al., 1998; Krapp et al., 2008; Song et al., 1996). As stated previously, upon mitotic entry, Byr4-Cdc16 dissociates from SPBs, allowing Spg1 to switch to its GTP-bound active state (Li et al., 2000; Rachfall et al., 2014). To date, no GEF for Spg1 has been identified. However, it is possible that high intrinsic GTPase activity and high nucleotide release might be sufficient for nucleotide turnover in the absence of a GEF (Furge et al., 1998).

Activation of Spg1 triggers the subsequent activity of three SIN kinases (Cdc7, Sid1 and Sid2)(Figure 1-4)(Guertin et al., 2000). Once Spg1 is in its active GTP-bound state, it binds to the kinase Cdc7 (Li et al., 2000; Mehta and Gould, 2006; Schmidt et al., 1997). While it is not known what kinases Cdc7 activates downstream, based on work in budding yeast, it is possible that Cdc7 activates Sid2 (Mah et al., 2005). Further downstream the SIN signaling cascade, the protein kinase Sid1 and its binding partner Cdc14 localize to the SPB with active Spg1 (Fankhauser and Simanis, 1993; Guertin et al., 2000). Sid1 requires Sid4, Cdc11, Cdc14, Spg1 and Cdc7 for its SPB recruitment placing it downstream of Cdc7 recruitment (Guertin et al., 2000). Currently, we do not know any substrates of Sid1. However, it is possible that the terminal SIN kinase Sid2 and/or its binding partner Mob1 are potential substrates.

The terminal SIN kinase Sid2 and its partner Mob1 localize constitutively to SPBs and function downstream of Sid1-Cdc14 (Hou et al., 2004; Hou et al., 2000; Salimova et al., 2000; Sparks et al., 1999). Sid2-Mob1 also localizes to the division site (Sparks et al., 1999), where Sid2 phosphorylates the actin nucleating protein, Cdc12. Phosphorylation of Cdc12 by Sid2-Mob1 facilitates mature CR assembly and maintenance thereby promoting cytokinesis (Bohnert et al., 2013). Lastly, Sid2 promotes

cytokinesis through regulation of the Cdc14-like phosphatase Clp1 (Chen et al., 2008). During interphase Clp1 localizes to the nucleolus and is released to the cytoplasm and CR during early mitosis (Trautmann et al., 2001). Sid2- dependent phosphorylation of Clp1 maintains cytoplasmic Clp1 during cytokinesis and allows for dephosphorylation of the essential cytokinetic F-BAR protein Cdc15 (Chen et al., 2008; Mishra et al., 2005). Improper dephosphorylation of Cdc15 by Clp1 results in inefficient CR assembly (Clifford et al., 2008; Roberts-Galbraith et al., 2010). In the future, it will be critical to identify further SIN substrates to achieve a complete understanding of how the SIN promotes cytokinesis.

The SIN is inhibited during a mitotic checkpoint

In the event of a mitotic stress, cells must inhibit mitosis and cytokinesis until the stress is corrected to avoid genomic damage and possible cell death. In *S.* pombe, when chromosomes are not properly attached to the mitotic spindle, SIN activity is inhibited to prevent the CR from cutting through unsegregated chromosomes. One protein that inhibits the SIN during a mitotic stress is the E3 ubiquitin ligase Dma1 (Guertin et al., 2002b; Murone and Simanis, 1996). Dma1 was first identified as a SIN inhibitor in a screen aimed at identifying multi-copy suppressors of the SIN inhibitor *cdc16* (Murone and Simanis, 1996). During a mitotic stress wherein spindle microtubules are depolymerized, Dma1 inhibits SIN signaling by ubiquitinating Sid4 and impeding localization of Plo1 (Figure 1-5). In the absence of Dma1, cells exposed to a mitotic stress are unable to inhibit SIN signaling and undergo cytokinesis leading to chromosomal segregation errors (Guertin et al., 2002b; Murone and Simanis, 1996). Previous work established that during a spindle stress, two redundant *S. pombe* CK1s,

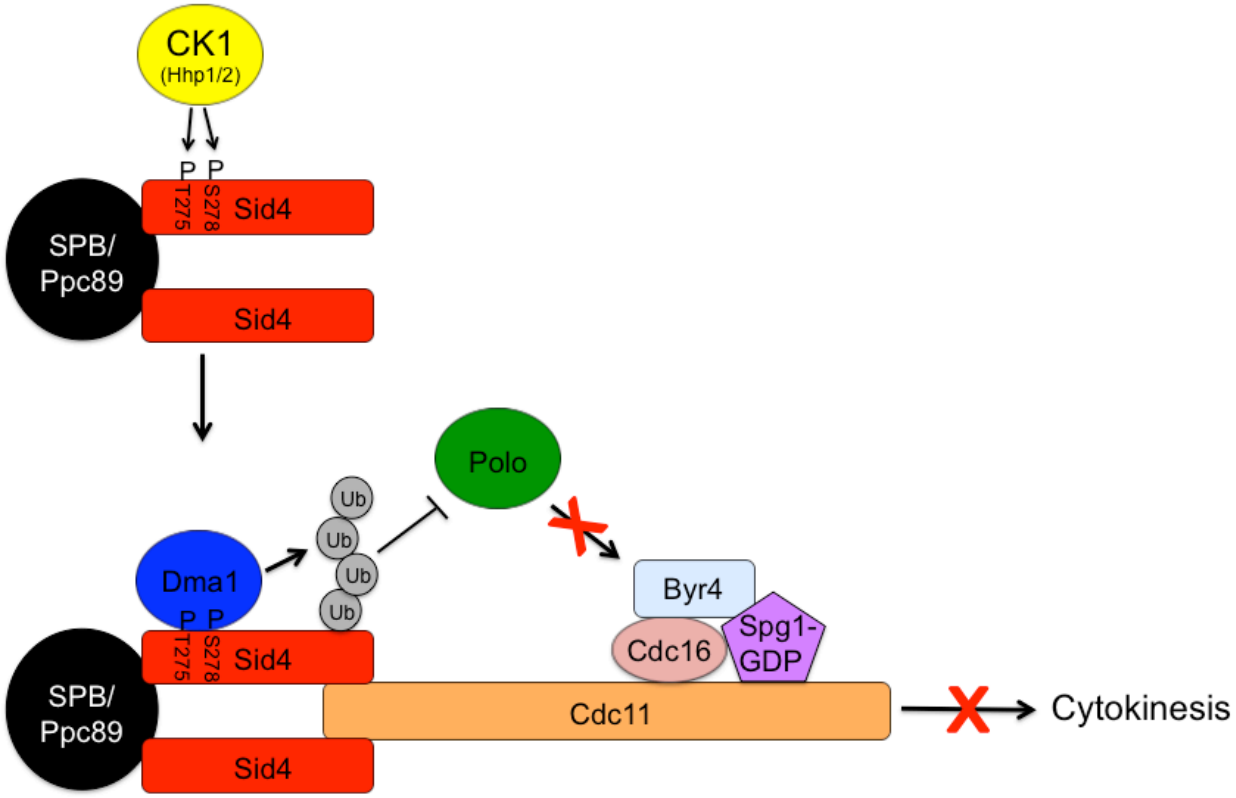

Figure 1-5. Hhp1/2 activates the Dma1-mediated mitotic checkpoint
During a mitotic spindle stress, Hhp1/2 phosphorylates Sid4 on two residues whereby creating a docking site for the FHA domain of the E3 ubiquitin ligase Dma1. Once docked, Dma1 ubiquitinates Sid4 and blocks Plo1 binding thus preventing SIN activation.

Hhp1 and Hhp2 (hereafter referred to as Hhp1/2), phosphorylate Sid4 on two residues, T275 and S278 (Figure 1-5) (Johnson et al., 2013). Phosphorylation of these residues recruits Dma1 through its Forkhead Associated (FHA) domain and promotes ubiquitination of Sid4 and subsequent SIN inhibition. Dma1 binds the SIN scaffold, Sid4, through its FHA domain and inhibits SIN signaling when over-expressed (Guertin et al., 2002; Murone and Simanis, 1996). Dma1 is a non-essential protein and loss of Dma1 causes no apparent defects to normal cell cycle progression (Murone and Simanis, 1996). However, cells lacking Dma1 fail to arrest in mitosis when the mitotic spindle is perturbed (Murone and Simanis, 1996). Previous work demonstrated that the protein

Dnt1 inhibits Dma1 function through direct binding of Dma1's FHA domain (Wang et al., 2012). However, it is still not clear what DUB, if any, antagonizes Dma1 ubiqutin ligase function.

Casein kinase 1 (CK1) enzymes

Casein kinases are among the most abundant serine/threonine protein kinases found in eukaryotic cells (Carpy et al., 2014; Desjardins et al., 1972; Hathaway and Traugh, 1979; Matsumura and Takeda, 1972; Tuazon and Traugh, 1991) and generally recognize substrates consisting of acidic or phosphorylated amino acid residues (Agostinis et al., 1989; Flotow et al., 1990; Flotow and Roach, 1991; Graves et al., 1993; Meggio et al., 1992; Meggio et al., 1991). Hhp1/2 are the sole soluble CK1s in *S. pombe* and are orthologs of *Saccharomyces cerevisiae* Hrr25p and human CK1δ and CK1ε (hereafter referred to as CK1δ/ε) (Dhillon and Hoekstra, 1994; Hoekstra et al., 1994)(Figure 1-6).

CK1 kinases share highly related catalytic domains (Figure 1-6)(53%-98% sequence identity). However, CK1family members contain unique kinase domain extensions (KDE) and have divergent C-terminal non-catalytic domains that are thought to dictate intracellular localization and govern catalytic activity (Babu et al., 2002; Cegielska et al., 1998; Dahlberg et al., 2009; Gietzen and Virshup, 1999; Graves and Roach, 1995; Greer and Rubin, 2011; Ianes et al., 2015; Longenecker et al., 1996; Longenecker et al., 1998; Meng et al., 2016). Indeed, some CK1 isoforms are anchored to membranes via C-terminal palmitoylation (Babu et al., 2004; Sun et al., 2004; Vancura et al., 1994; Wang et al., 1992).

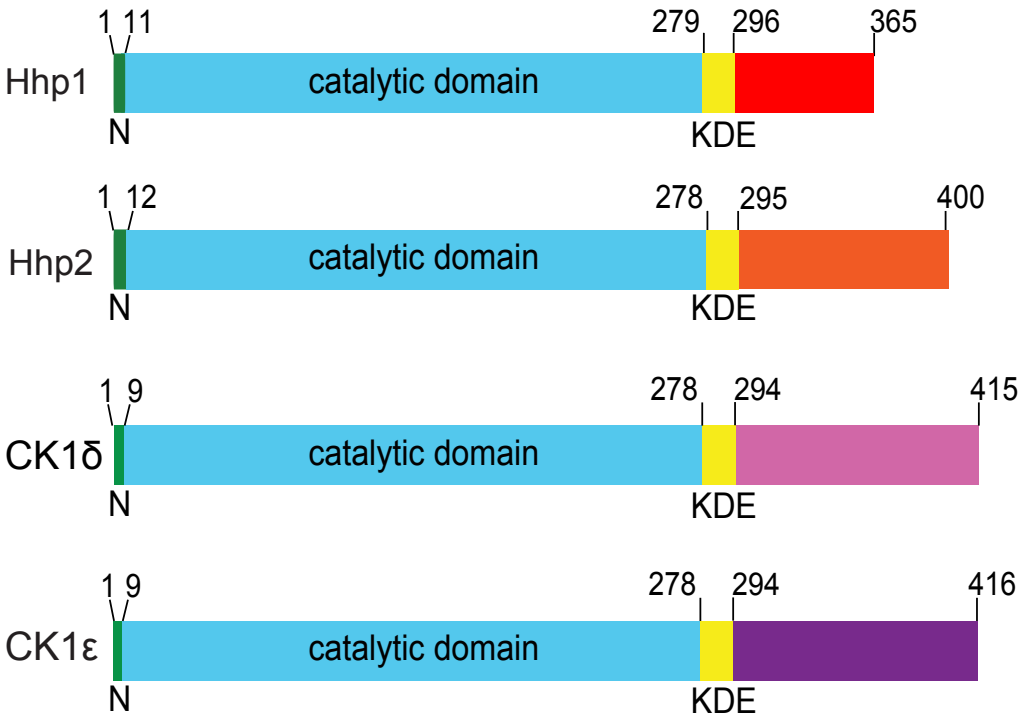

Figure 1-6. *S. pombe* Hhp1 and Hhp2 are orthologs of human CK1δ and CK1ε Schematic diagrams of Hhp1, Hhp2, CK1δ and CK1ε with relative positions of N-terminal extensions (N) (green), catalytic domains (blue), kinase domain extensions (yellow) and unrelated C-termini in red, orange, pink or purple indicated.

CK1 structure and substrate recognition

CK1 represents the typical kinase domain fold consisting of a bi-lobed structure with a smaller N-terminal lobe consisting primarily of β- sheets and a larger, primarily α-helical C-terminal lobe. The two lobes are connected by a hinge region forming a catalytic cleft for substrate and ATP binding (Figure 1-7) (Carmel et al., 1994; Longenecker et al., 1996; Xu et al., 1995).

CK1 kinases are acidotropic protein kinases and recognize a canonical consensus motif consisting of pSer/Thr/-X-X-(X)-Ser/Thr where pSer/Thr indicates a

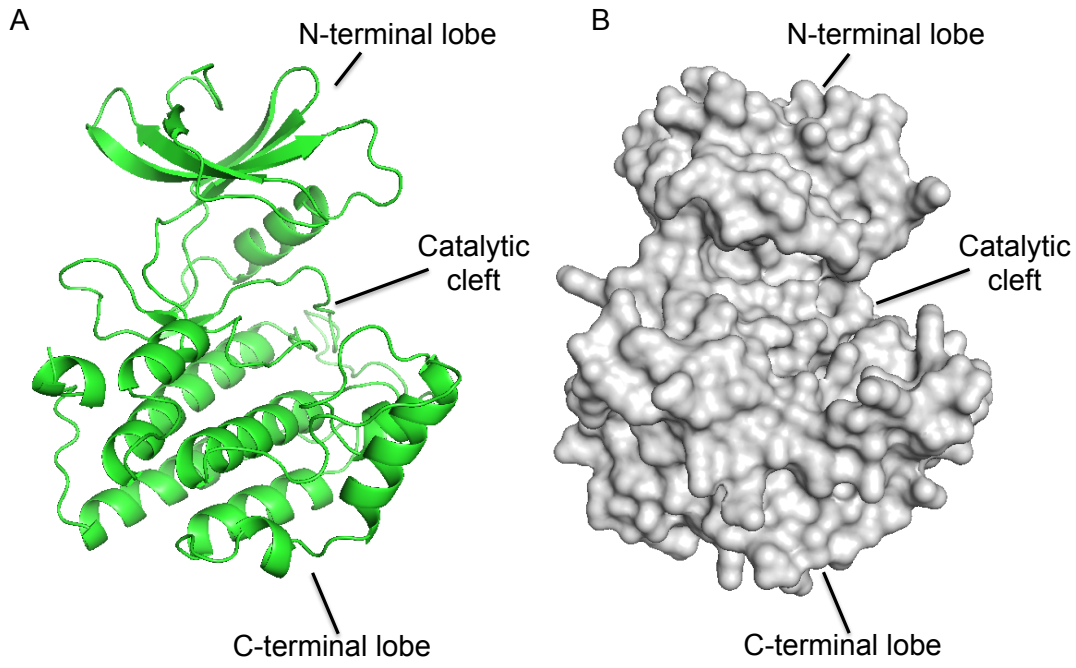

Figure 1-7. Structure of Hhp1 kinase domain
(A) Ribbon and (B) surface model of the catalytic domain of *S. pombe* Hhp1. The homology model was generated from Phyre[2] software and modeled with MacPymol.

phosphorylated serine or threonine residue. However, CK1 can also recognize motifs that are not phospho-primed but instead consist of a cluster of negatively charged acidic amino acids. CK1 also can phosphorylate "non-canonical" sites that are specified by local determinants and remote recognition elements. This is exemplified in the CK1 mediated phosphorylation of non-consensus sites on NF-AT (nuclear factor of activated T-cells) (Marin et al., 2002), β-catenin (Bustos et al., 2006; Marin et al., 2003), APC (adenomatous polyposis coli) (Ferrarese et al., 2007) and p53 (Venerando et al., 2010). At present, more than 140 *in vitro* and *in vivo* CK1 substrates have been identified signifying the importance of CK1 in cellular signaling (reviewed in (Knippschild et al., 2014).

CK1 regulation

Although members of the CK1 family are expressed ubiquitously throughout eukaryotes, their expression levels differ based on cell and tissue type. Multiple factors can change the expression or activity of CK1 isoforms including viral transformation (Elias et al., 1981), insulin stimulation (Cobb and Rosen, 1983) or DNA damage (Santos et al., 1996). Furthermore, multiple regulatory mechanisms affect CK1 activity at the protein level including subcellular localization, interaction with scaffolding proteins, and post-translational modifications.

Sequestration of CK1 enzymes to specific subcellular compartments is crucial in regulating their access to substrates (Sillibourne et al., 2002; Vancura et al., 1994; Wang et al., 1992). Therefore, cells can utilize scaffolds to tether members of signaling pathways into complexes thereby increasing the interaction efficiency between partner molecules . Scaffolds have also been implicated in allosterically regulating their binding partners thereby exerting control of their activity (Good et al., 2011; Locasale et al., 2007). In the case of CK1, scaffolds have been implicated in altering the affinity of CK1 for their substrates as well as regulating the activation of CK1 kinase activity (Good et al., 2011; Kholodenko et al., 2010). Examples of this include the role of A-kinase anchoring protein 450 (AKAP450) and its role in controlling CK1δ/ε centrosomal localization (Sillibourne et al., 2002).

CK1 activity can be further controlled through post-translational modifications such as phosphorylation. Within the C-terminal domain of CK1δ/ε, multiple amino acid residues can be autophosphorylated or phosphorylated by cellular kinases to regulate enzymatic activity. It is thought that phosphorylation of the C-terminal domain acts as a

pseudo-substrate blocking the catalytic center of the kinase (Cegielska et al., 1998; Gietzen and Virshup, 1999; Graves and Roach, 1995; Rivers et al., 1998). Conversely, dephosphorylation or truncation of the C-terminal domain of CK1 results in an increase in kinase activity (Bedri et al., 2007; Cegielska et al., 1998; Gietzen and Virshup, 1999).

Summary

In this work, I will describe multiple mechanisms of protein regulation that contribute to mitotic progression and cytokinesis. In chapter 2, I will describe a genetic screen performed to identify DUBs that antagonize the function of the APC/C. In chapter 3, I will describe an overexpression screen used to determine what DUB(s) counteract the function of the E3 ubiquitin ligase Dma1. Lastly, in chapter 4 I describe how a master kinase, CK1, is targeted to a major subcellular signaling hub, the SPB/centrosome and how this targeting is critical to maintain a mitotic checkpoint. Taken together, these studies have advanced our understanding of the subcellular targeting mechanisms of eukaryotic protein kinases and highlight new roles of DUBs in regulating cell division.

CHAPTER II

HISTONE H2B UBIQUITINATION PROMOTES THE FUNCTION OF THE ANAPHASE-PROMOTING COMPLEX/CYCLOSOME IN *SCHIZOSACCHAROMYCES POMBE*

Zachary C. Elmore, Janel R. Beckley, Jun-Song Chen and Kathleen L. Gould

Genes, Genomes, Genetics (G3), 4(8);1529-38, (2014)

Introduction

The purpose of cell division is to accurately replicate the genetic material of a dividing cell and evenly distribute it between mother and daughter cells. Precise degradation of critical cell cycle regulators by the ubiquitin proteasome system (UPS) ensures unidirectionality of cell cycle progression (reviewed in (Mocciaro and Rape, 2012; Wickliffe et al., 2009).

Targeting of cellular proteins for degradation by the UPS involves the covalent attachment of ubiquitin to substrate proteins, creating a degradation signal that targets substrates to the 26S proteasome. Ubiquitin is attached to substrates through a tightly coordinated enzyme cascade including and E1 activating, E2 conjugating and E3 ligating enzymes (reviewed in (Komander and Rape, 2012; Teixeira and Reed, 2013; Tomko and Hochstrasser, 2013).

In *Schizosaccaromyces pombe* and other eukaryotic organisms, the metaphase to anaphase transition is controlled by the anaphase promoting complex/cyclosome (APC/C) E3 ubiquitin ligase. The APC/C carries out its mitotic function by promoting

the degradation of securin and cyclin B through the UPS (reviewed in (McLean et al., 2011; Primorac and Musacchio, 2013; Teixeira and Reed, 2013). To prevent precocious sister chromatid separation, the APC/C is inhibited by the spindle assembly checkpoint (SAC) (reviewed in (Jia et al., 2013; Musacchio, 2011) which is only silenced when all kinetochores achieve bipolar attachment to spindle poles. SAC inactivation promotes APC/C activation, leading to chromosome segregation and mitotic exit (Jia et al., 2013; McLean et al., 2011; Musacchio, 2011).

Ubiquitin is removed from proteins by deubiquitinating enzymes (DUBs) (reviewed in (Komander et al., 2009; Reyes-Turcu et al., 2009). DUBs are cysteine or metallo-proteases that are classified based on their catalytic domain structure. The 5 DUB families include ubiquitin C-terminal hydrolases (UCHs), ubiquitin-specific proteases (USPs), Machado-Joseph disease proteases, JAB1/MPN/Mov34 metalloenzymes (JAMMs) and ovarian tumor proteases (OTUs) (Kouranti et al., 2010; Nijman et al., 2005). DUBs have diverse roles in regulating the ubiquitin cycle. They are responsible for processing ubiquitin precursors into their conjugation competent form, cleaving ubiquitin from target proteins, trimming of ubiquitin chains, and replenishing the free ubiquitin pool (Komander et al., 2009; Kouranti et al., 2010; Nijman et al., 2005; Reyes-Turcu et al., 2009). In mammalian cells, the DUB USP44 reverses APC/C mediated ubiquitination of the APC/C activator Cdc20 to maintain the SAC (Stegmeier et al., 2007). Though it is plausible that reversal of APC/C ubiquitination is a conserved mechanism, there is no known USP44 homolog in non-mammals.

In this work, we utilized a genetic approach to determine if any single DUB antagonizes the function of the APC/C in *S. pombe*, a model organism with many

mechanisms of conserved cell cycle control. In contrast to mammals, which encode approximately 80 DUB genes (reviewed in (Komander et al., 2009; Reyes-Turcu et al., 2009), the *S. pombe* genome encodes only 20 catalytically active DUBs belonging to 4 of the 5 DUB subfamilies (UCH, USP, OTU and JAMM) (Kouranti et al., 2010). All *S. pombe* DUBs except for the proteasomal DUB Rpn11, are nonessential for viability (Iwaki et al., 2007; Kim et al., 2010; Shimanuki et al., 1995; Stone et al., 2004; Zhou et al., 2003) making our genetic screen straightforward. Here, we provide evidence that a single DUB, Ubp8, antagonizes the APC/C in a mechanism independent of the SAC. Genetic analysis reveals that Ubp8's ability to antagonize APC/C function depends on its catalytic activity and the ubiquitination status of histone H2B. Accordingly, our work reveals a new interaction between chromatin signatures and cell cycle progression, mediated by a DUB.

Results

ubp8 antagonizes the function of the APC/C in S. pombe

We surmised that if a DUB antagonizes APC/C function in *S. pombe*, the deletion of that DUB should suppress a mutant defective in APC/C activity. Thus, we crossed each of the 19 non-essential DUB deletion mutants and a temperature sensitive mutant of *rpn11* (the essential DUB) to *cut9-665*, an APC/C mutant (Kouranti et al., 2010; Penney et al., 1998; Samejima and Yanagida, 1994). Only three mutations affected growth of *cut9-665* (Figure 2-1A,B). In a serial dilution growth test, only *ubp8*Δ suppressed *cut9-665* at its semi-permissive temperature (32°C) (Figure 2-1A). *cut9-665* showed a negative genetic interaction with *ubp14*Δ and *pad1-1* (a temperature sensitive allele of the proteasomal DUB *rpn11)* (Figure 2-1A,B). These DUB mutants decrease the cellular

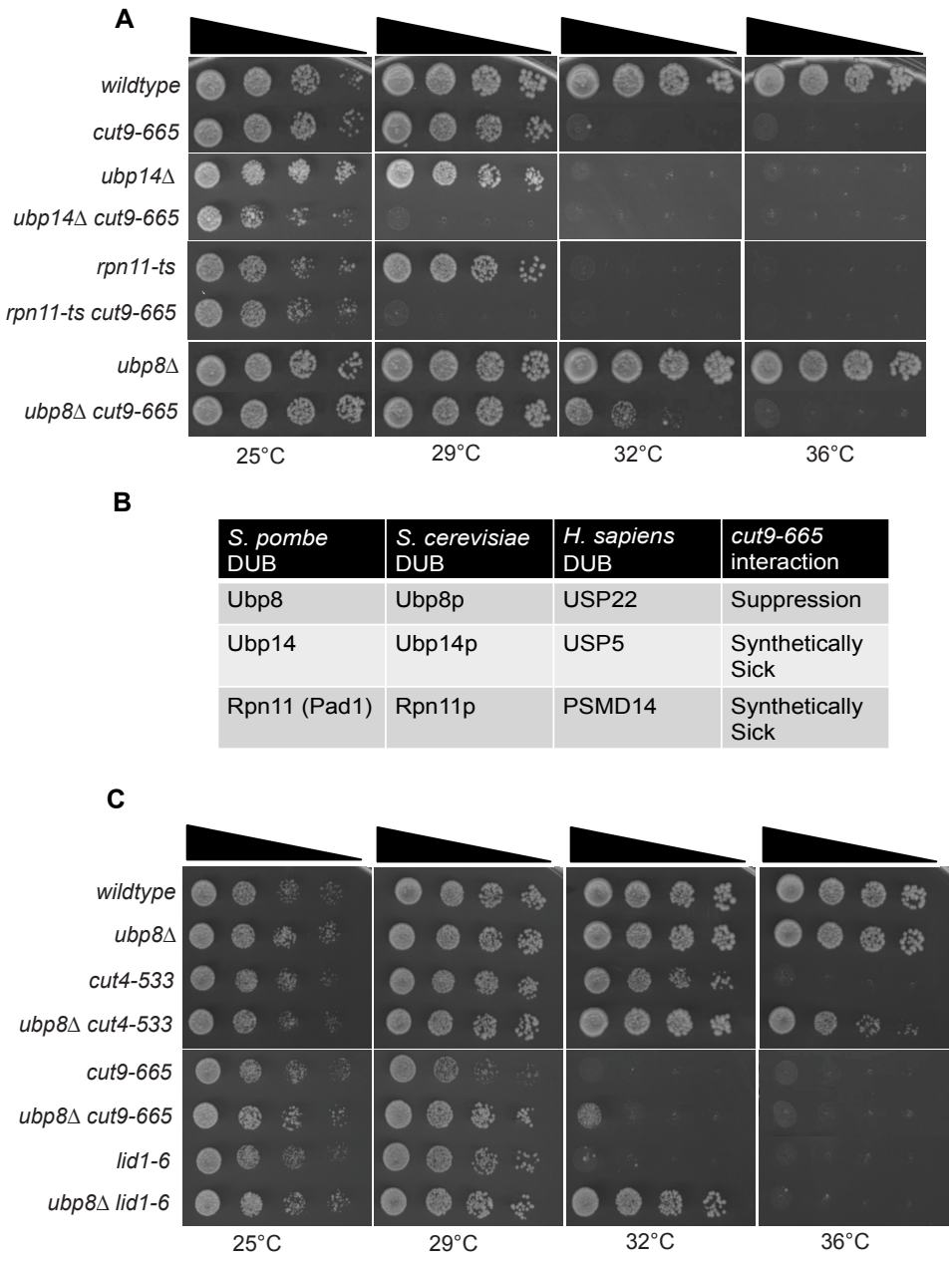

B

S. pombe DUB	*S. cerevisiae* DUB	*H. sapiens* DUB	*cut9-665* interaction
Ubp8	Ubp8p	USP22	Suppression
Ubp14	Ubp14p	USP5	Synthetically Sick
Rpn11 (Pad1)	Rpn11p	PSMD14	Synthetically Sick

Figure 2-1. *ubp8* antagonizes APC/C function in *S. pombe*. (A) *ubp8*Δ suppresses the temperature sensitive growth of *cut9-665*. Strains were grown at 25°C to an OD_{595}=0.2. Serial dilutions (10-fold) of the indicated single and double mutant strains were spotted on YE and incubated at the indicated temperatures for 3-4 days. (B) List of the *S. pombe* DUBs that showed genetic interactions with *cut9-665* and their homologs. (C) *ubp8*Δ suppresses the temperature sensitive phenotype of APC/C temperature sensitive mutants *cut4-533* and *lid1-6*. Strains were grown and spotted as described in (B).

ubiquitin pool most likely contributing to the exacerbated APC/C temperature sensitive phenotype (Penney et al., 1998; Verma et al., 2002) (see discussion).

lid1+ and cut4+ encode other components of the APC/C while *slp1+* encodes an APC/C co-activator homologous to Cdc20p (*S. cerevisiae)*. Temperature-sensitive *lid1-6, cut4-533, cut9-665* and *slp1-362* mutants all display a "cut" phenotype at restrictive temperatures where chromosome segregation and spindle elongation fail to occur; therefore, subsequent cytokinesis bisects the nucleus or results in segregation of DNA to only one daughter cell (Berry et al., 1999; Matsumoto, 1997; Yamashita et al., 1996). To determine if suppression of *cut9-665* by *ubp8*Δ was indicative of general suppression of hypomorphic APC/C function, we tested other APC/C mutants and found that *ubp8*Δ suppressed *lid1-6*, *cut4-533*, and *slp1-362* (Figure 2-1C), data not shown]. Based on these data, we conclude that Ubp8 antagonizes APC/C function.

Suppression of APC/C temperature sensitive mutants is not dependent on the SAC or enhanced proteasome function

The SAC is a well-characterized APC/C inhibitor (Jia et al., 2013; Musacchio, 2011). Therefore, we investigated whether suppression of *cut9-665* by *ubp8*Δ was achieved by diminished SAC activity. Deletion of key SAC components *mph1*Δ, *mad2*Δ, and *mad3*Δ *(He et al., 1998; Sczaniecka et al., 2008)* suppressed APC/C mutations as expected, but also enhanced the suppression of the APC/C by *ubp8*Δ (Figure 2-2) additively. Thus, Ubp8 antagonizes the APC/C through SAC-independent mechanism(s).

The APC/C is responsible for ubiquitinating critical cell cycle regulatory proteins, targeting them for their subsequent degradation by the 26S proteasome (reviewed in (McLean et al., 2011; Primorac and Musacchio, 2013; Teixeira and Reed, 2013). Thus, it

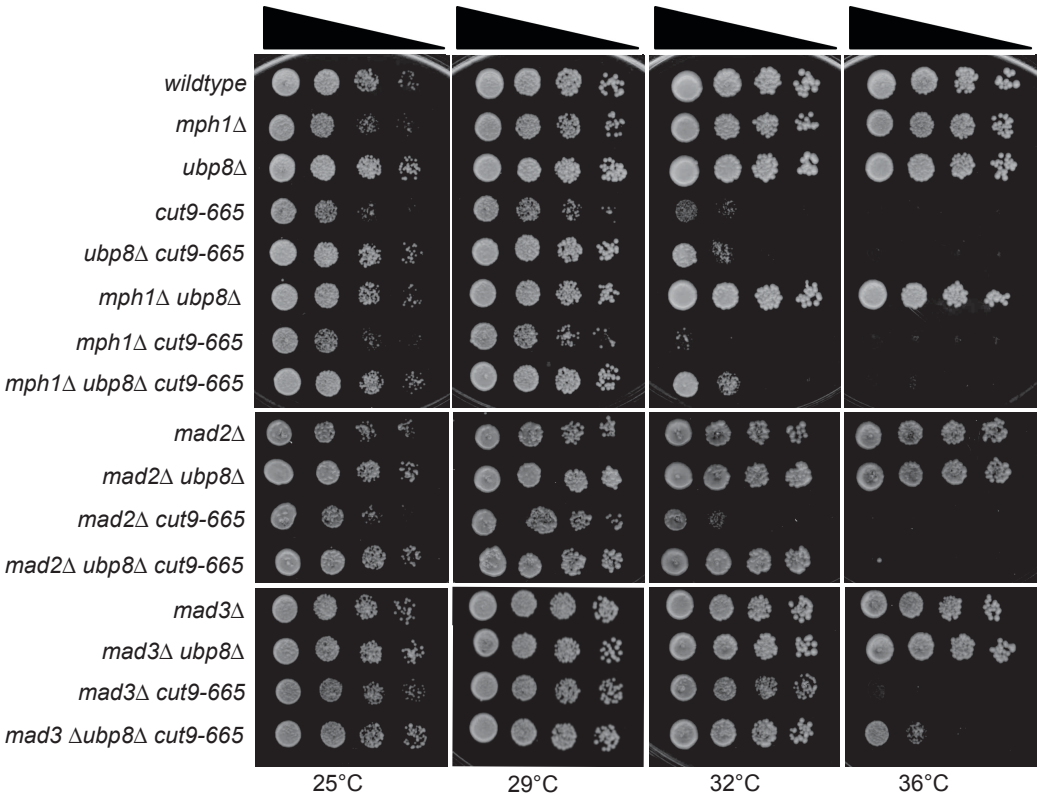

Figure 2-2. *ubp8*Δ suppression of *cut9-665* is independent of the SAC. (A) *ubp8*Δ suppresses the temperature sensitive phenotype of *cut9-665* in both *mph1*$^{+}$ and *mph1*Δ strains. *ubp8*Δ suppression of *cut9-665* is enhanced in *mad2*Δ and *mad3*Δ strains. Serial dilutions (10-fold) of the indicated single, double and triple mutant strains were spotted on YE plates and incubated at the indicated temperatures

was possible that *ubp8*Δ lowered the threshold for APC/C function by enhancing proteasome-mediated degradation. To test this idea, we combined *ubp8*Δ with a mutation in the proteasome subunit Mts3, *mts3-1*. This mutant is defective in proteasome-mediated proteolysis and in the metaphase to anaphase transition (Gordon et al., 1993; Gordon et al., 1996; Seeger et al., 1996). *ubp8*Δ did not suppress the temperature

sensitive growth o*f mts3-1* (Figure 2-3) indicating that suppression of APC/C mutants is not mediated by enhanced proteasome function. Therefore, we conclude Ubp8 does not antagonize the APC/C via inhibition of proteasome function.

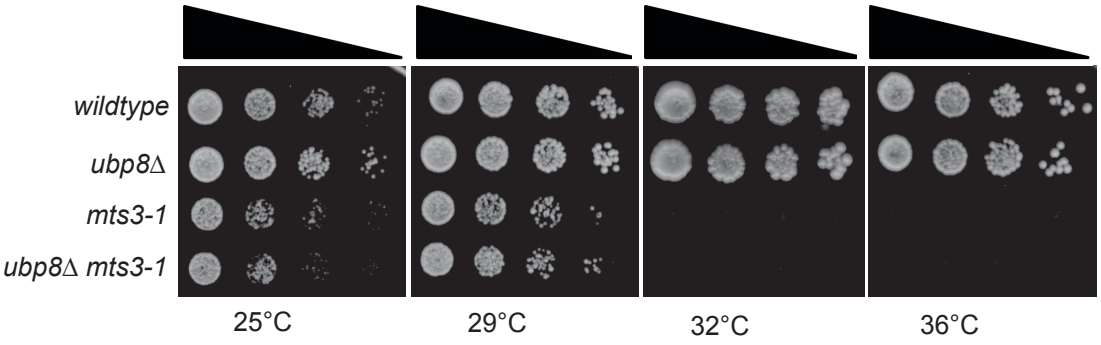

Figure 2-3. *ubp8*Δ does not suppress the temperature sensitive phenotype of proteasome mutants. Serial dilutions (10 fold) of the indicated single and double mutant strains were spotted on YE plates and incubated at the indicated temperatures.

Suppression of APC/C temperature sensitive mutants is dependent on Ubp8 catalytic activity

We next tested whether suppression of APC/C temperature-sensitive mutants was due to loss of Ubp8 catalytic activity or loss of the entire protein. Ubp8 is a papain-like cysteine protease that utilizes an Asn-His-Cys triad for catalytic function. We mutated the ubp8 sequence at the endogenous locus, resulting solely in production of Ubp8-C154S H387A, a catalytically inactive mutant based on sequence homology (Ingvarsdottir et al., 2005). To ensure that Ubp8-C154S H387A lacked activity, we assayed the levels of ubiquitinated histone H2B, a known substrate of Ubp8 (Ingvarsdottir et al., 2005; Lang et al., 2011; Lee et al., 2005; Tanny et al., 2007; Zhao et al., 2008). We observed increased levels of ubiquitinated histone H2B in both *ubp8*Δ and *ubp8-C154S H387A* cells (Figure 2-4A). Like *ubp8*Δ, *ubp8-C154S H387A* suppressed

the temperature sensitive phenotype of multiple APC/C mutants (Figure 2-4B) indicating that antagonization of the APC/C by Ubp8 is dependent on its catalytic function.

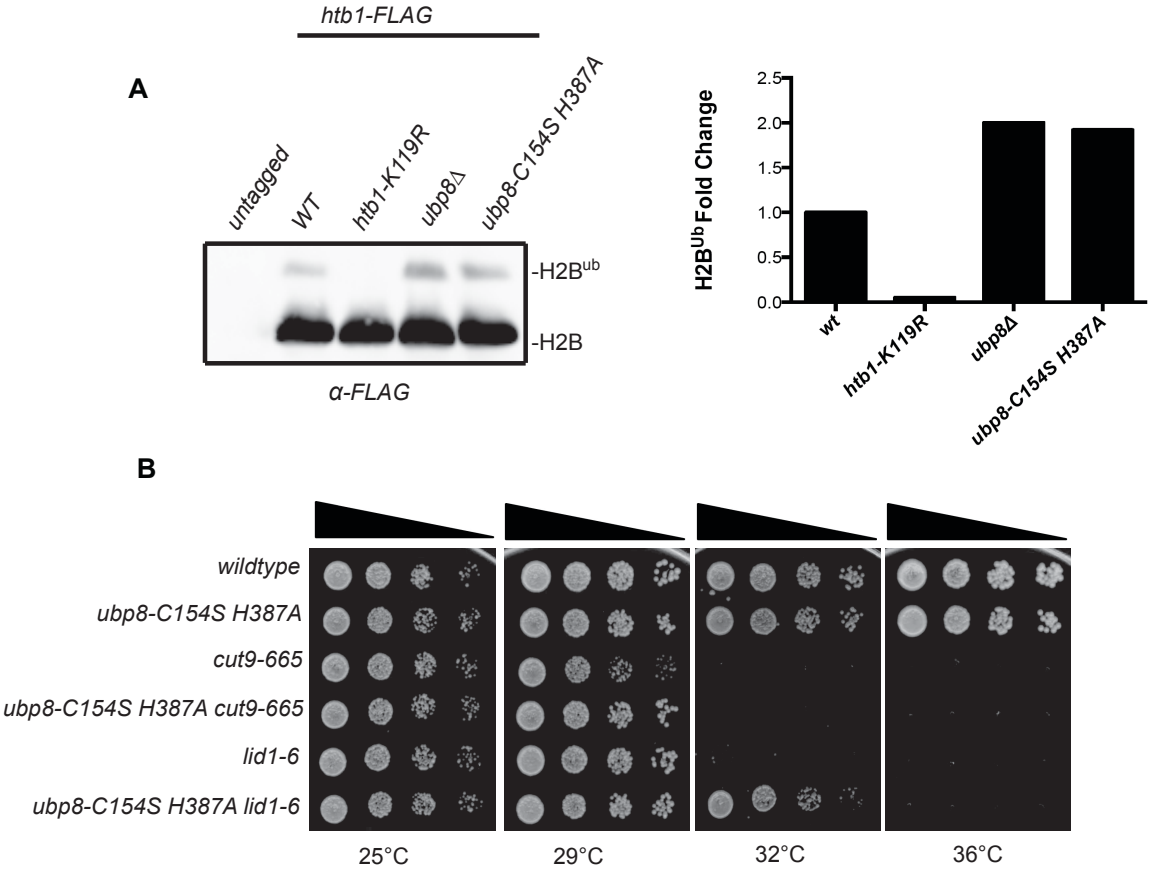

Figure 2-4. Suppression of APC/C mutants is dependent on the catalytic activity of Ubp8. (A) Anti-FLAG western blots of whole-cell extracts prepared from untagged and the indicated FLAG tagged strains. $H2B^{ub}$ corresponds to the slower migrating ubiquitinated form of H2B. (B) *ubp8-C154S H387A* suppressed the temperature sensitive phenotype of *cut4-533, slp1-362, lid1-6*, and *cut9-665* mutants. Serial dilutions (10-fold) of the indicated single and double mutant strains were spotted on YE and incubated at the indicated temperatures.

Suppression of APC/C temperature sensitive mutants is dependent on the activity of the SAGA DUB module

Ubp8 is part of the evolutionarily conserved DUB module of the SAGA transcriptional complex. The *S. pombe* SAGA DUB module consists of four proteins:

Sgf11, Sgf73, Sus1, and Ubp8 (Helmlinger et al., 2011). In *S. cerevisiae,* each of the DUB module components is required for ubiquitin protease activity *in vitro* and *in vivo (Lee et al., 2005; Samara et al., 2010; Samara et al., 2012)*. Like deletion of *ubp8*, deletion of each SAGA DUB module component (*sgf11*Δ, *sgf73*Δ*, or sus1*Δ) led to increased levels of ubiquitinated H2B *in vivo* (Figure 2-5A) and suppressed the temperature sensitive phenotype of APC/C mutants (Figure 2-5B). These results indicate that suppression of APC/C mutants is achieved by loss of the DUB activity associated with the SAGA complex.

Suppression of APC/C temperature sensitive mutants is specific to the SAGA DUB module

The SAGA complex is organized into distinct subcomplexes, each with discrete regulatory activities. In *S. pombe*, these modules include the DUB, histone acetyltransferase (HAT), TATA-binding protein (TBP), structural, Tra1 and Sgf29 (Helmlinger, 2012) (Figure 2-6A). The main function of the DUB module is to deubiquitinate histone H2B to regulate gene expression (Ingvarsdottir et al., 2005; Lang et al., 2011; Lee et al., 2005; Tanny et al., 2007; Zhao et al., 2008). The HAT module is responsible for acetylation of histone H2B and H3 while the TBP module regulates pre-initiation complex assembly and transcriptional activation (Koutelou et al., 2010; Samara and Wolberger, 2011). Tra1 has an important role in the recruitment of transcriptional co-activator complexes to specific promoters while Sgf29 plays a role in the binding of methylated histones (Helmlinger, 2012). Components of the structural module TBP-associated factors (TAFs) are responsible for maintaining SAGA architectural integrity

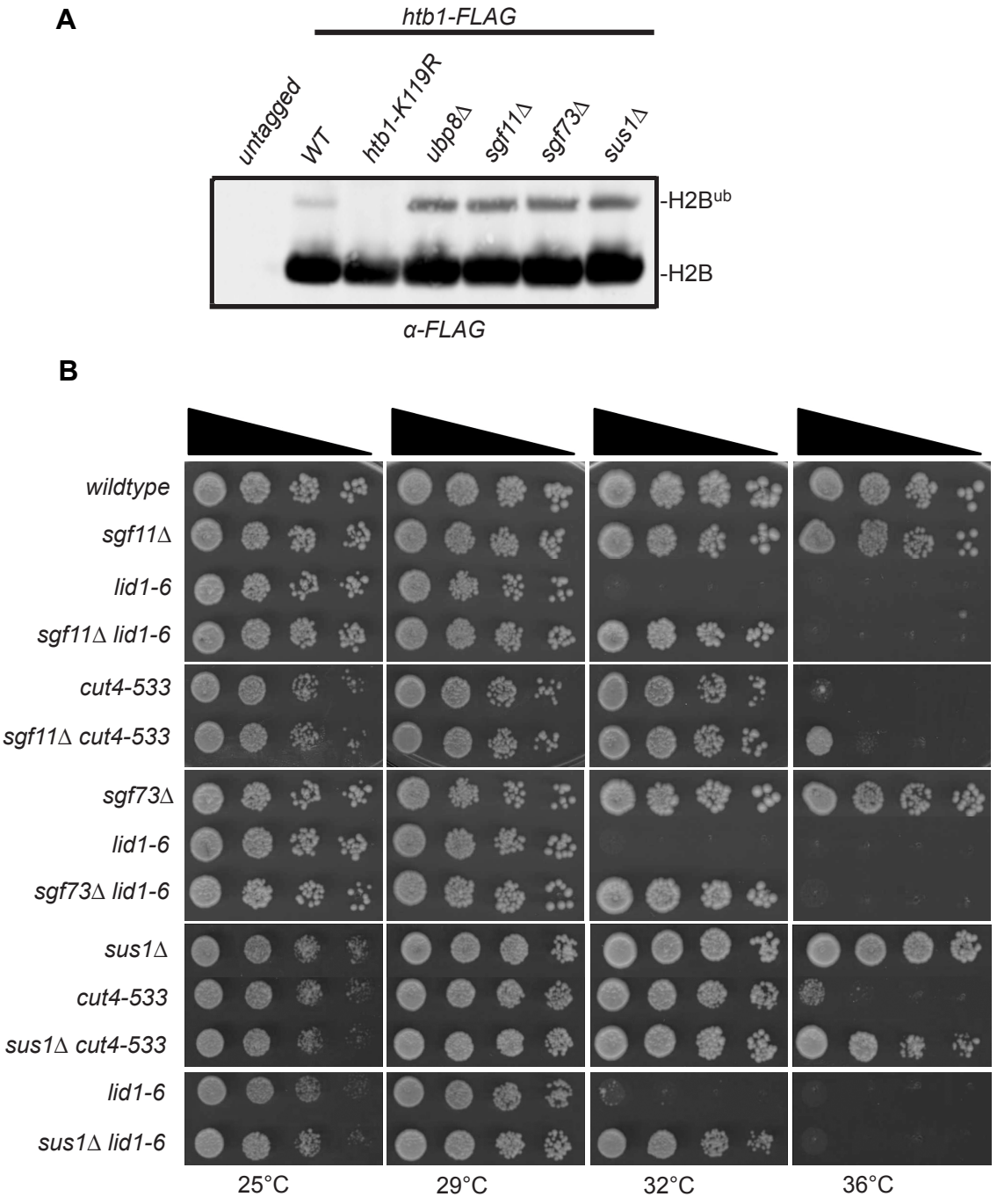

Figure 2-5. Suppression of APC/C temperature sensitive mutants is dependent on the SAGA DUB module. (A) Anti-FLAG western blots of whole-cell extracts prepared from untagged and the indicated FLAG tagged strains. $H2B^{ub}$ corresponds to the slower migrating ubiquitinated form of H2B. (B) Individual deletions of SAGA DUB module components (*sgf11*Δ, *sgf73*Δ and *sus1*Δ) suppress the temperature sensitive phenotype of APC/C mutants. Serial dilutions (10-fold) of the indicated single and double mutant strains were spotted on YE plates and incubated at the indicated temperatures.

and are involved in regulating gene expression through their association with the TFIID general transcription factor complex (Grant et al., 1998). In accordance with their role in multiple complexes, TAF components are encoded by essential genes in *S. pombe* (Helmlinger et al., 2011).

To determine whether SAGA subunits outside the DUB module affect the cells' requirement for APC/C function, we tested whether deletion mutants of non-DUB SAGA components could suppress APC/C mutants. *gcn5*Δ, *sgf29*Δ, *ada2*Δ, *ngg1*Δ, and *tra1*Δ, did not suppress the temperature sensitive phenotype of *lid1-6* (Figure 2-6B). Further, *spt8*Δ had a negative growth phenotype in combination with *lid1-6* (Figure 2-6B). These data indicate that the activity of the DUB module of the SAGA complex is responsible for antagonizing APC/C function.

Suppression of APC/C temperature sensitive mutants is dependent on H2B ubiquitination

To better understand how Ubp8 inhibits APC/C function, we identified putative substrates of the SAGA DUB module by semi-quantitative comparison of all ubiquitinated proteins (the ubiquitinome) in wildtype cells relative to that of *ubp8*Δ. We overexpressed a His-Biotin-His (HBH)-Ub fusion in *wildtype* and *ubp8*Δ strains, performed purifications under fully denaturing conditions, and identified all ubiquitinated proteins using 2D-LC-MS/MS. We compared the abundance of each protein in *ubp8*Δ to wildtype to identify potential Ubp8 substrates (i.e. ubiquitinated proteins enriched in the *ubp8*Δ strain). Histone H2B, an important substrate of Ubp8, was the only protein more

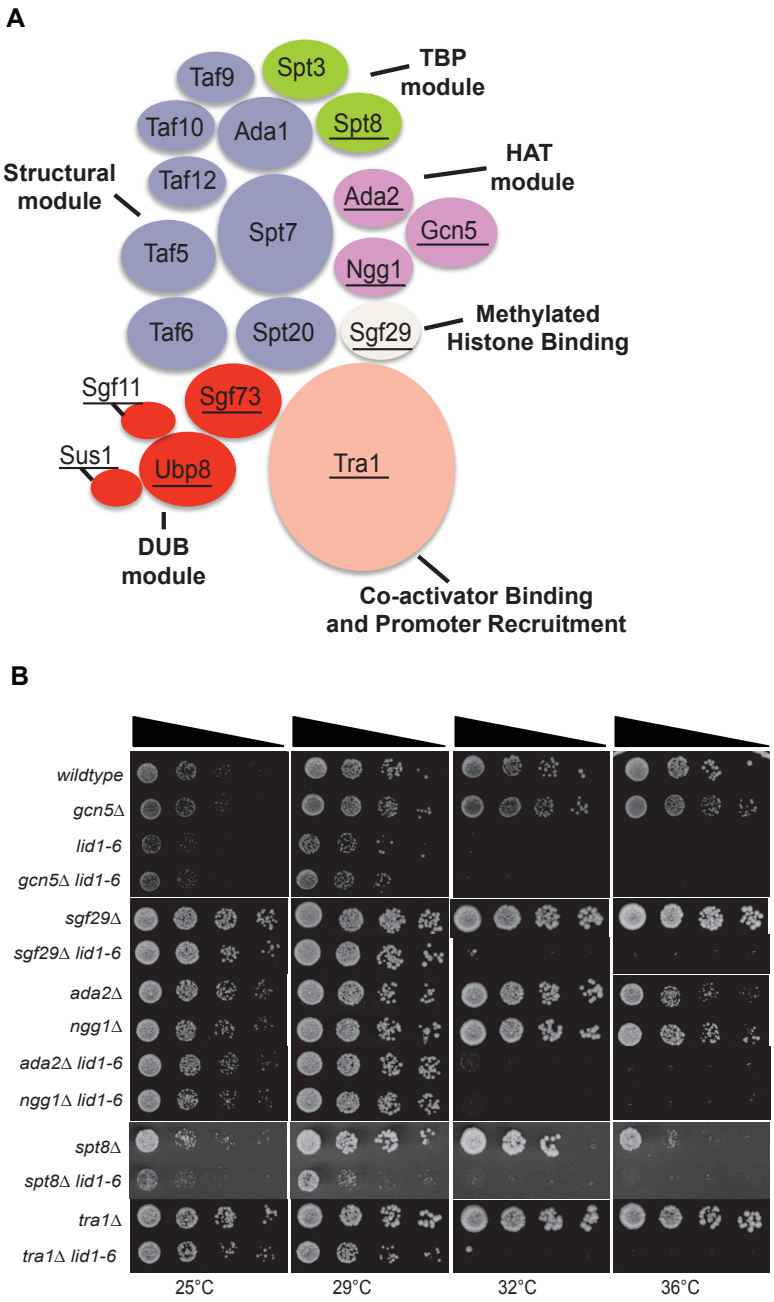

Figure 2-6. Suppression of APC/C temperature sensitive mutants is specific to the SAGA DUB module. (A) Schematic organization of *S. pombe* SAGA complex. Structural subunits are colored blue, Tra1 (Co-activator binding and promoter recruitment)-pink, Histone acetyltransferase (HAT)-purple, TATA-box binding protein module (TBP)-green, DUB module-red, Sgf29 (methylated histone binding)-gray. Underlined subunits indicate mutants used in this study. (B) Single deletions of SAGA complex components and the effect on the temperature sensitive phenotype of *lid1-6*. Serial dilutions (10-fold) of the indicated single and double mutant strains were spotted on YE and incubated at the indicated temperatures.

than 2 fold more abundant in *ubp8*Δ relative to wildtype (Figure 2-7), suggesting that it may be the only relevant target of Ubp8.

With this knowledge in mind, we investigated whether suppression of APC/C mutants required histone H2B ubiquitination. BRE1-like Brl1 and small histone ubiquitination factor Shf1, components of the HULC ubiquitin ligase complex, are required in *S. pombe* for H2B ubiquitination (Tanny et al., 2007; Zofall and Grewal, 2007). Deletions of *brl1* and *shf1* (*brl1*Δ and *shf1*Δ) abolished ubiquitination of histone H2B as did a lysine to arginine mutant of histone H2B in which the ubiquitin acceptor site is lost (*htb1-K119R*) (Figure 2-8A). Mutants in which H2B ubiquitination was abolished did not suppress APC/C temperature mutants when combined with *ubp8*Δ (Figure 2-8B). Furthermore, H2B ubiquitination mutants exhibited a negative growth phenotype when combined with *cut9-665* (Figure 2-8B). Together these results indicate that elevated levels of histone H2B ubiquitination reduce the requirement for APC/C function in *S. pombe*.

Discussion

In this work we found that of all DUB single deletions, only one, *ubp8*Δ, reduced the requirement for APC/C function in *S. pombe*. Our data support a model wherein Ubp8 antagonizes APC/C indirectly via modulating the ubiquitination status of H2B.

Multiple DUBs influence APC/C function

In our genetic approach to identify DUB(s) that antagonize APC/C function, we found that *ubp14*Δ and *pad1-1*, mutations in the conserved DUBs Ubp14 and Rpn11, respectively, showed negative genetic interactions with APC/C mutants indicating that

these DUBs were important for APC/C function. Based upon what is known about the function of these DUBs, we can provide plausible explanations for this behavior. Ubp14 cleaves free ubiquitin chains to liberate monomeric ubiquitin, thereby replenishing the ubiquitin pool (Amerik et al., 1997). Deletion of *ubp14* leads to the accumulation of free ubiquitin chains that compete with other cellular proteins for proteasome binding, thereby interfering with normal proteasome function and presumably the degradation of APC/C substrates (Amerik et al., 1997). We would thus predict that *ubp14*Δ would synergize negatively with mutants of the APC/C. Similarly, Rpn11, an essential proteasomal DUB, cleaves the proximal ubiquitin molecule in a ubiquitin chain when polyubiquitinated substrates bind the proteasome (Verma et al., 2002). This proximal cleavage releases the ubiquitin chain from the proteasome and allows target proteins to be properly degraded. *pad1-1 (rpn11 ts)* mutants have compromised ubiquitin dependent proteasome function and arrest at metaphase at the restrictive temperature (Penney et al., 1998; Verma et al., 2002). Therefore, through decreased proteasome function in *ubp14*Δ and *pad1-1 (rpn11 ts)* mutants, we predict that the degradation of APC/C substrates is compromised, further exacerbating the *cut9-665* temperature sensitive phenotype.

Suppression of APC/C mutants is dependent on SAGA DUB module activity

The yeast SAGA DUB module is a highly conserved complex in which the proteins Sgf11, Sgf73, Sus1 and Ubp8 are orthologous to the human proteins ATXN7L3, ATXN7, ENY2 and USP22 respectively (Lang et al., 2011; Zhao et al., 2008). In our work, we found that suppression of APC/C mutants was specific to the SAGA DUB module. Interestingly, mutants that decreased H2B ubiquitination (*spt8*Δ) showed a

ORF	Protein	Description	MW	Ratio	Normalized TSC		TSC		Coverage	
				ubp8Δ/ubp8$^+$	ubp8Δ	ubp8$^+$	ubp8Δ	ubp8$^+$	ubp8Δ	ubp8$^+$
SPBC337.08c	Ubi4	ubiquitin	43 kDa	1.0	1000	1000	1840	464	19%	27%
SPCC622.09	Htb1	histone H2B Htb1	14 kDa	3.0	176	58	324	27	52%	52%
SPAC16C9.02c		S-methyl-5-thioadenosine phosphorylase	34 kDa	1.3	3	2	5	1	8%	4%
SPCC1281.06c		acyl-coA desaturase	54 kDa	0.8	10	13	19	6	11%	11%
SPBC3H7.02		sulfate transporter	96 kDa	0.7	6	9	11	4	6%	6%
SPAC1F12.05		endocytosis regulator	42 kDa	0.6	8	13	14	6	9%	5%
SPAC18G6.14c	Rps7	40S ribosomal protein S7	22 kDa	0.6	49	86	90	40	52%	56%
SPBC1652.02		APC amino acid transporter	65 kDa	0.5	9	17	17	8	4%	4%
SPAC29B12.11c		human WW domain binding protein-2 orthol	20 kDa	0.5	2	4	4	2	10%	5%
SPBC1289.16c	Cao2	copper amine oxidase-like protein Cao2	90 kDa	0.5	1	2	2	1	5%	2%
SPCC757.03c		ThiJ domain protein	27 kDa	0.4	2	4	3	2	6%	7%
SPCP1E11.04c	Pal1	membrane associated protein Pal1	47 kDa	0.3	8	24	15	11	28%	21%
SPBC1685.13	Fhn1	Fhn1 plasma membrane organization protein	20 kDa	0.3	2	6	4	3	9%	9%
SPCC1020.10	Oca2	serine/threonine protein kinase Oca2	73 kDa	0.3	1	4	2	2	2%	4%
SPAC29B12.10c	Pgt1	glutathione transporter Pgt1	96 kDa	0.3	1	4	2	2	1%	1%
SPAC630.08c	Erg25	C-4 methylsterol oxidase	36 kDa	0.3	1	4	2	2	5%	5%
SPBC1711.04		methylenetetrahydrofolate reductase	36 kDa	0.3	1	4	2	2	8%	7%
SPBC16E9.02c		CUE domain protein	64 kDa	0.3	5	22	10	10	9%	9%
SPBC1604.21c	Ptr3	ubiquitin activating enzyme E1	113 kDa	0.3	3	11	5	5	3%	3%

Figure 2-7. Proteomic identification of SAGA DUB module substrates. Indicated are proteins identified from *S. pombe* ubiquitinome purifications in *wildtype* and *ubp8*Δ strains. Total spectral counts (Stone et al., 2004) for each protein were normalized to the TSC for ubiquitin.

negative genetic intraction with APC/C mutants, further implicating H2B ubiquitination status as a key factor in the regulation of APC/C function. In *S. cerevisiae*, each subunit of the Ubp8-Sgf11-Sus1-Sgf73 complex makes extensive contact with all other subunits and all four components are required for DUB activity *in vitro* and *in vivo* (Ingvarsdottir et al., 2005; Kohler et al., 2010; Lee et al., 2005; Samara et al., 2010; Samara et al., 2012). In contrast, in Drosophila and in human cells, the presence of Ataxin-7 (Sgf73) is not necessary for DUB activity, and, instead, loss of Ataxin-7 results in increased

negative genetic intraction with APC/C mutants, further implicating H2B ubiquitination status as a key factor in the regulation of APC/C function. In *S. cerevisiae*, each subunit of the Ubp8-Sgf11-Sus1-Sgf73 complex makes extensive contact with all other subunits and all four components are required for DUB activity *in vitro* and *in vivo* (Ingvarsdottir et al., 2005; Kohler et al., 2010; Lee et al., 2005; Samara et al., 2010; Samara et al., 2012). In contrast, in Drosophila and in human cells, the presence of Ataxin-7 (Sgf73) is

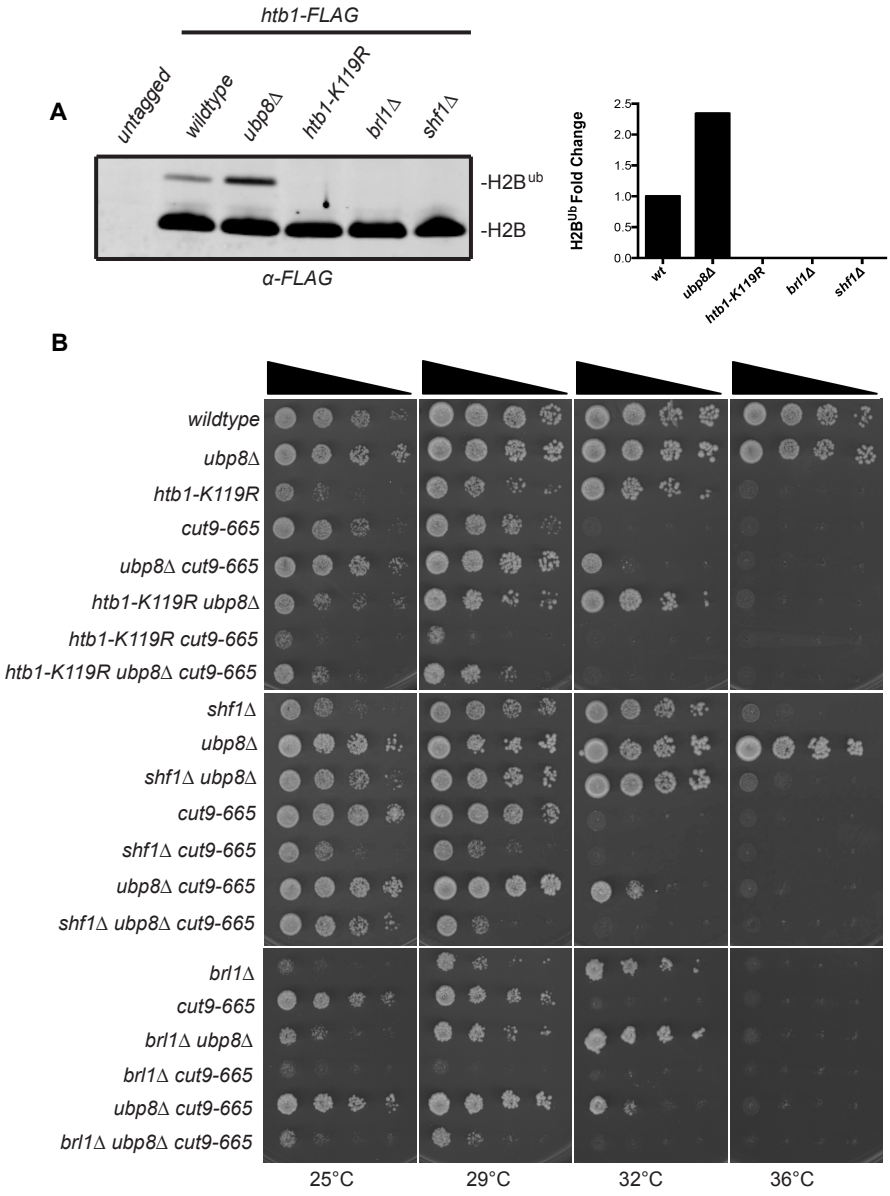

Figure 2-8. Suppression of APC/C temperature sensitive mutants is dependent on H2B ubiquitination. (A) Anti-FLAG western blots of whole-cell extracts prepared from untagged and the indicated FLAG tagged strains. (B) Individual deletions and point mutants (*brl1*Δ*, htb1-K119R, shf1*Δ) that abolish H2B ubiquitination did not suppress the temperature sensitive phenotype of APC/C mutants when combined with *ubp8*Δ. Serial dilutions of the indicated single, double and triple mutant strains were spotted on YE plates and incubated at the indicated temperatures.

not necessary for DUB activity, and, instead, loss of Ataxin-7 results in increased deubiquitination and reduced levels of H2B ubiquitination (Mohan et al., 2014). This is

presumably through the release of an active DUB module population no longer regulated by other components of the SAGA complex. These results reveal the complexity of regulation of H2B ubiquitination and present an interesting backdrop for understanding the role of the DUB module in regulating APC/C function in higher eukaryotes.

Suppression of APC/C mutants is dependent on increased histone H2B ubiquitination

Histone H2B ubiquitination regulates many cellular processes including transcriptional activation and silencing, maintenance of chromatin structure and DNA repair (Weake and Workman, 2008). In *S. pombe*, H2B is ubiquitinated by the multi-subunit histone H2B ubiquitin ligase complex (HULC). The HULC consists of the Rad6 homolog Rhp6, the Bre1 homologs Brl1 and Brl2 and an additional protein Shf1 (Tanny et al., 2007; Zofall and Grewal, 2007). Each HULC subunit is required for ubiquitination of residue K119 on histone H2B (Zofall and Grewal, 2007). Ubp8 deubiquitinates histone H2B *in vitro* and *in vivo* (Lang et al., 2011; Lee et al., 2005; Samara et al., 2010; Samara et al., 2012) and we have now linked this modification to a function in APC/C regulation in *S. pombe*.

The exact mechanism by which H2B ubiquitination promotes APC/C function remains unclear. Because of its known role in transcriptional regulation, it is possible that increased H2B ubiquitination in *ubp8*Δ modulates the levels of APC/C components, inhibitors or activators. However, there is no evidence in support of this explanation from the results of extensive transcriptome analyses (Helmlinger *et al*., 2011). For example, the transcript level of the *S. pombe* APC/C co-activator *slp1*, which is known to be cell cycle regulated (Anderson et al., 2002), is not altered in deletions of DUB module

components. Furthermore, transcript levels of members of the PKA pathway, an APC/C inhibitor, are also unaltered in DUB module mutants (Helmlinger et al., 2011).

A second possibility is that the reduced requirement for APC/C function is related to the effects of H2B ubiquitination on centromere structure and function. In accordance with this, H2B mutations that affect H2B structure decrease H2B ubiquitination and cause centromeric defects (Maruyama et al., 2006). Additionally, monoubiquitination of H2B maintains active centromeric chromatin and promotes proper kinetochore formation (Sadeghi et al., 2014). Based on these data, it is possible that increased H2B

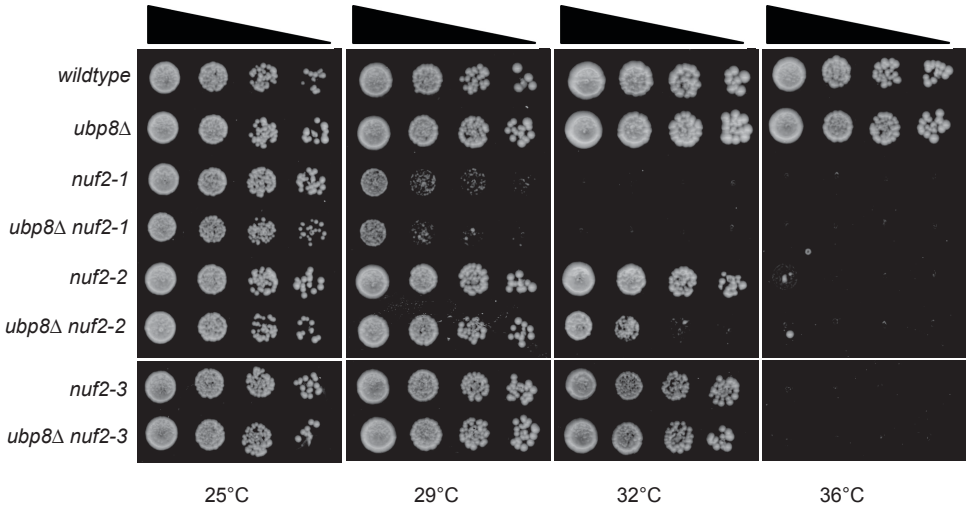

Figure 2-9. *ubp8*Δ does not suppress the temperature sensitive phenotype of *nuf2* kinetochore mutants. Serial dilutions (10 fold) of the indicated single and double mutant strains were spotted on YE plates and incubated at the indicated temperatures.

ubiquitination in a *ubp8*Δ mutant augments kinetochore formation. Moreover, improved kinetochore formation could promote microtubule-kinetochore attachment allowing for enhanced chromosome segregation and suppression of APC/C temperature sensitivity. To test this, we combined *ubp8*Δ with temperature sensitive mutants of the essential kinetochore protein Nuf2 (*nuf2-1*, *nuf2-2*, and *nuf2-3*) *(Nabetani et al., 2001)*. *ubp8*Δ did

not suppress the *nuf2* temperature sensitive phenotype (Figure 2-9) indicating that *ubp8*Δ does not suppress APC/C mutants through augmented kinetochore function.

Our work defines a new role for DUBs in regulating APC/C function indirectly through ubiquitination of histone H2B. Antagonization of APC/C function is dependent on SAGA DUB module activity and independent of the SAC. Further work is needed to dissect the exact mechanism in which H2B ubiquitination regulates APC/C activity.

Because of its essential roles in chromosome segregation and mitotic progression, the APC/C has become a therapeutic target for the treatment of multiple neoplastic diseases (Bassermann et al., 2014). Interestingly, the Ubp8 homolog USP22 has been identified as a member of an 11-gene "death from cancer" signature that acts as a predictor of tumor aggressiveness, treatment resistance and metastatic probability in cancer patients (Atanassov and Dent, 2011; Glinsky, 2006; Liu et al., 2010). Therefore, advancing our understanding of how the SAGA DUB module controls cell division may provide insights into the role of USP22 in tumor progression.

CHAPTER III

IDENTIFICATION OF DUB(S) THAT ANTAGONIZE THE FUNCTION OF THE E3 UBIQUITIN LIGASE, DMA1

(Adapted from "RELIEF OF THE DMA1-MEDIATED CHECKPOINT REQUIRES DMA1 AUTOUBIQUITINATION AND DYNAMIC LOCALIZATION")

Christine M. Jones*, Jun-Song Chen*, Alyssa E. Johnson, Zachary C. Elmore, Janel R. Beckley, and Kathleen L. Gould

*These authors contributed equally to this work

-Manuscript in preparation

Introduction

The post-translational modification of proteins by conjugation of monomers or chains of ubiquitin is a regulatory mechanism for tuning protein stability, localization and function. Given these vital functions, ubiquitination has to be highly regulated so that protein degradation and cell signaling are controlled in space and time.

Ubiquitin is attached to substrates through a tightly coordinated enzyme cascade (E1, E2, E3)(Hershko and Ciechanover, 1998; Komander and Rape, 2012; Tomko and Hochstrasser, 2013). Conversely, ubiquitin is removed from target substrates by deubiquitinating enzymes (DUBs) (Komander et al., 2009; Kouranti et al., 2010; Reyes-Turcu et al., 2009). E3 ubiquitin ligases facilitate the final step in protein ubiquitination by promoting transfer of ubiquitin from the E2 enzyme to a target lysine residue on the substrate (Pickart, 2004). Two distinct classes of E3 ligases exist, which are classified by the presences of either a RING or HECT domain. RING domain E3 ligases have been

thought to mainly act as scaffolds to bring the E2~Ub complex in proximity to the substrate (Deshaies and Joazeiro, 2009); however, recent evidence suggests that RING domains might also allosterically activate their cognate E2 (Ozkan et al., 2005). In contrast, HECT domain E3s first ligate ubiquitin to an active cysteine residue on themselves before actively catalyzing ubiquitination of the substrate (Rotin and Kumar, 2009). In addition to either a HECT or RING domain, many E3s also contain a substrate recognition motif that provides substrate specificity.

In the fission yeast *Schizosaccharomyces pombe,* the checkpoint protein and E3 ubiquitin ligase, Dma1, delays cytokinesis by inhibiting the septation initiation network (SIN) when a spindle error occurs. During a mitotic checkpoint, Dma1 ubiqutinates the SIN scaffold Sid4 (Chang and Gould, 2000b; Morrell et al., 2004), and this ubiquitination is required for SIN inhibition (Johnson and Gould, 2011b). Sid4 ubiquitination antagonizes the SPB localization of the Polo-like kinase Plo1 (Guertin et al., 2002b; Johnson and Gould, 2011b), the major SIN activator (Mulvihill et al., 1999; Ohkura et al., 1995; Tanaka et al., 2001) so that SIN signaling is blocked and cytokinesis is delayed. Overproduction of Dma1 completely blocks SIN activity and results in cell death (Guertin et al., 2002b), indicating its levels and activity must be properly regulated. Furthermore, upon resolution of the mitotic spindle defect, the Dma1-dependent checkpoint signal must be extinguished in order to resume SIN activation and cell division. In this chapter, we utilized an overexpression screen to identify the DUBs that antagonize Dma1 activity *in vivo*. We show that multiple DUBs can antagonize Dma1 activity and that fusion of a Dub to the SPB scaffold, Ppc89, inhibits Sid4 ubiquitination.

Results

To identify the Dub(s) that antagonize Dma1 function, we screened eighteen of the twenty *S. pombe* DUBs for their ability to rescue Dma1 overexpression-induced cytokinesis failure and cell death (Guertin et al., 2002b; Murone and Simanis, 1996). Four of the eighteen DUBs (Ubp1, Ubp2, Ubp7, and Ubp14) suppressed Dma1-induced cell death, presumably by reversing Sid4 ubiquitination (Figure 3-1).

DUB	Rescue
Ubp1	Yes
Ubp2	Yes
Ubp3	No
Ubp6	No
Ubp7	Yes
Ubp8	No
Ubp9	No
Ubp11	No
Ubp12	No
Ubp14	Yes
Ubp15	No
Ubp16	No
Uch1	No
Uch2	No
Otu1	No
Otu2	No
Sst2	No
Rpn11	No

Figure 3-1. Identification of DUBs that antagonize Dma1 activity
Wildtype *S. pombe* was transformed with pREP42*dma1*$^{+}$ and each of the listed deubiquitinating enzyme genes in pREP1 (except *rpn11*$^{+}$ which was expressed from pREP3X and *upb12*$^{+}$ which was expressed from pREP3). URA+LEU+ transformants were tested for the ability to grow in medium lacking thiamine at 29°C and rescue the Dma1-induced cell death phenotype.

Next we wanted to determine if fusion of these DUBs to Sid4 could abrogate Sid4 ubiquitination. Of the DUBs that rescued Dma1-induced cell death, only Ubp7 has

diffuse cytoplasmic localization and functions independently of other subunits *in vivo* (Kouranti et al., 2010), making it well-suited for our purpose. The ubiquitin specific protease (USP) domain of Ubp7 was fused to the C-terminus of Sid4 (Sid4-Ubp7) and produced under control of the native *sid4*$^{+}$ promoter as the sole version of Sid4 in the cell. The fusion did not affect cell viability, but the Sid4-Ubp7 fusion was still ubiquitinated (Figure 3-2), indicating that Ubp7 was not able to access Sid4 ubiquitination sites.

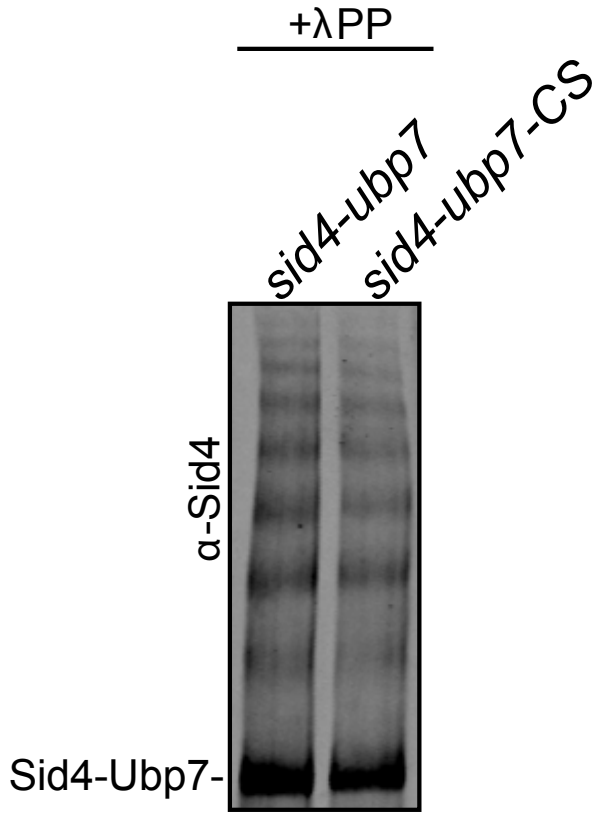

Figure 3-2. Sid4-Ubp7 fusion does not inhibit Sid4 ubiquitination
A Sid4-Ubp7 and a catalytically inactive DUB fusion (Sid4-Ubp7-CS) were immunoprecipitated from the indicated strain, treated with phosphatase, and visualized by immunoblotting.

We next tested whether adding the Ubp7 USP domain to the C-terminus of the Sid4 binding partner Ppc89 (Rosenberg et al., 2006a) eliminated Sid4 ubiquitination. The

Ppc89-Ubp7 USP fusion (hereafter called Ppc89-DUB) (Figure 3-3A) abolished Sid4 ubiquitination comparable to deletion of *dma1* (Figure 3-3B). The *ppc89-DUB* strain

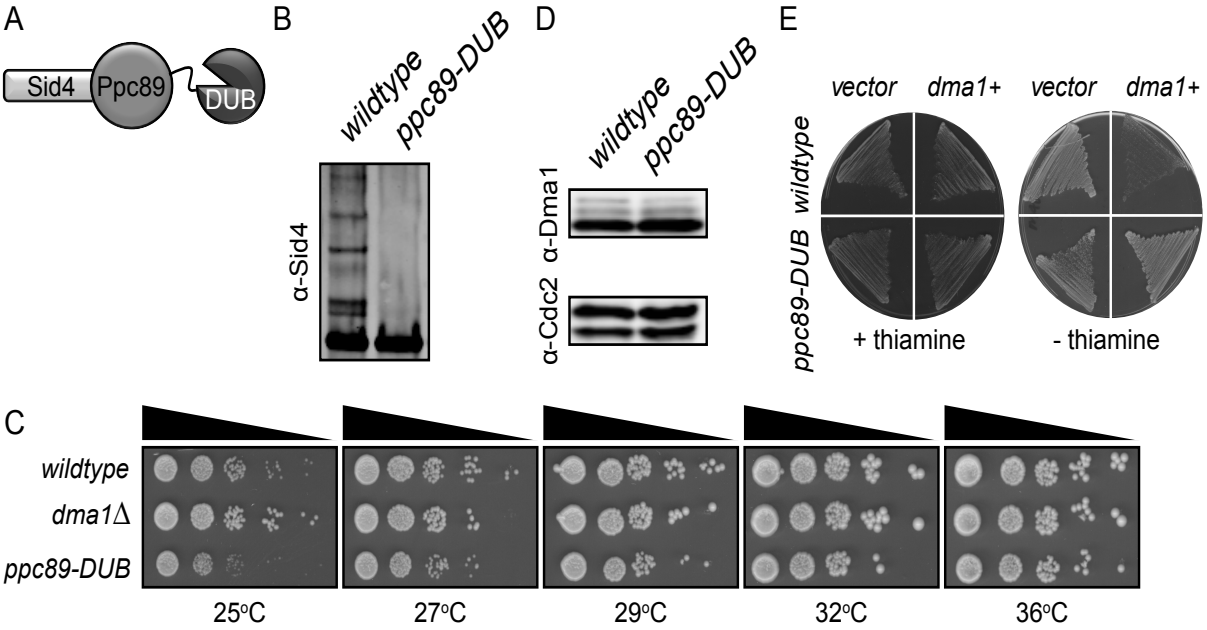

Figure 3-3. A Ppc89-DUB fusion eliminates Sid4 ubiquitination. (A) Schematic of Ppc89-DUB fusion (B) Sid4 was immunoprecipitated from equal amounts of protein lysates from the indicated strains, treated with phosphatase, and visualized by immunoblotting. (C) The indicated strains were grown at 29°C, and then the same number of cells were spotted in 10-fold serial dilutions and incubated at the indicated temperatures on YE plates. (D) Relative protein levels of Dma1-FLAG in the indicated strains as determined by immunoblotting of immunoprecipitates from the same amount of protein lysates as determined by immunoblotting for Cdc2. (E) *wildtype* and *ppc89-DUB* strains were transformed with either vector alone (pREP42) or vector containing *dma1*$^{+}$ (pREP42*dma1*$^{+}$). Transformants were incubated on medium containing thiamine (left) or lacking thiamine (right) at 29°C.

grew similarly to wildtype at a variety of temperatures (Figure 3-3C), and the levels of Dma1 and Sid4 were unchanged relative to their levels in wildtype cells (Figure 3-3D and B). As would be expected when Sid4 cannot accumulate ubiquitin modifications, the *ppc89-DUB* strain resisted Dma1 overexpression-induced cell death (Figure 3-3E). Taken together, these data indicate that our Ppc89-DUB fusion can abrogate Dma1-mediated Sid4 ubiquitination.

Discussion

Our work reveals new insights into the role of DUBs in regulating a mitotic checkpoint. The ability of 4 DUBs to antagonize the activity of Dma1 reveals there may be underlying redundancy in DUB-mediated Dma1 inhibition. This would be in agreement with previous work demonstrating functional overlap between DUBs in *S. pombe* (Beckley et al., 2015). Future work will be important in determining the substrate overlap between the 4 DUBs to gain a deeper understanding of how they abrogate Dma1 function.

Our work identifying the DUBs that antagonize Dma1 function has led to the creation of a powerful tool to study the Dma1-mediated mitotic checkpoint. While it is well characterized how Dma1 is recruited to Sid4 to activate the mitotic checkpoint, it is not clear how the checkpoint is shut off. The Ppc89-DUB fusion can be used in future studies to analyze the role of Sid4 ubiquitination in mediating Dma1 localization at the SPB. Work is presently underway to determine if Sid4 ubiquitination plays a role in removing Dma1 from the SPB to shut off the mitotic checkpoint.

CHAPTER IV

THE KINASE DOMAIN OF CK1 ENZYMES CONTAINS THE SPINDLE POLE LOCALIZATION CUE ESSENTIAL FOR THE YEAST DMA1-MEDIATED MITOTIC CHECKPOINT

Zachary C. Elmore, Rodrigo X. Guillen, and Kathleen L. Gould

-In revision

Introduction

Casein kinases are among the most abundant serine/threonine protein kinases found in eukaryotic cells (Carpy et al., 2014; Desjardins et al., 1972; Hathaway and Traugh, 1979; Matsumura and Takeda, 1972; Tuazon and Traugh, 1991) and generally recognize substrates consisting of acidic or phosphorylated amino acid residues (Agostinis et al., 1989; Flotow et al., 1990; Flotow and Roach, 1991; Graves et al., 1993; Meggio et al., 1992; Meggio et al., 1991). Members of the casein kinase 1 (CK1) family have been implicated in multiple cellular processes including regulation of autophagy, DNA repair, circadian rhythm, ribosome assembly, intracellular trafficking, meiotic progression, and Wnt signaling (Ghalei et al., 2015; Knippschild et al., 2005; Nakatogawa, 2015; Schittek and Sinnberg, 2014). CK1 kinases share highly related catalytic domains (53%-98% sequence identity) that consist of a bi-lobed structure with a smaller N-terminal lobe consisting primarily of β- sheets and a larger, primarily α-helical C-terminal lobe (Carmel et al., 1994; Longenecker et al., 1996; Xu et al., 1995). However, CK1 family members have divergent C-terminal non-catalytic domains that are

thought to dictate intracellular localization and govern catalytic activity (Babu et al., 2002; Cegielska et al., 1998; Dahlberg et al., 2009; Gietzen and Virshup, 1999; Graves and Roach, 1995; Greer and Rubin, 2011; Ianes et al., 2015; Longenecker et al., 1996; Longenecker et al., 1998; Meng et al., 2016). Indeed, some CK1 isoforms are anchored to membranes via C-terminal palmitoylation (Babu et al., 2004; Sun et al., 2004; Vancura et al., 1994; Wang et al., 1992).

Hhp1 and Hhp2 (hereafter referred to as Hhp1/2) are the sole soluble CK1s in *Schizosaccharomyces pombe* and are orthologs of *Saccharomyces cerevisiae* Hrr25p and human CK1δ and CK1ε (hereafter referred to as CK1δ/ε) (Dhillon and Hoekstra, 1994; Hoekstra et al., 1994). In addition to functioning redundantly in meiosis, DNA damage repair, and mitotic commitment (Chan et al., 2017; Dhillon and Hoekstra, 1994; Sakuno and Watanabe, 2015), Hhp1/2 are essential for preventing cytokinesis during a mitotic stress imposed by microtubule depolymerization (Johnson et al., 2013). In this checkpoint pathway, Hhp1/2 function redundantly upstream of the ubiquitin ligase Dma1 to inhibit the septation initiation network (SIN) (Guertin et al., 2002b; Murone and Simanis, 1996), a *hippo*-related signaling pathway localized at the spindle pole body (SPB) that triggers cytokinesis (Johnson and Gould, 2011a; Johnson et al., 2012; Simanis, 2015). Specifically, Hhp1/2 phosphorylate the SIN scaffold Sid4 at T275 and S278 to create a docking site for Dma1's FHA domain (Johnson et al., 2013). Dma1 then concentrates at SPBs and ubiquitinates Sid4, also a scaffold for Polo kinase Plo1, to inhibit Plo1's SPB localization and ability to activate the SIN (Guertin et al., 2002b; Johnson and Gould, 2011a).

In addition to other subcellular localizations, Hhp1/2, as well as Hrr25p and human CK1δ/ε localize to the SPB or its equivalent in vertebrates, the centrosome (Greer and Rubin, 2011; Hutchins et al., 2010; Johnson et al., 2013; Peng et al., 2015b). Interaction with AKAP450 and the gamma-tubulin complex is reported to be important for anchoring CK1δ and Hrr25p to the centrosome and SPB, respectively (Peng et al., 2015b; Sillibourne et al., 2002). However, the residues within CK1 enzymes required for SPB/centrosome recruitment are unknown, as is the SPB binding partner(s) in *S. pombe*.

In this work, we establish that Hhp1/2 localize throughout the cell cycle to the SPB and also to the nucleus and cell division site with Hhp2 showing additional localization to cell tips. We report that the catalytic domains of Hhp1/2 are sufficient to support this localization pattern independently of enzymatic function. Further, we define conserved residues at the base of the Hhp1/2 catalytic domains necessary for SPB localization. Mutation of these residues eliminates Hhp1/2's SPB localization and mitotic checkpoint function by disrupting the interaction with the core SPB protein, Ppc89 (Rosenberg et al., 2006b), but does not affect other critical Hhp1/2 functions. We also find that the centrosomal targeting information in human CK1δ/ε is analogously contained within their respective kinase domains indicating conservation of this localization mechanism from yeast to human. This study provides novel insight into how specific docking residues within the catalytic domain of protein kinases can direct them to subcellular locations to control substrate phosphorylation and downstream signaling.

Results

Hhp1/2 localization during a normal and perturbed cell cycle

Both Hhp1 and Hhp2 localize to SPBs and either is sufficient to promote the Dma1-mediated mitotic checkpoint that delays cytokinesis (Johnson et al., 2013). To determine their intracellular distribution throughout the cell cycle and during a mitotic arrest, each was tagged at its endogenous C-terminus with mNeonGreen (mNG) (Willet et al., 2015) and co-imaged with the SPB protein Sid4-RFP (Chang and Gould, 2000a). Both Hhp1 and Hhp2 localize to the nucleus and the division site in addition to SPBs; Hhp2 was also detected at cell tips (Figure 4-1A). By immunoblotting whole cell lysates from a strain producing both enzymes tagged with GFP, we determined that Hhp1 is more abundant than Hhp2 (Figure 4-2A), consistent with the relative protein levels determined by quantitative mass spectrometry (Carpy et al., 2014; Marguerat et al., 2012), and the more severe growth defects and phenotypes associated with the deletion of *hhp1*$^{+}$ relative to *hhp2*$^{+}$ (Figure 4-2B-D) (Bimbo et al., 2005; Carpy et al., 2014; Chen et al., 2015; Dhillon and Hoekstra, 1994; Hoekstra et al., 1994). To better define the localization of Hhp1/2 during the mitotic checkpoint signaling window, we performed time-lapse imaging of cells progressing through mitosis. Hhp1-mNG and Hhp2-mNG localized to the SPB and nucleus throughout mitosis, and then the division site following the completion of spindle elongation with comparable timing (Figure 4-2E and F). These data indicate that Hhp1 and Hhp2 spatial and temporal distributions are similar but not identical.

When the mitotic checkpoint is activated by preventing microtubule polymerization in the *nda3-KM311* ß-tubulin mutant (Toda et al., 1983), Sid4 is

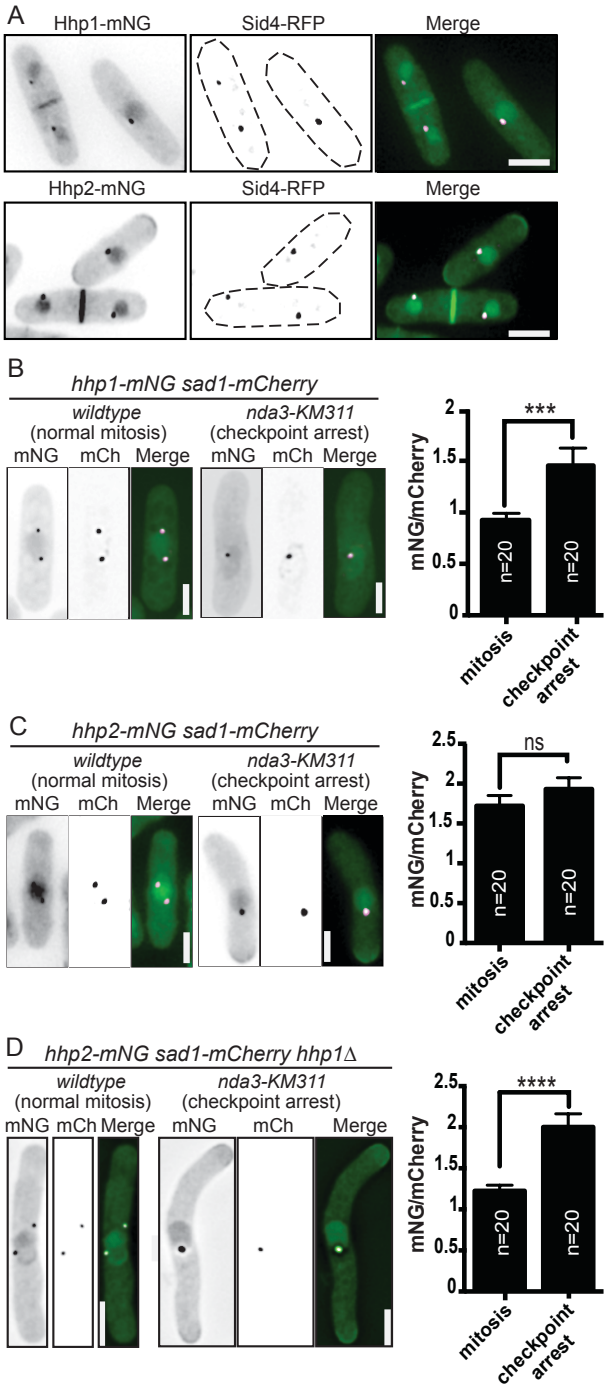

Figure 4-1. Intracellular localization patterns of Hhp1/2. (A) Live-cell imaging of Hhp1-mNG and Hhp2-mNG with Sid4-RFP. (B-D) Hhp1-mNG (B) and Hhp2-mNG (C and D) were imaged in prometaphase arrested and wildtype mitotic *sad1-mCherry* or *sad1-mCherry hhp1*Δ cells. Representative inverted grayscale images are shown in left panels with quantitation to the right. Scale bars, 5 µm. Values are represented as mNG/mCherry intensity ratios. ***p<0.001, ****p<0.001 determined using Student's *t*-test. ns=not significant. Error bars represent standard error of the mean (SEM).

hyperphosphorylated by Hhp1/2, and Hhp1 increases in intensity at SPBs (Johnson et al., 2013) (Figure 4-1B). By co-imaging with the SPB marker Sad1-mCherry in checkpoint activated and unperturbed mitotic cells, we found that Hhp2 intensity at duplicated but unseparated SPBs was also increased in checkpoint activated cells but only if they lacked Hhp1 (Figure 4-1C and D). These results indicate that both Hhp1/2 can accumulate at SPBs during the checkpoint.

Hhp1/2 catalytic domains direct SPB localization and checkpoint function

To determine the mechanism of Hhp1/2 SPB targeting, we first defined the regions of the enzymes necessary for this localization. Hhp1/2 contain conserved N-terminal catalytic domains and kinase domain extensions (KDEs) that are conserved among mammalian but not *S. cerevisiae* CK1 family members (reviewed in (Knippschild et al., 2014)) (Figure 4-3A). Given that both Hhp1/2 localize to SPBs and participate in checkpoint signaling, we anticipated that homologous sequences dictated these functions and that their unrelated C-termini were not involved. Accordingly, Hhp1/2 C-terminal truncations, constructed by inserting sequences encoding GFP in the endogenous *hhp1/2* loci to produce Hhp1-(1-296)-GFP and Hhp2-(1-295)-GFP (Figure 4-3B), both co-localized with Sid4-RFP at SPBs (Figure 4-3C). Moreover, Hhp1-(1-296)-GFP and Hhp2-(1-295)-GFP also localized to the nucleus and division site while Hhp2-(1-295)-GFP was also detected at cell tips (Figure 4-3C). The C-terminus of Hhp1 fused to GFP was not targeted to any particular subcellular location although it could be produced (Figure 4-4A and B), indicating that the C-terminus is neither necessary nor sufficient for SPB localization of Hhp1/2.

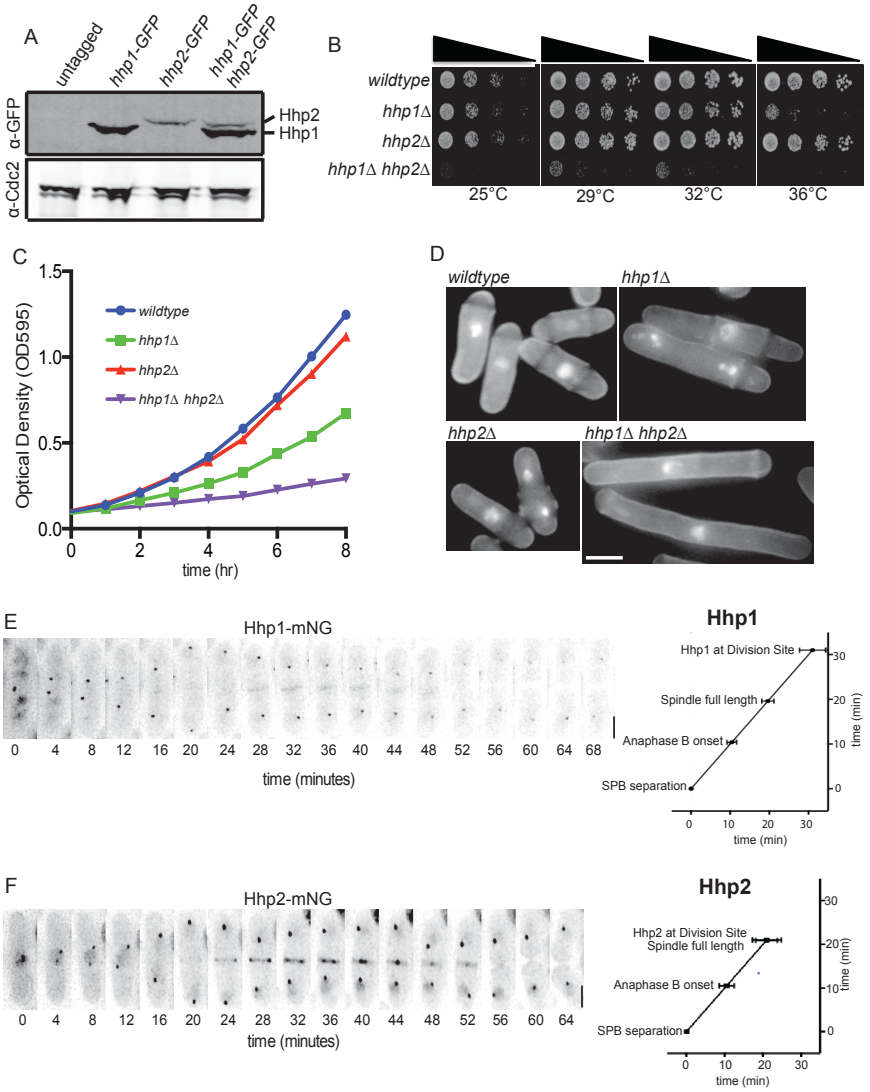

Figure 4-2. Comparison of Hhp1 and Hhp2 functions and localizations. (A) Anti-GFP western blot of whole-cell extracts prepared from untagged and the indicated GFP-tagged strains. Anti-PSTAIRE antibody served as loading control for lysates. (B) Serial dilutions (10-fold) of the indicated strains were spotted on YE plates and incubated at the indicated temperatures. (C) Liquid growth assay of wildtype, *hhp1*Δ, *hhp2*Δ and *hhp1*Δ *hhp2*Δ mutants. Cells were grown in liquid YE at 32°C to log phase and cut back to an OD_{595}=0.1. OD_{595} measurements were taken every hour for 8 h to determine growth rates of mutants. (D) wildtype, *hhp1*Δ, *hhp2*Δ, and *hhp1*Δ *hhp2*Δ mutant phenotypes were analyzed by DAPI (DNA) and methyl blue (cell wall) staining. (E and F) (Left panels) Representative montages of Hhp1-mNG (E) and Hhp2-mNG (F) movies. Images are shown in 4 min intervals with T=0 defined as the time of SPB separation. Right panels are timelines showing when Hhp1-mNG and Hhp2-mNG are detected at the division site. The mean time of detection of each protein ± SD is plotted from 20 cells each. The onset of anaphase B was determined to be 10.4 ± 1.2 min for *hhp1-mNG* and 10.5 ± 1.9 min for *hhp2-mNG* cells. Hhp1-mNG was detected at the division site at 31 ± 3.3 min and Hhp2-mNG at 21 ± 3.8 min. Scale bars, 5 μm.

To ascertain the functionality of the C-terminal truncation mutants of Hhp1/2, we performed growth, *in vitro* kinase, and mitotic checkpoint assays. First, we found that each of the *hhp1/2* C-terminal truncation mutants integrated as the sole *hhp1/2* allele in cells rescued the severe growth defect of the double deletion mutant *in vivo* (Figure 4-3D). Consistent with this finding and previous reports (Cegielska et al., 1998; Gietzen and Virshup, 1999; Graves and Roach, 1995), recombinant Hhp1/2 C-terminal truncation mutants phosphorylated the exogenous substrate casein *in vitro* even more robustly than the full-length proteins (Figure 4-3E). Importantly, we found that the truncation mutants were sufficient to inhibit the SIN during the mitotic checkpoint. GFP-tagged Hhp1 and Hhp2 C-terminal truncations accumulated at SPBs during a mitotic checkpoint arrest compared to a normal mitosis (Fig. 4-4C and D) and Sid4 was appropriately ubiquitinated (Figure 4-3F). Taken together, these data indicate that the C-termini of Hhp1/2 are dispensable for their SPB localization and function during the Dma1-mediated mitotic checkpoint.

Because the KDE of CK1δ was reported to mediate its centrosomal localization (Greer and Rubin, 2011), we tested whether Hhp1/2 KDEs influence SPB targeting. Further C-terminal truncations of Hhp1/2 were made such that only the predicted catalytic domains (Hhp1-(1-280)-GFP and Hhp2-(1-278)-GFP) were produced from endogenous loci (Figure 4-5A). While these Hhp1/2 truncation mutants were still SPB-targeted as evidenced by co-localization with Sid4-RFP (Figure 4-5B), functional tests of these more severely truncated enzymes revealed that neither was able to suppress the growth defect associated with loss of the other gene when expressed as the sole alleles at their respective genetic loci (Figure 4-5C) and they did not support mitotic checkpoint

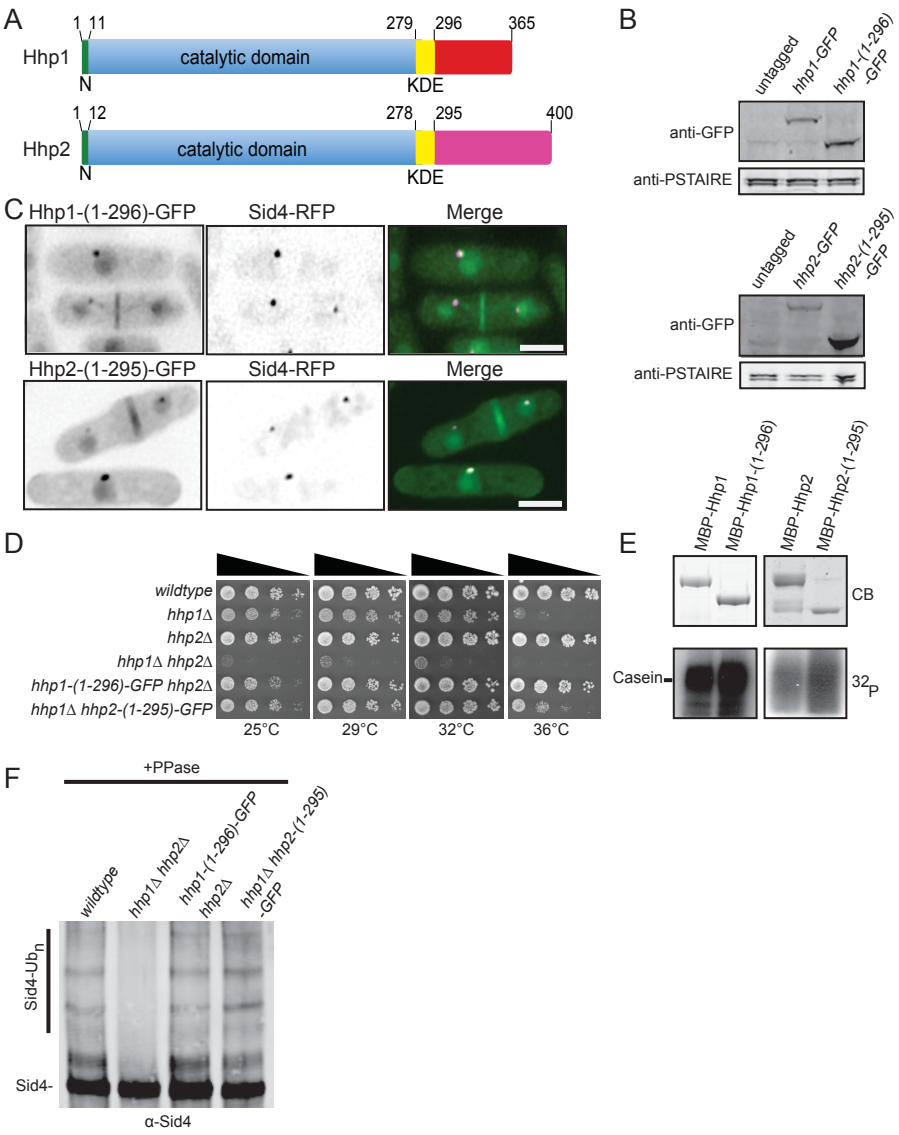

Figure 4-3. The C-termini of Hhp1/2 are dispensable for their functions. (A) Schematic diagrams of Hhp1/2 with relative positions of N-terminal extension (N), kinase domains (blue), kinase domain extensions (KDE) (yellow) and unrelated C-termini in red or purple indicated drawn to scale. (B) Anti-GFP western blots of whole-cell extracts prepared from untagged and the indicated GFP-tagged strains. Anti-PSTAIRE (Cdc2) immunoblots served as protein loading controls. (C) Live-cell imaging of endogenously tagged Hhp1-(1-296)-GFP and Hhp2-(1-295)-GFP with Sid4-RFP. Scale bars, 5 μm. (D) Serial 10-fold dilutions of the indicated strains were spotted on YE plates and incubated at the indicated temperatures. (E) *in vitro* kinase assays of recombinant MBP-Hhp1, MBP-Hhp1-(1-296), MBP-Hhp2 and MBP-Hhp2-(1-295), detected by Coomassie blue (CB) staining of SDS-PAGE gels, with casein. Phosphorylated casein was detected by autoradiography (^{32}P). (F) Sid4 from the indicated strains was immunoprecipitated from denatured cell lysates, treated with phosphatase, and visualized by immunoblotting.

signaling as assayed by Sid4 ubiquitination (Figure 4-5D). This loss of *in vivo* function is likely due to significantly reduced kinase activity (Figure 4-5E and F). We conclude that while the KDEs of Hhp1/2 are required for their full enzymatic function, SPB targeting information is contained within the Hhp1/2 kinase domains.

Hhp1/2 localize to SPBs independent of catalytic activity

It was previously reported that the kinase activity of CK1δ and of Hrr25 is necessary for their proper centrosomal and SPB localization, respectively (Milne et al., 2001; Peng et al., 2015a; Peng et al., 2015b). To determine if Hhp1/2 kinase activity impacts their SPB targeting, catalytically inactive mutants of each enzyme were generated (Hhp1-K40R and Hhp2-K41R), and their inactivity was verified *in vitro* (Figure 4-6A). When produced at the endogenous loci as sole gene copies tagged with mNG in cells, these mutants mimicked null alleles in growth and checkpoint assays (Figure 4-7A and B) although they were produced at wild-type levels as determined by immunoblotting (Figure 4-6B) and measuring whole cell fluorescence intensities (Figure 4-7C and D). Co-imaging of Sid4-RFP and Hhp1-(K40R)-mNG or Hhp2-(K41R)-mNG showed that both catalytically inactive mutants localized to SPBs (Figure 4-6C), indicating that Hhp1/2 kinase activity is not necessary for SPB localization.

Residues in the C-terminal lobe of the Hhp1 kinase domain are required for SPB localization

To identify which residues in the CK1 catalytic domain are responsible for SPB targeting, we performed a comparative analysis of Hhp1 and its paralog, Cki2. Cki2 does not localize to SPBs; Cki2 C-terminally tagged with GFP localized to vacuolar membranes (Figure 4-8A and B, top) as previously reported (Matsuyama et al., 2006).

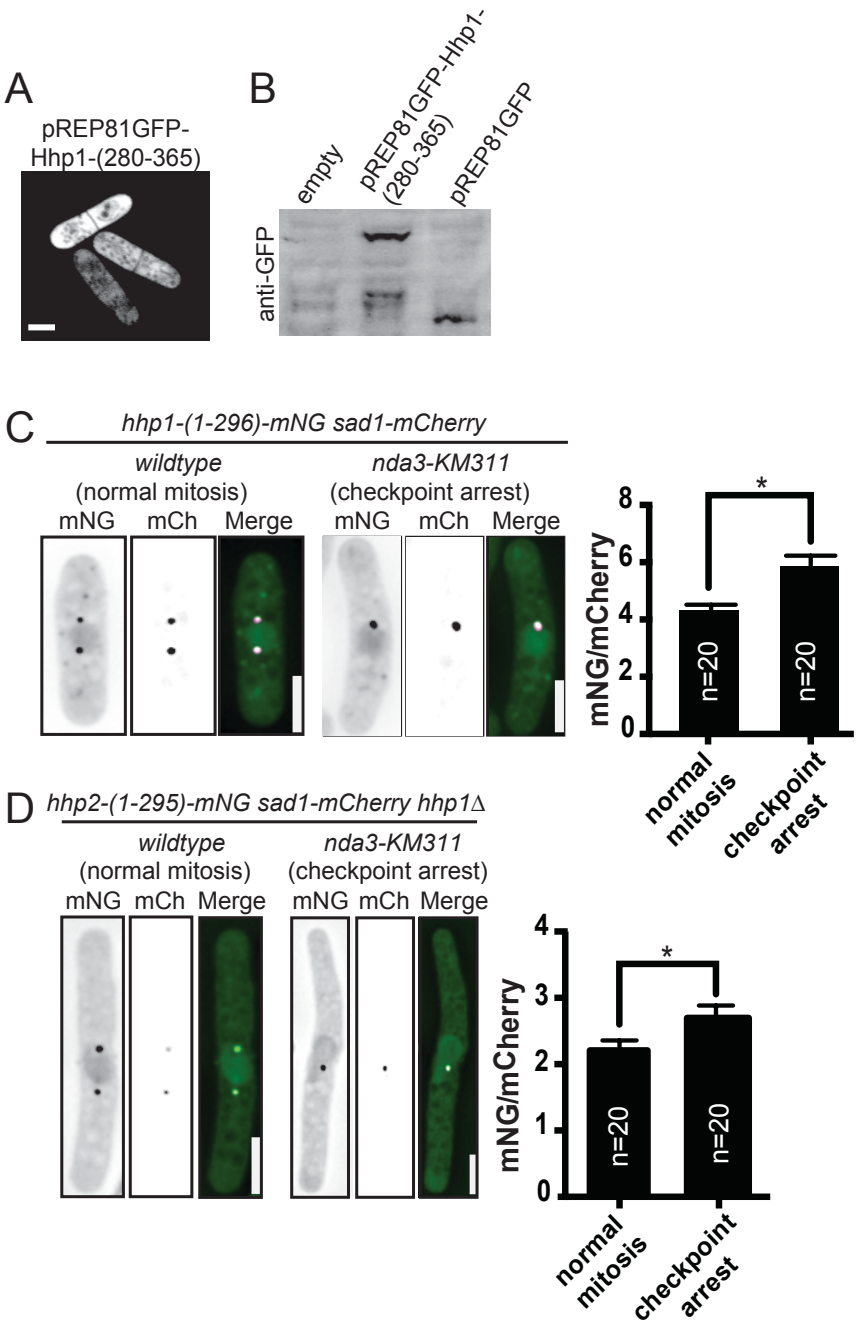

Figure 4-4. SPB targeting information of Hhp1/2 resides within the kinase domain
(A) Live cell imaging of wildtype cells expressing *pREP81-GFP-hhp1-(280-365)* grown in the absence of thiamine for 20 hours at 32°C. (B) Anti-GFP western blot of whole-cell extracts prepared from wildtype cells carrying *pREP81*, *pREP81-GFP*, and *pREP81-GFP-hhp1-(280-365)* grown in the absence of thiamine for 20 h at 32°C. (C and D) Representative images of the indicated strains. Inverted grayscale images are shown for mNG and mCherry (mCh). Quantitation of Hhp1-(1-296)-mNG and Hhp2-(1-295)-mNG at SPBs is shown on the right represented as mNG/Sad1-mCherry ratios. *p<0.001 determined using Students *t*-test. Error bars represent SEM. Scale bars, 5 μm.

Furthermore, a C-terminally tagged mutant of Cki2 lacking the predicted palmitoylation sites (Cki2-(1-429) (Sun et al., 2004) localized to the nucleus, cytoplasm, and division site, but it still did not localize to the SPB (Figure 4-8A and B bottom), indicating that Cki2 lacks SPB targeting information.

To detect differences between Cki2 and Hhp1/2, we generated structural models of the kinase domains of Hhp1, Hhp2, and Cki2 (Figure 4-9A and Figure 4-8C) using the Protein Homology/analogY Recognition Engine V 2.0 (Phyre^2) (Kelley et al., 2015). A comparison revealed 19 surface residues of Cki2 that differed in charge potential from analogous residues on Hhp1 (Figure 4-8C and D). To determine if any of these residues mediate SPB localization, the corresponding residues in Hhp1 were mutated to either mimic the Cki2 residue or reverse charge, and the resultant mutants were integrated at the *hhp1* endogenous locus and tagged at their C-termini with mNG. Of the 14 mutants tested, only Hhp1-(R261E)-mNG and Hhp1-(R272E K273E)-mNG failed to localize to SPBs (Figure 4-9B and Figure 4-8D). Hhp1-(R261E)-mNG and Hhp1-(R272E K273E)-mNG were still recruited to other subcellular locations including the nucleus and division site. Both mutant proteins were produced at similar levels to wildtype (Figure 4-9C). Interestingly, the mutants retained function as measured by their ability to support wildtype *S. pombe* growth and phosphorylate casein in *in vitro* kinase assays (Fig. 4-8E and F).

Interaction with Ppc89 mediates Hhp1/2 SPB localization

Though Sid4 is a SPB-localized Hhp1/2 target (Johnson et al., 2013), it is not known what protein(s) tether(s) Hhp1/2 to the SPB. Sid4 is not required for Hhp1 (Johnson et al., 2013) or Hhp2 (Figure 4-10A) localization; however, Hhp1/2 co-purifies

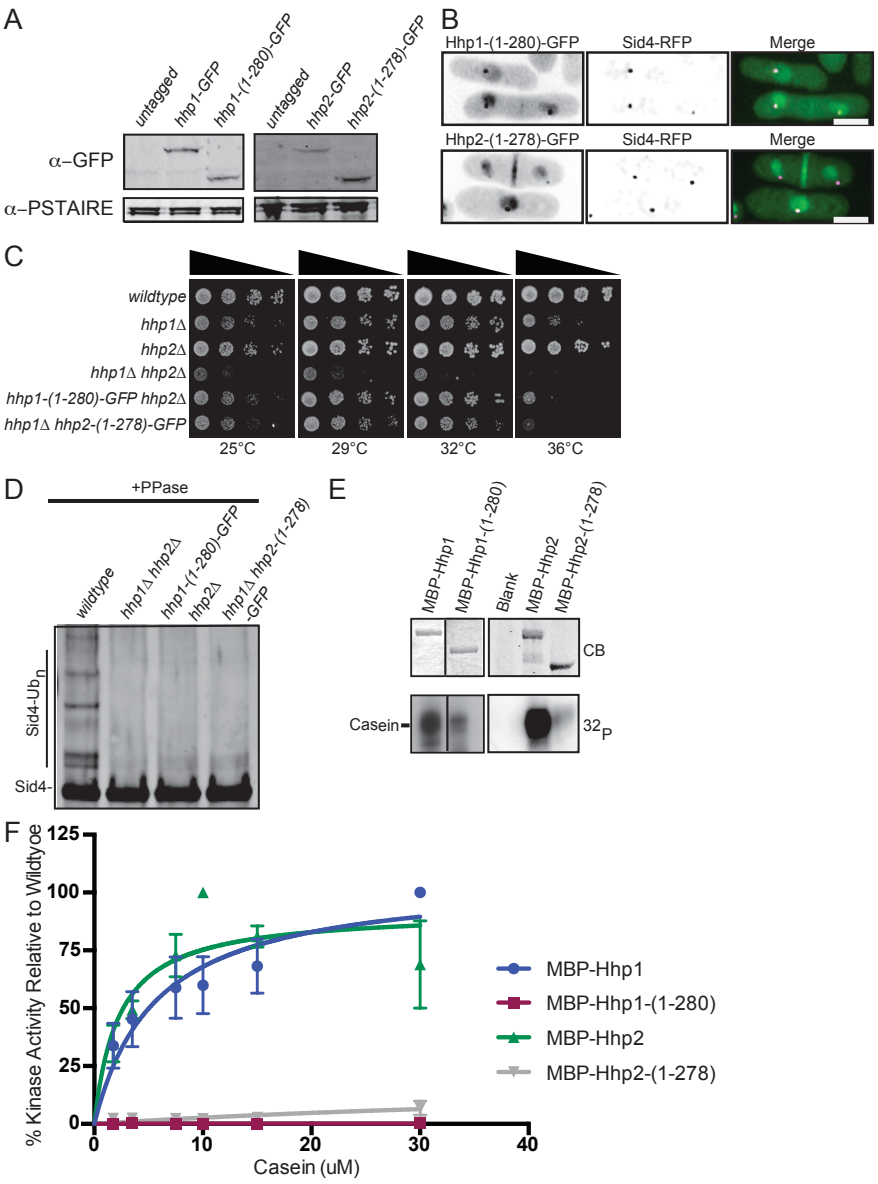

Figure 4-5. The KDE of Hhp1/2 is required for enzymatic function *in vivo* and *in vitro* (A) Anti-GFP western blot of whole-cell extracts prepared from untagged and the indicated GFP-tagged strains. Anti-PSTAIRE antibody served as loading control for lysates. (B) Live-cell imaging of endogenously tagged Hhp1-(1-280)-GFP, Hhp2-(1-278)-GFP with Sid4-RFP. Bars, 5 µm. (C) Serial 10-fold dilutions of the indicated strains were spotted on YE plates and incubated at the indicated temperatures. (D) Sid4 was immunoprecipitated from denatured cell lysates of the indicated strains, treated with phosphatase, and visualized by immunoblotting. (E) *In vitro* phosphorylation of casein by recombinant MBP-Hhp1-(1-280) and MBP-Hhp2-(1-278). Kinases were detected by CB staining of SDS-PAGE gels, and phosphorylated casein was detected by autoradiography (^{32}P). (F) Recombinantly purified full length Hhp1/2 and the indicated Hhp1/2 truncation mutants were dephosphorylated with λ-phosphatase and used in *in vitro* kinase assays with increasing levels of casein (0-60 µM). Phosphorylation of casein was quantified by Phophorimager.

with multiple SPB proteins, including a central component of the SPB, Ppc89, which also secures Sid4 at the SPB (Johnson et al., 2013; Rosenberg et al., 2006b). *ppc89* is required for Hhp1 (Johnson et al., 2013) and Hhp2 SPB localization (Figure 4-10B) and it interacts with *hhp1* (Vo et al., 2016) and *hhp2* in a yeast two-hybrid assay (Figure 4-11A-C). We further determined that it is the middle coiled-coil region of Ppc89 that supports two-hybrid interactions with *hhp1/2* (Figure 4-11A), a region distinct from the Sid4 binding site (Rosenberg et al., 2006b).

We next tested if the residues that were critical for Hhp1 SPB localization affected their interaction with Ppc89. We found that *hhp1-R261E* and *hhp1-R272E K273E* mutants did not interact with *ppc89* in the two-hybrid assay (Figure 4-11B and C). Thus, an interaction with Ppc89 may position Hhp1 proximal to its mitotic checkpoint substrate, Sid4.

Hhp1 SPB localization is required for checkpoint signaling

To test the hypothesis that CK1 must be present at SPBs to execute its checkpoint function, we examined the ability of Hhp1-R261E and Hhp1-R272E K273E to prevent septation when a mitotic checkpoint is imposed. Because either Hhp1 or Hhp2 can redundantly activate the Dma1-mediated mitotic checkpoint, we combined *hhp1-R261E* and *hhp1-R272E K273E* with an *hhp2*Δ mutant to analyze mitotic checkpoint function. We found that the tubulin mutant *nda3-KM311* and *nda3-KM311* with either the *hhp1* SPB localization mutant held a checkpoint arrest for 6-7 hours, whereas *nda3-KM311 hhp1-(R272E K273E) hhp2*Δ bypassed the arrest similar to cells lacking *dma1* (Figure 4-12A). Consistent with checkpoint failure, Sid4 ubiquitination was not detected in checkpoint-activated *hhp1-(R261E) hhp2*Δ and *hhp1-(R272E K273E) hhp2*Δ cells (Figure

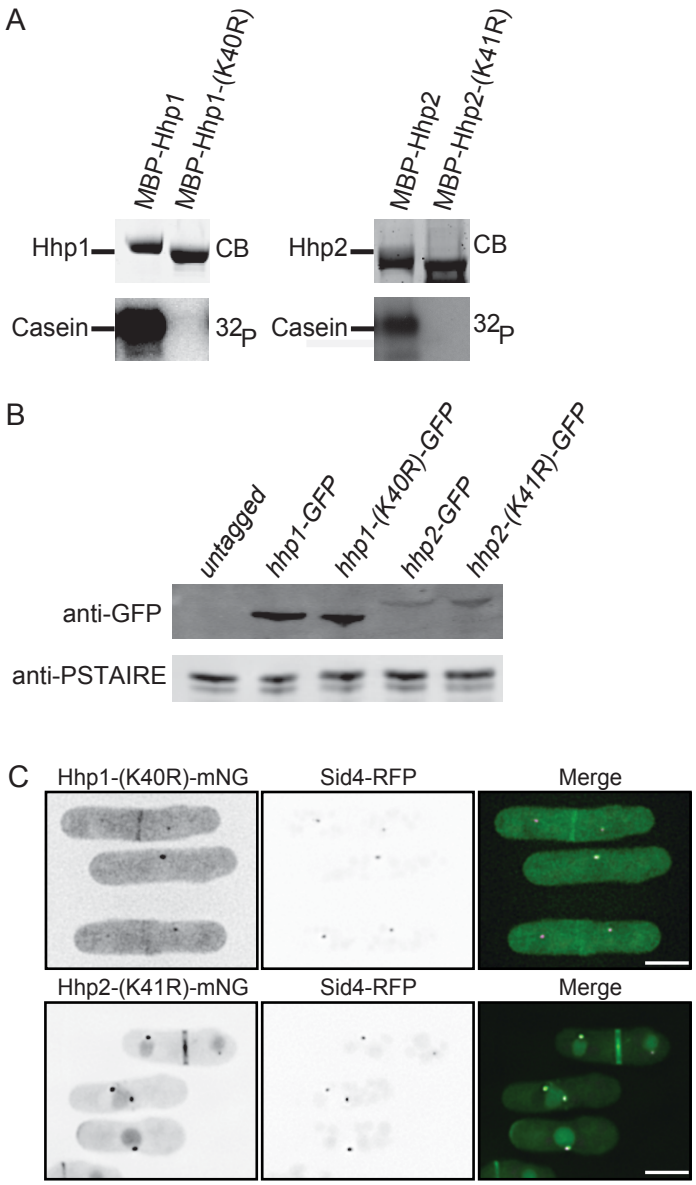

Figure 4-6. Kinase activity of Hhp1/2 is not required for SPB localization.
(A) *in vitro* kinase assays of recombinant MBP-Hhp1-(K40R) and MBP-Hhp2-(K41R) detected by CB staining of SDS-PAGE gels, with casein. Phosphorylated casein was detected by autoradiography. (B) Anti-GFP western blot of whole-cell extracts prepared from untagged and the indicated GFP-tagged strains. Anti-PSTAIRE antibody served as loading control for lysates. (C) Live-cell imaging of endogenously tagged Hhp1-(K40R)-mNG and Hhp2-(K41R)-mNG with Sid4-RFP. Scale bars, 5 um.

4-12B). Because of its ability to inhibit the SIN via Sid4 ubiquitination, overexpression of *dma1* is lethal (Guertin et al., 2002a). Consistent with the lack of Sid4 ubiquitination, *hhp1-(R261E) hhp2*Δ and *hhp1-(R272E K273E) hhp2*Δ mutants were refractory to *dma1*

overexpression-induced lethality (Figure 4-12C). Taken together, these data indicate that Hhp1/2 localization to SPBs is critical for their role in mitotic checkpoint signaling.

The kinase domains of CK1δ/ε dictate centrosomal localization

CK1δ/ε, the vertebrate orthologs of Hhp1/2, localize to the centrosome (Hutchins et al., 2010; Milne et al., 2001) (Rodrigo Guillen, data not shown). To determine if the intrinsic cues necessary for Hhp1/2 SPB localization are conserved in CK1δ/ε, we made C-terminal truncations of CK1δ/ε analogous to the truncations of Hhp1/2 that did or did not contain the KDE (Rodrigo Guillen, data not shown). These truncation mutants or wildtype versions of the proteins were then expressed in RPE- 1 cells as N-terminal eGFP fusions (Rodrigo Guillen, data not shown). In the majority of transfected cells, all three versions of the proteins co-localized with the centrosomal marker γ-tubulin although truncation of the KDE from either protein resulted in a lower percentage of centrosomal localization compared to wildtype or truncations including the KDEs (Rodrigo Guillen, data not shown). These data support the idea that as in Hhp1/2, the spindle pole targeting information is contained within the CK1δ/ε kinase domains and the KDE may impart stability to their association with centrosomes.

We next tested whether kinase activity was important for CK1δ/ε centrosomal localization. K38R mutations in both enzymes render them inactive (Gietzen and Virshup, 1999) (Rodrigo Guillen, data not shown). When these mutations were expressed in RPE-1 cells as eGFP fusions, both co-localized at centrosomes with γ-tubulin as well as wildtype (Rodrigo Guillen, data not shown) indicating that protein kinase activity is dispensable for their centrosomal targeting. Taken together, these data indicate that

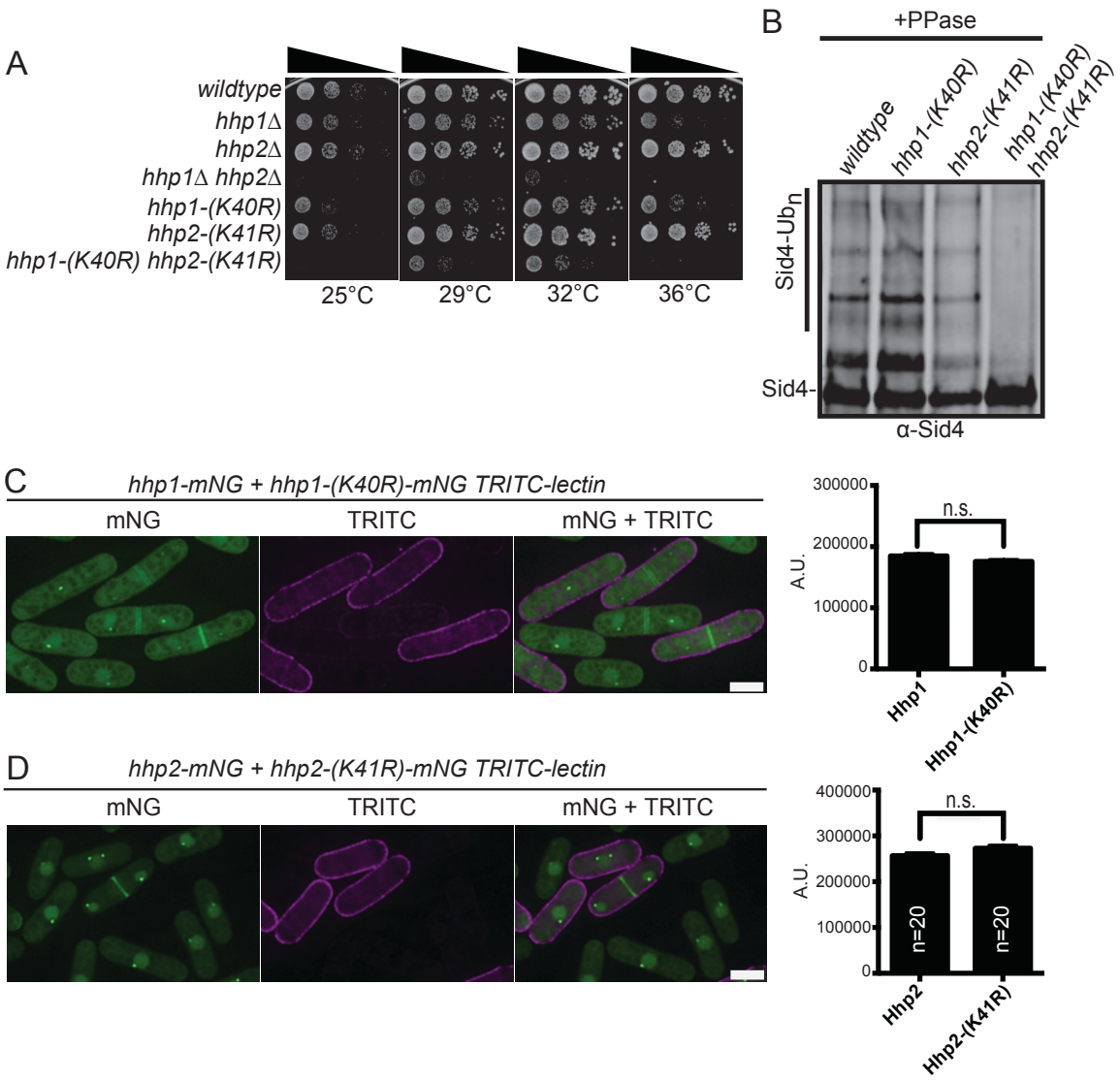

Figure 4-7. Hhp1/2 kinase-dead mutants localize to the SPB. (A) Growth assay of *hhp1-(K40R)*, *hhp2-(K41R)*, and *hhp1-(K40R) hhp2-(K41R)* mutants. Serial dilutions (10-fold) of the indicated single and double mutant strains were spotted on yeast extract plates and incubated at the indicated temperatures. (B) Sid4 from the indicated strains was immunoprecipitated from denatured cell lysates, treated with phosphatase, and visualized by immunoblotting. (C and D) *hhp1-(K40R)-mNG* (C) or *hhp2-(K41R)-mNG* (D) cells were labeled with tetramethylrhodamine isothiocyanate (TRITC)–lectin and mixed with *hhp1-mNG* (C) or *hhp2-mNG* (D) cells and imaged live. Representative images are shown in the left panels and quantitation of fluorescence intensities are shown on the right. A.U.=arbitrary units. Scale bar, 5 μm. p values determined using Student's *t*-test. ns=not significant. Error bars represent SEM.

soluble CK1 family members utilize their catalytic domains to associate with mitotic microtubule organizing centers (MTOC).

Discussion

The mechanisms governing CK1 enzyme targeting to specific intracellular locales are not well defined. To gain insight into how the *S. pombe* CK1 enzymes Hhp1/2 participate in mitotic checkpoint signaling, we defined residues at the base of the Hhp1/2 catalytic domains that support an interaction with a key SPB scaffold, Ppc89. This interaction is necessary for Hhp1/2 SPB association, Sid4 phosphorylation, and a mitotic checkpoint response, but not for other functions carried out by these enzymes that promote cell proliferation. Similar to our findings in yeast, human CK1δ/ε utilize their catalytic domains to mediate an interaction with the centrosome. Our findings reveal a conserved mechanism by which CK1 enzymes can be tailored to perform a specific function at a discreet subcellular location and time.

Hhp1/2 have overlapping subcellular localizations

Hhp1/2 have redundant roles in the Dma1-dependent mitotic checkpoint (Johnson et al., 2013), and deletion of either enzyme also renders cells sensitive to multiple types of DNA damaging agents (Bimbo et al., 2005; Chen et al., 2015; Dhillon and Hoekstra, 1994), observations that are congruent with these enzymes having similar functions. However, in addition to detecting Hhp1/2 in the nucleus, in accord with their known roles in DNA damage repair, and at SPBs and cell division site, we found that Hhp2 but not Hhp1 is present at cell tips. This observation raises the possibility that these enzymes could have, in addition to common functions, variable, specialized roles that remain to be determined.

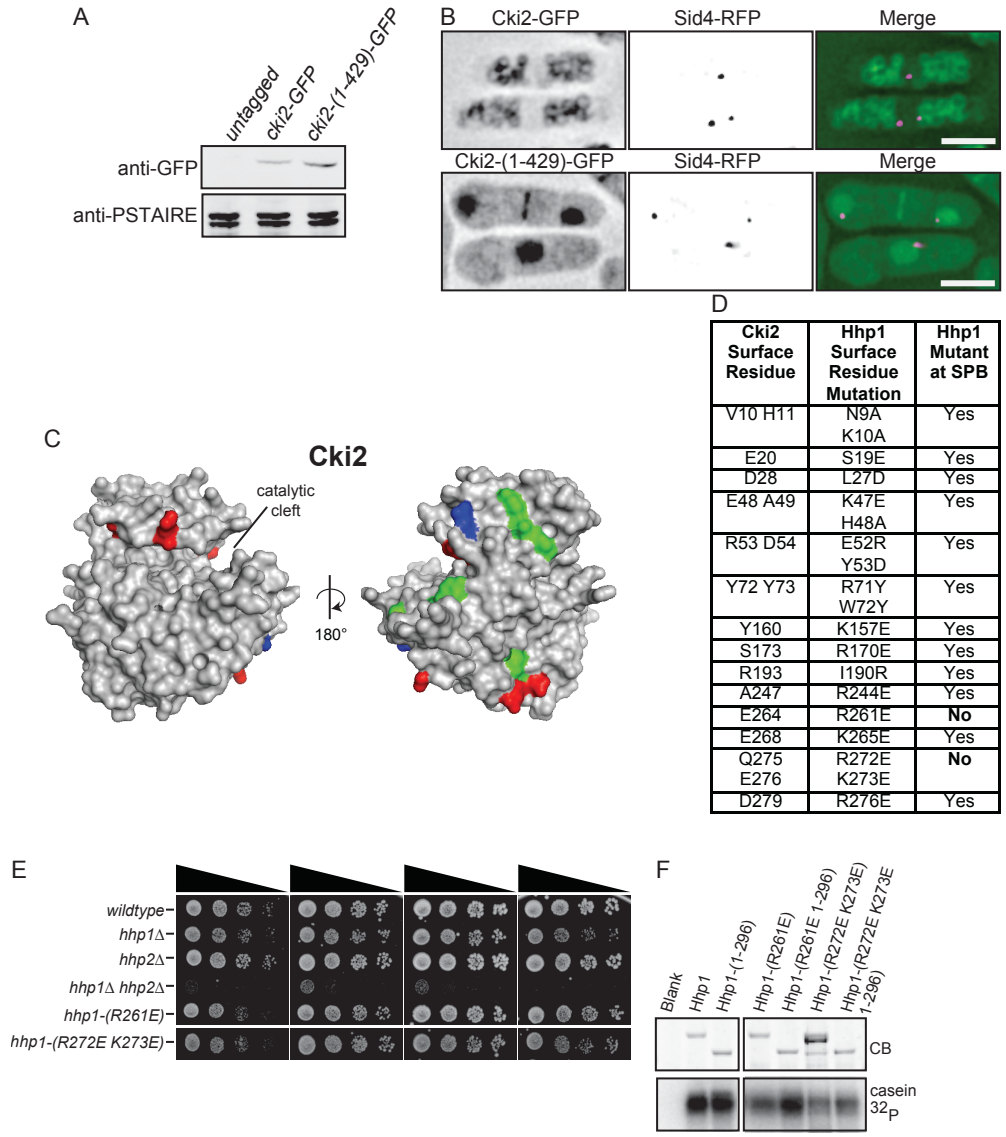

Cki2 Surface Residue	Hhp1 Surface Residue Mutation	Hhp1 Mutant at SPB
V10 H11	N9A K10A	Yes
E20	S19E	Yes
D28	L27D	Yes
E48 A49	K47E H48A	Yes
R53 D54	E52R Y53D	Yes
Y72 Y73	R71Y W72Y	Yes
Y160	K157E	Yes
S173	R170E	Yes
R193	I190R	Yes
A247	R244E	Yes
E264	R261E	**No**
E268	K265E	Yes
Q275 E276	R272E K273E	**No**
D279	R276E	Yes

Figure 4-8. Cki2 does not localize to the SPB. (A) Anti-GFP western blot of whole-cell extracts prepared from untagged and the indicated GFP-tagged strains. Anti-PSTAIRE antibody served as loading control for lysates. (B) Live-cell imaging of endogenously tagged Cki2-GFP and Cki2-(1-429)-GFP with Sid4-RFP. Scale bars, 5 um. (C) Homology model of Cki2 catalytic domain generated from Phyre[2] software and modeled with MacPymol. Surface residues with charge differences between Cki2 and Hhp1 are colored. Green=hydrophobic residues, Red=acidic residues, Blue=basic residues. (D) Table of Cki2 surface residues with the corresponding mutations made in Hhp1 and the effect of those mutations on SPB localization. (E) Growth assay of *hhp1-(R261E)* and *hhp1-(R272E K273E)* mutants. Serial 10-fold dilutions of the indicated single and double mutant strains were spotted on YE plates and incubated at the indicated temperatures. (F) *in vitro* kinase assays of recombinant MBP-Hhp1, MBP-Hhp1-(1-296), MBP-Hhp1-(R261E), MBP-Hhp1-(R261E 1-296), MBP-Hhp1-(R272E K273E) and MBP-Hhp1-(R272E K273E 1-296) detected by CB staining of SDS-PAGE gels, with casein. Phosphorylated casein was detected by autoradiography (^{32}P).

Kinase domains mediate spindle pole recruitment of Hhp1/2 and CK1δ/ε

Because neither *hhp1* nor *hhp2* are essential genes (the double deletion mutant can also be maintained, *e.g.* Figure 4-2B and D), we were able to clearly define the requirements for their SPB localization without the potentially confounding effects of overexpression and/or the presence of wildtype enzymes. By making gene replacement strains producing C-terminal truncations, the SPB targeting information of Hhp1/2 was pinpointed to within their kinase domains. In contrast, the non-catalytic C-terminus of *S. cerevisiae* Hrr25 was reported to be necessary for SPB localization (Peng et al., 2015b). This difference may be explained by a 'central domain' in the Hrr25 kinase that is not conserved in the *S. pombe* or mammalian CK1 enzymes and which has been found to confer functions specific to *Saccharomyces* species (Ye et al., 2016). Interestingly, we found that the cell tip localization of Hhp2 is also supported by its kinase domain. Because of the high degree of sequence similarity between the Hhp1/2 kinase domains (Dhillon and Hoekstra, 1994), it seems likely that a subtle difference in the enzymes' structures imparts this distinction in localization pattern.

In terms of requirements for CK1δ/ε centrosomal targeting, conflicting evidence has been previously reported. While one report indicated that the kinase domain of human CK1δ is necessary and sufficient for proper subcellular localization (Milne et al., 2001), another suggested that a C-terminal centrosomal localization sequence (equivalent to what we have termed the KDE) in mouse CK1δ was necessary and sufficient for centrosomal localization (Greer and Rubin, 2011). Here, we found that the catalytic domains of CK1δ/ε (lacking the KDEs) are sufficient for centrosome targeting, although constructs containing the KDEs are more stably localized.

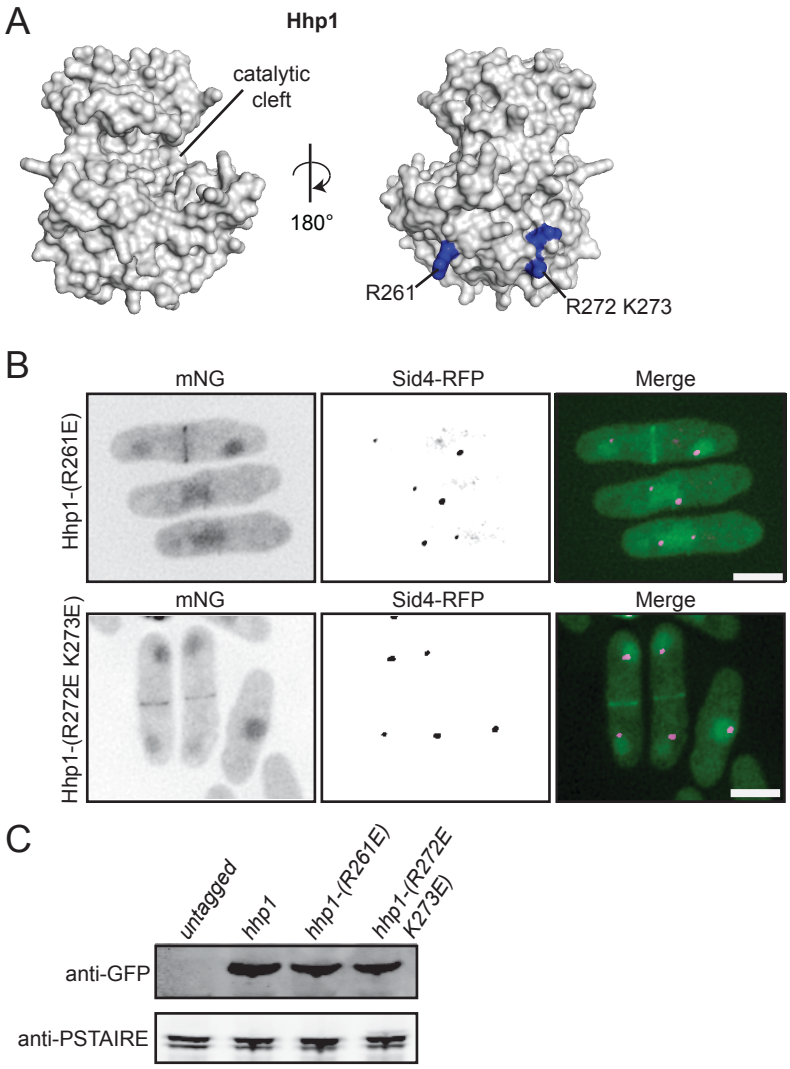

Figure 4-9. Residues at the base of the Hhp1 catalytic domain are critical for SPB localization. (A) Homology models of Hhp1 and Hhp2 catalytic domains generated from Phyre[2] software and modeled with MacPymol. Residues critical for Hhp1/2 SPB localization are in blue. (B) Live-cell imaging of endogenously tagged Hhp1-(R261E)-mNG and Hhp1-(R272E K273E)-mNG with Sid4-RFP. Scale bars, 5 µm. (C) Anti-GFP western blot of whole-cell extracts prepared from the indicated strains. Anti-PSTAIRE immunoblots served as protein loading controls.

In the course of characterizing the *hhp1/2* C-terminal truncation mutants, we found that removal of the C-terminal tails, but not the KDEs, led to increased catalytic activity towards an exogenous substrate *in vitro*. These findings agree with previous results demonstrating that phosphorylation of the C-terminal non-catalytic domain by

intramolecular auto-phosphorylation inhibits CK1 catalytic activity (Cegielska et al., 1998; Gietzen and Virshup, 1999; Graves and Roach, 1995; Longenecker et al., 1996; Longenecker et al., 1998). Interestingly, strains reliant on only *hhp1/2* C-terminal truncation mutants (*hhp1-(1-296)* and *hhp2-(1-295))* did not display any growth defects signifying that the auto-inhibition observed in vitro may not be important in vivo or that hypermorphic activity of Hhp1/2 is not detrimental to cells. Removal of the KDEs of Hhp1/2 however led to decreased function *in vitro* and *in vivo.* It is possible that KDEs interact with the C-terminal lobe of the kinase domain, as does the 'central domain' of Hrr25p (Ye et al., 2016) and such an interaction could influence the structure and function of Hhp1/2 and CK1δ/ε, thereby explaining both defects in localization and activity of mutants lacking KDEs.

Hhp1/2 and CK1δ/ε localize to spindle poles independently of kinase activity

We found that Hhp1/2 and CK1δ/ε do not require kinase activity for SPB or centrosomal localization. This differs from what has been reported for Hrr25 (Peng et al., 2015a; Peng et al., 2015b), and one report on CK1δ (Milne et al., 2001). However, our results agree with another report (Qi et al., 2015) indicating that CK1δ/ε kinase activity is dispensable for centrosomal targeting and suggest that Hhp1/2 and CK1δ/ε do not need to phosphoprime their tether. Instead, to accumulate at SPBs/centrosomes these enzymes may utilize scaffolds whose accessibility or abundance is modulated.

Notably, only one scaffolding protein, AKAP450, has been implicated in mediating CK1 localization and in this case to centrosomes (Sillibourne et al., 2002). In other signaling pathways scaffolds are essential organizing platforms that recruit a kinase and its substrate to the same intracellular location. For example, mitogen-activated

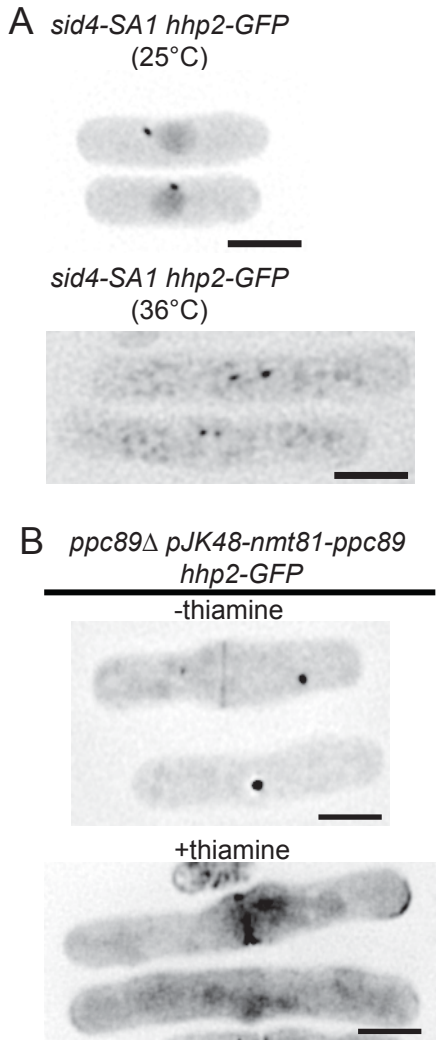

Figure 4-10. Hhp2 requires Ppc89 to localize to the SPB. (A) Localization of Hhp2-GFP in a *sid4-SA1* temperature sensitive strain at the permissive (25°C) and restrictive (36°C) temperatures. (B) Localization of Hhp2-GFP in a *ppc89* shut-off strain (-thiamine, ppc89 expression on; +thiamine, ppc89 expression off). Scale bars, 5 µm.

protein kinase cascades and protein kinase A pathways depend on scaffolding proteins to maintain kinase specificity (Schwartz and Madhani, 2004). In the context of Hhp1/2, interaction with Ppc89 may (i) provide an additional level of specificity by localizing Hhp1/2 and its substrate Sid4 to the appropriate site of action, (ii) contribute to signal amplification by concentrating Hhp1/2 and Sid4, and/or (iii) allow for coordination of the Hhp1/2-Dma1-dependent mitotic checkpoint with other signaling pathways that are

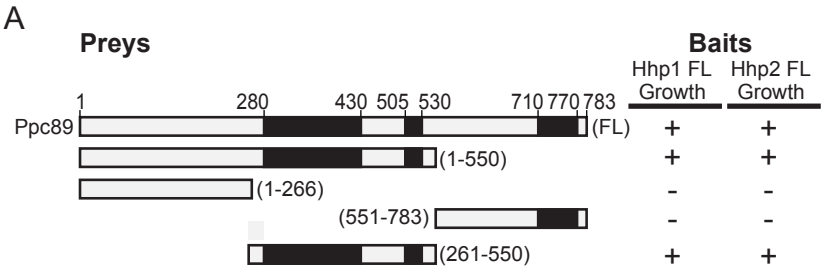

B

Bait	Prey	Growth
vector	*vector*	-
vector	*ppc89*	-
hhp1	*vector*	-
hhp2	*vector*	-
hhp1	*ppc89*	+
hhp2	*ppc89*	+
hhp1-(R261E)	*vector*	-
hhp1-(R261E)	*ppc89*	-
hhp1-(R272E K273E)	*vector*	-
hhp1-(R272E K273E)	*ppc89*	-

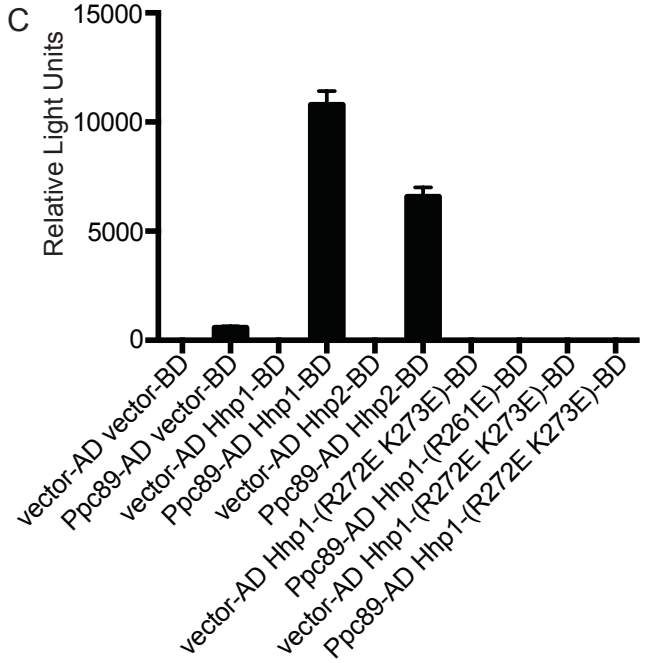

Figure 4-11. Basic residues within the kinase domain of Hhp1/2 are critical for interaction with the SPB protein Ppc89. (A,B) *S. cerevisiae* strain PJ69-4A was co-transformed with plasmids expressing the indicated regions of *hhp1/2* and *ppc89*. Black boxes indicate regions of predicted coiled-coil. In B, only full-length hhp1/2 genes were tested for interaction. Transformants were scored for growth on –Trp –Leu −His plates supplemented with 5mM 3-AT. Pluses indicate strong growth and minuses indicate no growth. (C) Bar graph shows β-galactosidase activity of the indicated bait and prey plasmids tested for growth in (B) (represented in relative light units). Each assay was performed in triplicate. ****$p<0.001$ determined using ANOVA. ns=not significant. Error bars represent SEM.

centered at the SPB. Given their involvement in multiple cellular processes and potentially constitutive activity, an additional utility of binding the scaffold Pcp89 may be to compartmentalize a subset of Hhp1/2 from a wider cellular population to direct CK1 enzymes to a specialized signaling complex.

Defining the CK1 SPB-binding interface

Our results, along with previous work, indicate that CK1 catalytic domains moonlight as protein interaction domains for kinase localization. Hhp1/2 require conserved basic residues on their C-terminal lobe to interact with the SPB. Hhp2's SPB docking interface is also needed by the kinase to localize to other subcellular localizations including the nucleus and cell tips.

In only one prior case have residues in the catalytic domain of CK1 enzymes been implicated in docking interactions. Specifically, residues in the N-terminal lobe of the Hrr25p catalytic domain, together with its central domain, bind the monopolin subunit Mam1 and promote phosphorylation of Dsn1 (Petronczki et al., 2006; Ye et al., 2016). Our findings therefore represent an important advance for the understanding of CK1 kinase domain-mediated subcellular targeting. Though new for CK1, there are several examples of other broadly acting protein kinase catalytic domains associating with scaffolds. As one example, the MAPK Fus3 is recruited and also allosterically regulated by the scaffold protein Ste5 (Bhattacharyya et al., 2006; Choi et al., 1994). Thus, Ppc89 may not only scaffold Hhp1/2 at the SPB, but also modulate its catalytic activity.

Our work demonstrates that CK1 interaction with SPBs is essential for mitotic checkpoint function in *S. pombe*. Similarly, CK1δ centrosomal localization has been reported to be required for Wnt-3a dependent neuritogenesis and proper ciliogenesis

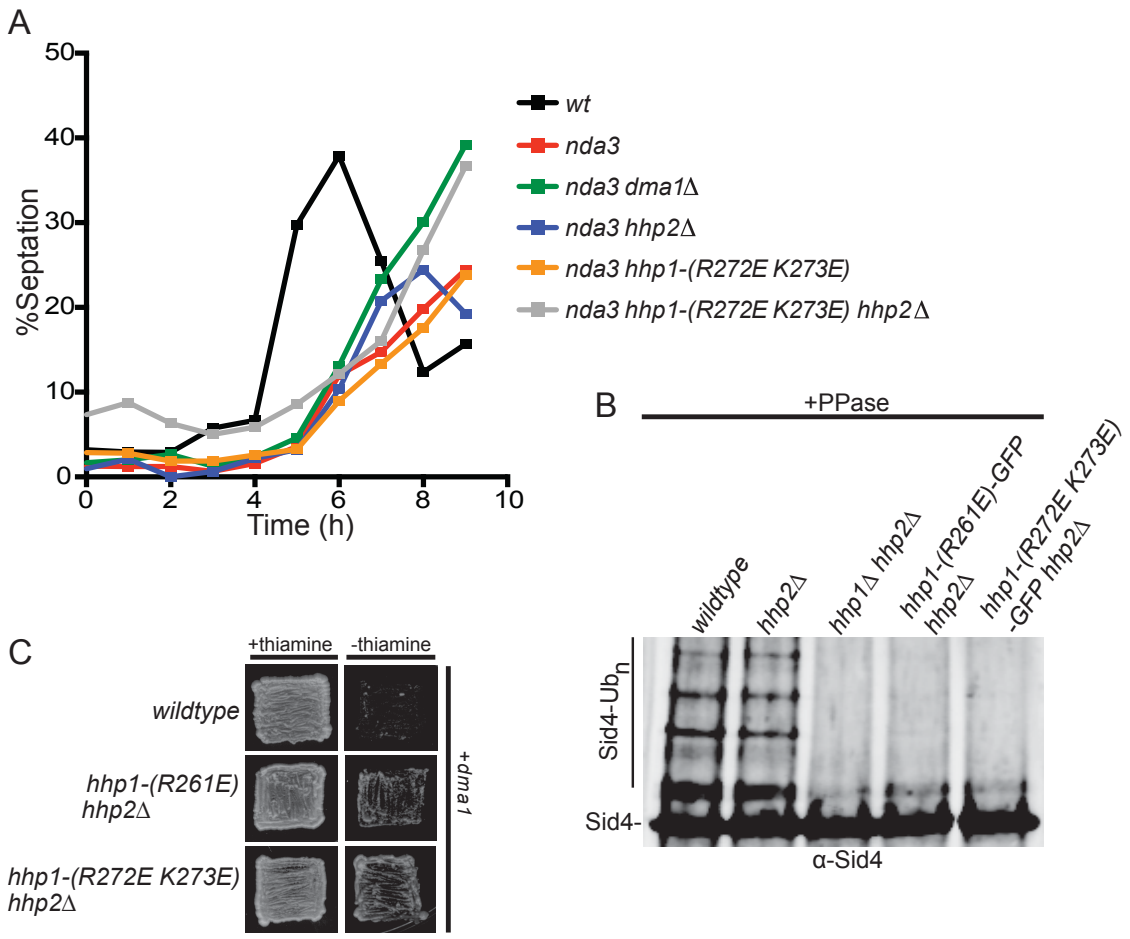

Figure 4-12. Hhp1 SPB localization is required for mitotic checkpoint function. (A) The indicated strains were synchronized in S-phase with hydroxyurea, shifted to 19°C to activate the spindle checkpoint, and septation indices were measured periodically for 9 hours. (B) Sid4 from the indicated strains was immunoprecipitated from denatured cell lysates, treated with phosphatase, and visualized by immunoblotting. (C) Over-expression of *dma1* from the *nmt41* promoter in wildtype, *hhp1-(R261E) hhp2*Δ *or hhp1-(R272E K273E) hhp2*Δ mutant cells. Growth of the transformants was observed on agar plates in the presence (repression) or absence (de-repression) of thiamine.

(Greer and Rubin, 2011; Greer et al., 2014), thus specific subcellular localization of CK1 enzymes is essential for mediating proper cellular signaling. Future work on the role of these enzymes at the SPB/centrosome is expected to reveal additional functions that are coordinated from this important cellular signaling nexus.

CHAPTER V

CONCLUSIONS AND FUTURE DIRECTIONS

Mitotic checkpoints ensure that the genome is accurately distributed when cells divide. To properly coordinate the division process, cells utilize multiple types of post-translational modifications to fine-tune the signaling that controls genomic duplication and segregation. In this work, I investigate the role of two post-translational modifications, ubiquitination and phosphorylation, and how they control mitotic progression in *S.* pombe.

In Chapter II, I presented work where I identified a DUB that antagonizes the APC/C. I found that the SAGA complex DUB, Ubp8, inhibits APC/C utilizing a mechanism independent of the SAC. The ability of Ubp8 to antagonize APC/C function depends on its catalytic activity and is specific to the DUB module of the SAGA complex. Furthermore, I discovered that Ubp8 impedes APC/C function through the deubiquitination of histone H2B. In mammalian cells, the DUB USP44 reverses APC/C mediated ubiquitination of the APC/C activator Cdc20 to maintain the SAC (Stegmeier et al., 2007). Though it is plausible that reversal of APC/C ubiquitination is a conserved mechanism, there is no known USP44 homolog in non-mammals. Therefore, our work uncovers a novel mechanism of APC/C inhibition by a DUB through the modification of chromatin signatures.

In Chapter III, I reveal the results of an overexpression screen for identifying DUBs that inhibit Dma1 function in *S. pombe*. Our screen revealed 4 DUBs (Ubp1, Ubp2, Ubp7, and Ubp14) that suppressed Dma1-induced cell death. The results of this

screen were used to inform the creation of a fusion protein, Ppc89-Ubp7, that inhibits Sid4 ubiquitination by Dma1. This work was the first to implicate DUBs in the regulation of the Dma1-mediated mitotic checkpoint and provides clues into possible mechanisms of mitotic checkpoint silencing.

In Chapter IV, I presented data demonstrating how the CK1 enzymes, Hhp1/2, target to SPBs using localization cues present within their respective kinase domains. We extended this analysis to the human CK1δ/ε enzymes and found their catalytic domains are also sufficient for centrosome targeting indicating conservation of this localization mechanism from yeast to human. We also clarified that the catalytic activities of Hhp1/2 and CK1δ/ε are dispensable for directing them to SPBs or centrosomes, respectively, resolving conflicting reports in the literature. We next defined basic residues at the base of the Hhp1/2 catalytic domains, far from their catalytic centers, that support an interaction with a key SPB protein, Ppc89. This interaction is necessary for Hhp1/2 SPB association, Sid4 phosphorylation and ubiquitination, and the checkpoint delay of cytokinesis, but not for other functions carried out by these enzymes that promote cell proliferation. This is the first evidence of specific docking residues within the catalytic domains of CK1 enzymes that can direct them to a particular subcellular localization to control substrate phosphorylation and downstream signaling. Collectively, these studies reveal a conserved mechanism by which CK1 enzymes can be tailored to perform a specific function at a discreet subcellular location and time.

Collectively, this work has identified new roles for DUBs in regulating cell division and has defined the molecular requirements necessary to direct a master kinase to a discreet subcellular location to enact a mitotic checkpoint. Looking forward, I view

identifying the molecular signal that cues CK1 to activate the mitotic checkpoint as the most pressing task to understand how the Dma1-mediated pathway is controlled. However, there are multiple problems that need to be addressed in order to gain a full understanding of the role of CK1 in cell division and I address some of these problems below.

Phosphoregulation of CK1

While Hhp1/2 are critically important for various biological processes, research has emphasized their effect on substrates rather than what controls their kinase activity and how they are integrated into signaling networks. Utilizing previous data from a former graduate student (Alyssa Johnson) and striking up a collaboration with a new post-doc (Sierra Culatti), I began investigating the role of autophosphorylation in regulating CK1 activity. Previous work demonstrated that CK1 family members have divergent C-terminal non-catalytic domains that are thought to dictate intracellular localization and govern catalytic activity. In particular, autophosporylation by CK1 on its C-terminus inhibits catalytic activity (Babu et al., 2002; Cegielska et al., 1998; Dahlberg et al., 2009; Gietzen and Virshup, 1999; Graves and Roach, 1995; Greer and Rubin, 2011; Ianes et al., 2015; Longenecker et al., 1996; Longenecker et al., 1998; Meng et al., 2016). We have identified many phosphorylation sites on Hhp1 and Hhp2 via MS and have confirmed most of these sites biochemically (Figure 5-1). Most of the autophosphorylation sites are within their respective C-terminal tails but some autophosphorylation sites were found within their catalytic domains and are conserved among the CK1δ/ε subfamily (Figure 5-1). To investigate the role of CK1 autophosphorylation, phosphomutants of both *hhp1* and *hhp2* are being generated and

analyzed for their catalytic activity *in vitro* and function *in vivo*. Experiments exploring *in vivo* function include examining their protein abundance, localization, and their ability to promote Sid4 ubiqutination. Understanding the mechanism(s) of autophosphorylation and the role this plays in modulating CK1 activity will give us a better understanding of how signaling events emanating from a mitotic defect leads to altered behavior of Hhp1/2.

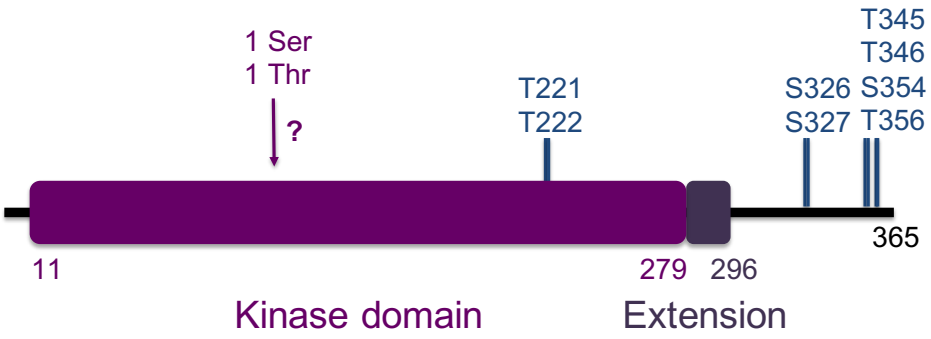

Figure 5-1. Summary of autophosphorylation sites in Hhp1
Schematic representation of the mapped autophosphorylation sites in Hhp1. Most sites are contained within the C-terminus with a still to be determined serine/threonine site left to be mapped in the kinase domain.

Identification of CK1 mitotic substrates

To date, only one CK1 mitotic substrate has been identified (Johnson et al., 2013). To identify more CK1 mitotic substrates and develop a clearer picture of the CK1 phosphoproteome, we developed and optimized a quantitative iTRAQ-based phosphoproteomics scheme. To inhibit CK1 activity, we created analog-sensitive (as) alleles of *hhp1* and *hhp2*. These alleles are inhibited by the ATP-analog 1NM-PP1 as demonstrated by reduced growth and inhibition of Sid4 phosphorylation and ubiquitination (Figure 5-2).

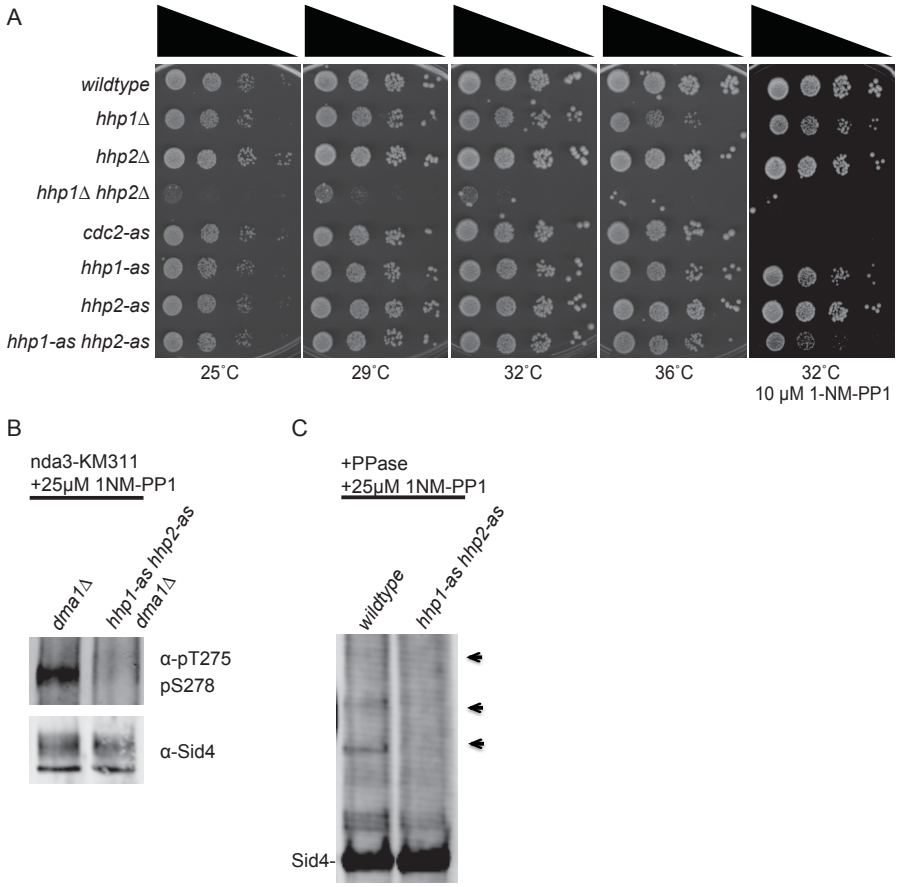

Figure 5-2. Development of *hhp1* and *hhp2* analog-sensitive alleles. (A) Serial 10-fold dilutions of the indicated strains were spotted on YE plates containing or lacking inhibitors and incubated at the indicated temperatures for 3 days. (B) Indicated strains were subjected to prometaphase arrest and treated with the ATP analogue 1NM-PP1. Sid4 was immunoprecipitated under denatured conditions with a Sid4 antibody and detected via immunoblot using a phospho-T275, S278 or Sid4 antibody. (C) Sid4 was immunoprecipitated from denatured cell lysates of the indicated strains, treated with phosphatase, and visualized by immunoblotting. Arrows indicate ubiquitinated forms of Sid4.

Specifically, we compared the phosphoproteomes of cells that were arrested in prometaphase with an active spindle checkpoint (triggered by the beta tubulin cold sensitive *nda3-KM11* allele) and contained either wildtype CK1 (*nda3-KM311*) or inhibitable CK1 (*hhp1-as hhp2-as nda3-KM311*). Both strains were treated with 10 μM of the analog for 30 minutes to selectively inhibit CK1 activity in the analog sensitive strain. Protein lysates were prepared and quantified prior to acetone precipitation

followed by tryptic digestion. Peptides from each sample were mixed together and subjected to phosphoenrichment using TiO2 beads, labeled with iTRAQ reagents, and analyzed by high resolution 2D-LC-MS/MS. Our preliminary analysis utilizing a previous mutant (*hhp1-as hhp2*Δ) (Cipak et al., 2011; Gregan et al., 2007) identified 39 proteins as potential Hhp1/2 substrates (more than 2 fold higher in kinase active strain). Several potential substrates from this analysis are of significant interest to us because they are involved in cytokinesis, spindle dynamics, or mitotic control and contain phosphosites consistent with CK1 preference for acidic motifs. Of special interest is the cytokinetic FBAR protein Imp2 which appears to be a CK1 and Cdk1 substrate. We are currently characterizing *imp2* phosphomutants to gain a deeper understanding of the role of CK1 in regulating mitosis and cytokinesis.

We are also exploring the mitotic role of CK1δ/ε in mammalian systems. We are currently investigating the mitotic substrates of CK1δ/ε using an approach similar to that described above for yeast Hhp1/2. To identify CK1δ/ε mitotic substrates, hTERT-RPE1 cells were blocked in mitosis using spindle poisons and subsequently treated with CK1δ/ε inhibitors (SR-2890 and SR-3029) (Bibian et al., 2013) or a vehicle control (DMSO). We also used older inhibitors that have some, but different, off-target effects (e.g. IC261 and D4476) (reviewed in (Schittek and Sinnberg, 2014)). Protein lysates were prepared and quantified prior to acetone precipitation followed by tryptic digestion. Peptides from each sample were labeled with iTRAQ reagents, mixed together and subjected to phosphoenrichment using TiO2 beads and then analyzed by high resolution 2D-LC-MS/MS. These experiments in mammalian cells have led to the discovery of multiple novel CK1δ/ε mitotic substrates that are currently being confirmed biochemically.

Conclusions

In this work, I have identified multiple new roles of DUBs in regulating cell division. First I show that the DUB Ubp8 inhibits the APC/C by deubiquitinating histone H2B. This is the first example of a post-translational chromatin mark regulating APC/C activity. I have also identified multiple DUBs that antagonize the activity of the mitotic checkpoint protein Dma1. Lastly, I have revealed a conserved mechanism of how the CK1 family of kinases are targeted to the major microtubule-organizing center of the cell, the SPB/centrosome, and how this targeting is critical for mitotic checkpoint function in *S. pombe*. Collectively, these studies have defined new roles and new modes of regulation of enzymes involved in post-translational control of cell division.

As previously mentioned, Hhp1/2 are orthologs of the mammalian kinases CK1δ/ε (Dhillon and Hoekstra, 1994; Hoekstra et al., 1994). While a clear Ppc89 homolog has not yet been identified in metazoans, the cues utilized by CK1δ/ε to target to the centrosome appear to be conserved. Thus, the mechanism that we have defined for Hhp1/2 recruitment to the SPB will likely inform us of the interaction between CK1δ/ε and its centrosomal scaffold. Future work solving a co-crystal structure between the kinase domain of Hhp1/2 and the scaffold Ppc89 will be critical in understanding how this interaction positions Hhp1/2 for substrate access. It is possible that Ppc89 not only regulates Hhp1/2 SPB localization but may also regulate Hhp1/2 kinase activity through allosteric mechanisms or through recruitment of a phosphatase. Therefore, further work investigating the interaction between CK1 and its MTOC scaffold will be important in gaining a full understanding of how CK1 activates the Dma1-mediated mitotic checkpoint.

Taken together, our work demonstrates that important mitotic kinases can be targeted to a specific subcellular localization to activate a signaling event strictly through interactions mediated by their kinase domains. This work could inform future drug design studies that inhibit kinase mediated signaling by disrupting interactions between kinases and their respective scaffolds.

Appendix

MATERIALS AND METHODS

Yeast strains, media, and genetic methods

S. pombe strains used in this study (Supporting Information, Table S1) were grown in yeast extract (YE) media (Moreno et al., 1991). Crosses were performed in glutamate medium (Moreno et al., 1991) and strains were constructed by tetrad analysis. *hhp1*, *hhp1-K40R*, *hhp1-R261E*, *hhp1-R272E K273E*, *hhp2*, and *cki2* were tagged endogenously at the 3′ end of their open reading frames (ORFs) with *GFP:kan*^{R} or *mNeonGreen:kan*^{R} (mNG) using pFA6 cassettes as previously described(Bahler et al., 1998). G418 (100 mg/mL; Sigma-Aldrich, St. Louis, MO) in YE media was used for selecting *kan*^{R} cells. mNG, a recently reported GFP derived from the lancelet *Branchiostoma lanceolatum*, was chosen for imaging experiments because of its superior brightness (Shaner et al., 2013; Willet et al., 2015). A lithium acetate transformation method (Keeney and Boeke, 1994) was used for introducing sequences encoding tags, and integration of tags was verified using whole-cell PCR and/or microscopy. Tagged *hhp1/2* alleles were fully functional as determined by growth assays and their ability to support Sid4 ubiquitination (Figure 4-3D and 4-3F and Figure 4-5C and D). Introduction of tagged loci into other genetic backgrounds was accomplished using standard *S. pombe* mating, sporulation, and tetrad dissection techniques. Fusion proteins were expressed from their native promoters at their normal chromosomal locus unless otherwise indicated. For *hhp1* and *hhp2* gene replacements, haploid *hhp1::ura4+* and *hhp2::ura4+* strains were transformed with linear *hhp1* and *hhp2* mutant gene fragments (digested with

BamHI and PstI from pIRT2-*hhp1* and pIRT2-*hhp2* plasmids) using standard lithium acetate transformations. Integrants were selected based on resistance to 1.5 mg/ml 5-fluoroorotic acid (Fisher Scientific) and validated by colony PCR using primers homologous to endogenous sequences that flank the genomic clone within pIRT2 in combination with those within the ORF. All constructs and integrants were sequenced to ensure their accuracy.

ubp8 was tagged at the 3' end of its endogenous open reading frame with sequences encoding the TAP tag (Tasto et al., 2001) by a PCR-mediated strategy (Bahler et al., 1998) using a lithium acetate–based transformation procedure (Keeney and Boeke, 1994). Proper integration of the epitope cassette was confirmed by whole cell PCR.

For serial dilution growth assays, cells were cultured in liquid YE at 25°C, three serial 10-fold dilutions starting at 4×10^6 cells/mL were made, 4 μL of each dilution was spotted on YE plates, and cells were grown at the indicated temperatures for 3-4 d. The GFP-Hhp1 (amino acids 280–365) fragment was placed under the control of the *nmt81* promoter in pREP81 vector. This construct and a construct with GFP alone were expressed in a wild-type strain. Cells were grown in media containing thiamine and then washed into media without thiamine to induce protein production, then grown for 22 hours at 32°C before imaging.

Molecular biology methods

All plasmids were generated by standard molecular biology techniques. *hhp1* and *hhp2* genes including 500 bp upstream and downstream of the ORFs were amplified by PCR and ligated into a PCR-Blunt vector (Life Technologies) and then subcloned into a

pIRT2 vector (Hindley et al., 1987). *hhp1* and *hhp2* mutants were created by mutagenizing pIRT2-plasmids containing *hhp1*$^{+}$ and *hhp2*$^{+}$ using a QuikChange site-directed mutagenesis kit (Agilent Technologies). Plasmids were validated by DNA sequencing. The ORF of CK1δ was amplified by PCR from a plasmid (CK1δ pGEX-6p-2) kindly provided by Dr. Fanni Gergely. V405 4HA-CK1ε, a gift from David Virshup (Duke University Medical School) (Addgene plasmid #13724), was used as a template for PCR amplification of the CK1ε ORF. Each PCR product was cloned into pEGFP-C1 and the correct sequence validated by DNA sequencing. Mutant CK1δ/ε variants were made using the QuikChange site-directed mutagenesis kit (Agilent Technologies) and confirmed by DNA sequencing.

The *ubp8* gene including 500 bp upstream and downstream of the open reading frame was amplified by PCR and ligated into a PCR-Blunt vector (Life Technologies) and then subcloned into a pIRT2 vector (Hindley et al., 1987). *ubp8-C154S H387A* was created by mutagenizing a pIRT2-plasmid containing *ubp8*$^{+}$ using a QuickChange® site-directed mutagenesis kit (Agilent Technologies). For *ubp8* gene replacements, a haploid *ubp8*::*ura4*$^{+}$ strain was transformed with a linear *ubp8* gene fragment (digested from pIRT2- *ubp8-C154S H387A* plasmid) using standard lithium acetate transformations. Integrants were selected based on resistance to 5'FOA and validated by colony PCR using primers homologous to endogenous sequences that flank the genomic clone within pIRT2 in combination with those within the ORF. All constructs were sequenced to ensure their accuracy

S. pombe strains used in this study were grown in yeast extract (YE) media (Moreno et al., 1991). Crosses were performed in glutamate medium (Moreno et al.,

1991) and strains were constructed by tetrad analysis. *hhp1*, *hhp1-K40R*, *hhp1-R261E*, *hhp1-R272E K273E*, *hhp2*, and *cki2* were tagged endogenously at the 3′ end of their open reading frames (ORFs) with *GFP:kan*^{R} or *mNeonGreen:kan*^{R} (mNG) using pFA6 cassettes as previously described(Bahler et al., 1998). G418 (100 mg/mL; Sigma-Aldrich, St. Louis, MO) in YE media was used for selecting *kan*^{R} cells. mNG, a recently reported GFP derived from the lancelet *Branchiostoma lanceolatum*, was chosen for imaging experiments because of its superior brightness (Shaner et al., 2013; Willet et al., 2015). A lithium acetate transformation method (Keeney and Boeke, 1994) was used for introducing sequences encoding tags, and integration of tags was verified using whole-cell PCR and/or microscopy. Tagged *hhp1/2* alleles were fully functional as determined by growth assays and their ability to support Sid4 ubiquitination (Figure 4-3D and F and Figure 4-5C and D). Introduction of tagged loci into other genetic backgrounds was accomplished using standard *S. pombe* mating, sporulation, and tetrad dissection techniques. Fusion proteins were expressed from their native promoters at their normal chromosomal locus unless otherwise indicated. For *hhp1* and *hhp2* gene replacements, haploid *hhp1::ura4+* and *hhp2::ura4+* strains were transformed with linear *hhp1* and *hhp2* mutant gene fragments (digested with BamHI and PstI from pIRT2-*hhp1* and pIRT2-*hhp2* plasmids) using standard lithium acetate transformations. Integrants were selected based on resistance to 1.5 mg/ml 5-fluoroorotic acid (Fisher Scientific) and validated by colony PCR using primers homologous to endogenous sequences that flank the genomic clone within pIRT2 in combination with those within the ORF. All constructs and integrants were sequenced to ensure their accuracy.

For serial dilution growth assays, cells were cultured in liquid YE at 25°C, three serial 10-fold dilutions starting at 4×10^6 cells/mL were made, 4 μL of each dilution was spotted on YE plates, and cells were grown at the indicated temperatures for 3-4 d. The GFP-Hhp1 (amino acids 280–365) fragment was placed under the control of the *nmt81* promoter in pREP81 vector. This construct and a construct with GFP alone were expressed in a wild-type strain. Cells were grown in media containing thiamine and then washed into media without thiamine to induce protein production, then grown for 22 hours at 32°C before imaging.

cDNAs encoding Ubp2, Ubp3, Ubp4, Ubp8, Ubp14, Ubp15, Ubp16, Uch1, were amplified by PCR from genomic *S. pombe* DNA using primers containing restriction sites. PCR products were digested with restriction enzymes (Nde1/BamHI for *ubp2* and *ubp3* and NdeI/XmaI for *ubp4*, *ubp8, ubp14, ubp15, ubp16*, and *uch1*), subcloned into pREP1, and verified by sequencing. DNAs encoding Ubp1, Ubp7, Ubp9, Ubp11, Otu1, Otu2, and Sst2, were digested from genomic constructs, subcloned into pREP1 and verified by sequencing. *ubp6* and *uch2* cDNAs in pREP1 vectors were gifts from Dr. Colin Gordon (Stone et al., 2004).

S. pombe protein methods

Cell pellets were frozen in a dry ice/ethanol bath and lysed by bead disruption in NP-40 lysis buffer under denaturing sodium dodecyl sulfate (SDS) lysis conditions as previously described (Gould et al., 1991), except with the addition of a complete protease inhibitor mixture (Calbiochem). Cell pellets for Hhp1 and Hhp2 immunoblots were lysed by bead disruption using a FastPrep cell homogenizer (MP Biomedicals). Cell pellets for Htb1-FLAG immunoblots were lysed by bead disruption using a FastPrep cell

homogenizer (MP Biomedicals). Proteins were immunoprecipitated with IgG sepharose beads (GE Healthcare) as described previously (Kouranti et al., 2010). Proteins were separated on a 4-12% Bis-Tris gel (Life Technologies), transferred to Immobilon-P PVDF (Millipore) membrane and immunoblotted with anti-FLAG (Sigma), anti-GFP (Roche), IgG primary and fluorescent mouse and rabbit secondary antibodies (LI-COR Biosciences) according to the manufacturers instructions. H2B ubiqutination was quantified relative to total H2B protein using Odyssey software (LI-COR Biosciences). For analysis of Sid4 phosphorylation and ubiquitination, Sid4 was immunoprecipitated under denaturing SDS conditions using Sid4 antiserum(Johnson et al., 2013). Proteins were separated on a 4–12% Bis-Tris gel (Life Technologies), transferred to Immobilon-P PVDF (Millipore) membrane, and immunoblotted with anti-GFP (Roche, 1:1000), anti-Sid4 (1:2000), anti-Sid4 pT275 pS278 (1:1000) (Johnson et al., 2013), and fluorescent anti-mouse and anti-rabbit secondary antibodies (LI-COR Biosciences) according to the manufacturer's instructions.

Microscopy methods

Live-cell images of *S. pombe* cells were acquired using a Personal DeltaVision microscope system (Applied Precision) that includes an Olympus IX71 microscope, 60× NA 1.42 PlanApo and 100× NA 1.40 UPlanSApo objectives, a Photometrics CoolSnap HQ2 camera, and softWoRx imaging software. Images in figures are maximum intensity projections of z-sections spaced at 0.2–0.5 μm. Images used for quantification were not deconvolved. Other images were deconvolved with 10 iterations. Time-lapse imaging was performed on cells in log phase using a microfluidics perfusion system (CellASIC ONIX; EMD Millipore). Cells were loaded into Y04C plates for 5 seconds at 8 psi, and

YE liquid medium was flowed into the chamber at 5 psi throughout imaging. Quantitative analysis of microscopy data was performed using Fiji (a version of ImageJ software) available at: https://fiji.sc/. To compare populations of cells for all genotypes, cells were imaged on the same day with the same microscope parameters. The average mNG fluorescence intensity of each protein at SPBs was measured in at least 20 cells with background correction calculated for each. The average mCherry fluorescence intensities were measured similarly, and final values for each cell are expressed as mNG/mCherry ratios. Measurements for the 20 cells in each group were averaged for statistical analysis using a two-tailed Student's t-test or ANOVA implemented in Prism 6 (GraphPad Software). All ANOVA statistical analyses used Tukey's post-hoc analysis.

In addition, to compare two populations of cells within the same field of view, one population was incubated with fluorescently conjugated lectin (Sigma-Aldrich), which labels cell walls. Specifically, 1 µl of a 5 mg/ml stock of TRITC-lectin in water was added to 1 ml of cells for a final concentration of 5 µg/ml. Cells were then incubated for 10 min at room temperature, washed three times, and resuspended in media. The lectin-labeled cell population and unlabeled cell population were mixed 1:1 immediately before imaging. The reciprocal labeling of populations was also performed to account for any signal bleed-through. The fluorescence intensity of the SPB was quantified and background fluorescence was subtracted (Willet et al., 2015).

in vitro kinase assays

MBP-Hhp1 and MBP-Hhp2 fusion proteins were purified on amylose beads (New England Biolabs in column buffer (20 mM Tris [pH 7.0], 150 mM NaCl, 2 mM EDTA and 0.1% NP40) and eluted with maltose (10mM). Kinase reactions were performed with

500 ng kinase, 500 ng casein, 10 μM ATP plus 1 μCi γ-[^{32}P]-ATP in kinase buffer (50 mM Tris [pH 7.5], 10 mM $MgCl_2$, and 5 mM DTT) in 20 μl at 30°C for 30 min. Reactions were quenched by adding SDS-PAGE sample buffer and proteins were separated by SDS-PAGE. Phosphorylated proteins were visualized by autoradiography and relative protein quantities were assessed by Coomassie blue staining relative to known standards utilizing Odyssey software (LI-COR Biosciences)**.** Kinetic assays were performed using recombinant MBP-Hhp1 and MBP-Hhp2 fusion proteins treated for 2 hours with lambda phosphatase (New England Biolabs). These kinase reactions were performed with 0.25 uM of kinase, 25 uM casein, 5 uM cold ATP, 2 μCi [γ^{32}P]-ATP in CK1 kinase buffer. Reactions were quenched at different time points by adding SDS sample buffer and proteins were separated by SDS-PAGE. Phosphorylated proteins were visualized and quantitated using an FLA7000IP Typhoon Storage Phosphorimager (GE Healthcare Life Sciences). Kinetic measurements were calculated using Prism 6 software. Relative protein quantities were assessed by Coomassie blue staining**.**

Two-hybrid analyses

Two-hybrid experiments were performed as described previously (Vo et al., 2016). *hhp1* and *ppc89,* cloned into pDEST DB and pDEST AD vectors, respectively, were generously provided by Dr. Haiyuan Yu (Cornell University). These or fragments thereof were co-transformed into *S. cerevisiae* strain PJ69-4A. Leu^+ and Trp^+ transformants were selected and then scored for positive interactions by streaking onto synthetic dextrose plates containing 5 mM 3-amino-1,2,4- triazole (3AT) and lacking tryptophan, leucine and histidine. ß-galactosidase reporter enzyme activity in the two-hybrid strains was measured using the Galacto-Star™ chemiluminescent reporter assay

system according to the manufacturer's instructions (Applied Biosystems, Foster City, California), except that cells were lysed by glass bead disruption. Each experiment was performed in triplicate. Reporter assays were recorded on a Multi-Detection Microplate Reader (Bio-TEK Instruments, Inc.).

Checkpoint assay

S. pombe cells were synchronized in S phase using hydroxyurea (HU) (Sigma) at a final concentration of 12 mM for 3–3.5 hours at 32°C. Cells were then filtered into HU-free media and immediately incubated at 19°C to activate the spindle checkpoint. Cells were fixed in 70% ethanol and septation indices were measured periodically for 9 hours by methyl blue staining of the septa.

in vivo Ubiquitinome Purifications

His-biotin-his tagged ubiquitin (HBH-Ub) was overexpressed in *wildtype* and *ubp8*Δ strains utilizing the thiamine repressible *nmt1* promoter in pREP1 (Kouranti et al., 2010; Maundrell, 1993). Ubiquitinated proteins were purified using two-step affinity purifications performed under denaturing conditions as described (Tagwerker et al., 2006). Briefly, cell pellets were lysed by bead disruption in buffer 1 (8 M urea, 300 mM NaCl, 50 mM NaPO4, 0.5% NP40 and 4 mM Imidazole, pH 8) and incubated with Ni^{2+}-NTA agarose beads (Qiagen) for 3–4 h at room temperature. After incubation, beads were washed 4 times with buffer 3 (8 M urea, 300 mM NaCl, 50 mM NaPO4, 0.5% NP40 and 20 mM Imidazole, pH 6.3) and eluted in buffer 4 (8 M urea, 200 mM NaCl, 50 mM NaPO4, 0.5% NP40 and 2% SDS, 100 mM Tris and 10 mM EDTA, pH 4.3). The pH of the eluate was adjusted to 8 and streptavidin ultra-link resin (Pierce) was added and incubated overnight at room temperature. After the second incubation, streptavidin beads were washed 4 times with buffer 6 (8 M urea, 200 mM NaCl, 2% SDS and 100 mM Tris,

pH 8) and once with buffer 7 (8 M urea, 200 mM NaCl and 100 mM Tris, pH 8). Purifications were performed in triplicate and purified proteins were subjected to mass spectrometric analysis.

Mass Spectrometry Methods

Purified ubiquitin-HBH on streptavidin beads was washed three times with Tris-urea buffer (100mM Tris, pH 8.5, 8M urea). Proteins were reduced with 3mM TCEP (Tris(2-carboxyethyl)phosphine hydrochloride), alkylated with 10mM iodoacetamide, and digested with trypsin (0.4 ug of Trypsin Gold, Promega). 2D-LC-MS analysis was performed in the following manner. Peptides were loaded onto 26 cm columns with a bomb pressure cell and then separated and analyzed by three-phase multidimensional protein identification technology on a Velos LTQ mass spectrometer (Thermo Scientific, West Palm Beach, FL) coupled to a nanoHPLC (NanoAcquity, Waters Corporation). The NanoAcquity autosampler was used for the 12 salt elution steps, each with 2 µl ammonium acetate. Each injection was followed by elution of peptides with a 0–40% acetonitrile gradient (60 minutes) except the first and last injections, in which a 0–90% acetonitrile gradient was used. One full precursor MS scan (400–2,000 mass-to-charge ratio) and five tandem MS scans of the most abundant ions detected in the precursor MS scan under dynamic exclusion was performed. Ions with a neutral loss of 98 Da (singly charged), 49 Da (doubly charged), or 32.7 Da (triply charged) from the parent ions during MS^2 were subjected to MS^3 fragmentation MS data analysis was done as previously described (Chen et al., 2013) with the following changes. A newer version of Scaffold (Scaffold v4.2.0) was used and the filtering criteria were changed to: minimum of 90.0%

peptide identification probability, minimum of 99.0% protein identification probability, and minimum of 2 unique peptides.

BIBLIOGRAPHY

Agostinis, P., L.A. Pinna, F. Meggio, O. Marin, J. Goris, J.R. Vandenheede, and W. Merlevede. 1989. A synthetic peptide substrate specific for casein kinase I. *FEBS Lett*. 259:75-78.

Amerik, A., S. Swaminathan, B.A. Krantz, K.D. Wilkinson, and M. Hochstrasser. 1997. In vivo disassembly of free polyubiquitin chains by yeast Ubp14 modulates rates of protein degradation by the proteasome. *EMBO J*. 16:4826-4838.

Amon, A. 1999. The spindle checkpoint. *Curr Opin Genet Dev*. 9:69-75.

Anderson, M., S.S. Ng, V. Marchesi, F.H. MacIver, F.E. Stevens, T. Riddell, D.M. Glover, I.M. Hagan, and C.J. McInerny. 2002. Plo1(+) regulates gene transcription at the M-G(1) interval during the fission yeast mitotic cell cycle. *EMBO J*. 21:5745-5755.

Atanassov, B.S., and S.Y. Dent. 2011. USP22 regulates cell proliferation by deubiquitinating the transcriptional regulator FBP1. *EMBO Rep*. 12:924-930.

Avruch, J., D. Zhou, J. Fitamant, N. Bardeesy, F. Mou, and L.R. Barrufet. 2012. Protein kinases of the Hippo pathway: regulation and substrates. *Semin Cell Dev Biol*. 23:770-784.

Babu, P., J.D. Bryan, H.R. Panek, S.L. Jordan, B.M. Forbrich, S.C. Kelley, R.T. Colvin, and L.C. Robinson. 2002. Plasma membrane localization of the Yck2p yeast casein kinase 1 isoform requires the C-terminal extension and secretory pathway function. *J Cell Sci*. 115:4957-4968.

Babu, P., R.J. Deschenes, and L.C. Robinson. 2004. Akr1p-dependent palmitoylation of Yck2p yeast casein kinase 1 is necessary and sufficient for plasma membrane targeting. *The Journal of biological chemistry*. 279:27138-27147.

Bahler, J., J.Q. Wu, M.S. Longtine, N.G. Shah, A. McKenzie, 3rd, A.B. Steever, A. Wach, P. Philippsen, and J.R. Pringle. 1998. Heterologous modules for efficient and versatile PCR-based gene targeting in Schizosaccharomyces pombe. *Yeast*. 14:943-951.

Balasubramanian, M.K., R. Srinivasan, Y. Huang, and K.H. Ng. 2012. Comparing contractile apparatus-driven cytokinesis mechanisms across kingdoms. *Cytoskeleton (Hoboken)*. 69:942-956.

Bassermann, F., R. Eichner, and M. Pagano. 2014. The ubiquitin proteasome system - implications for cell cycle control and the targeted treatment of cancer. *Biochim Biophys Acta*. 1843:150-162.

Beckley, J.R., J.S. Chen, Y. Yang, J. Peng, and K.L. Gould. 2015. A Degenerate Cohort of Yeast Membrane Trafficking DUBs Mediates Cell Polarity and Survival. *Mol Cell Proteomics*. 14:3132-3141.

Bedri, S., S.M. Cizek, I. Rastarhuyeva, and J.R. Stone. 2007. Regulation of protein kinase CK1alphaLS by dephosphorylation in response to hydrogen peroxide. *Arch Biochem Biophys*. 466:242-249.

Beltraminelli, N., M. Murone, and V. Simanis. 1999. The S. pombe zfs1 gene is required to prevent septation if mitotic progression is inhibited. *J Cell Sci*. 112 Pt 18:3103-3114.

Berry, L.D., A. Feoktistova, M.D. Wright, and K.L. Gould. 1999. The schizosaccharomyces pombe dim1(+) gene interacts with the anaphase-promoting complex or cyclosome (APC/C) component lid1(+) and is required for APC/C function. *Mol Cell Biol*. 19:2535-2546.

Bhattacharyya, R.P., A. Remenyi, M.C. Good, C.J. Bashor, A.M. Falick, and W.A. Lim. 2006. The Ste5 scaffold allosterically modulates signaling output of the yeast mating pathway. *Science*. 311:822-826.

Bibian, M., R.J. Rahaim, J.Y. Choi, Y. Noguchi, S. Schurer, W. Chen, S. Nakanishi, K. Licht, L.H. Rosenberg, L. Li, Y. Feng, M.D. Cameron, D.R. Duckett, J.L. Cleveland, and W.R. Roush. 2013. Development of highly selective casein kinase 1delta/1epsilon (CK1delta/epsilon) inhibitors with potent antiproliferative properties. *Bioorg Med Chem Lett*. 23:4374-4380.

Bimbo, A., Y. Jia, S.L. Poh, R.K. Karuturi, N. den Elzen, X. Peng, L. Zheng, M. O'Connell, E.T. Liu, M.K. Balasubramanian, and J. Liu. 2005. Systematic deletion analysis of fission yeast protein kinases. *Eukaryotic cell*. 4:799-813.

Bohnert, K.A., A.P. Grzegorzewska, A.H. Willet, C.W. Vander Kooi, D.R. Kovar, and K.L. Gould. 2013. SIN-dependent phosphoinhibition of formin multimerization controls fission yeast cytokinesis. *Genes Dev*. 27:2164-2177.

Bustos, V.H., A. Ferrarese, A. Venerando, O. Marin, J.E. Allende, and L.A. Pinna. 2006. The first armadillo repeat is involved in the recognition and regulation of beta-catenin phosphorylation by protein kinase CK1. *Proc Natl Acad Sci U S A*. 103:19725-19730.

Carmel, G., B. Leichus, X. Cheng, S.D. Patterson, U. Mirza, B.T. Chait, and J. Kuret. 1994. Expression, purification, crystallization, and preliminary x-ray analysis of casein kinase-1 from Schizosaccharomyces pombe. *J Biol Chem*. 269:7304-7309.

Carpy, A., K. Krug, S. Graf, A. Koch, S. Popic, S. Hauf, and B. Macek. 2014. Absolute proteome and phosphoproteome dynamics during the cell cycle of Schizosaccharomyces pombe (Fission Yeast). *Molecular & cellular proteomics : MCP*. 13:1925-1936.

Cegielska, A., K.F. Gietzen, A. Rivers, and D.M. Virshup. 1998. Autoinhibition of casein kinase I epsilon (CKI epsilon) is relieved by protein phosphatases and limited proteolysis. *The Journal of biological chemistry*. 273:1357-1364.

Chan, K.Y., M. Alonso-Nunez, A. Grallert, K. Tanaka, Y. Connolly, D.L. Smith, and I.M. Hagan. 2017. Dialogue between centrosomal entrance and exit scaffold pathways regulates mitotic commitment. *J Cell Biol*.

Chang, L., and K.L. Gould. 2000a. Sid4p is required to localize components of the septation initiation pathway to the spindle pole body in fission yeast. *Proceedings of the National Academy of Sciences of the United States of America*. 97:5249-5254.

Chang, L., and K.L. Gould. 2000b. Sid4p is required to localize components of the septation initiation pathway to the spindle pole body in fission yeast. *Proc Natl Acad Sci U S A*. 97:5249-5254.

Chang, L., J.L. Morrell, A. Feoktistova, and K.L. Gould. 2001. Study of cyclin proteolysis in anaphase-promoting complex (APC) mutant cells reveals the requirement for APC function in the final steps of the fission yeast septation initiation network. *Mol Cell Biol*. 21:6681-6694.

Chen, C.T., A. Feoktistova, J.S. Chen, Y.S. Shim, D.M. Clifford, K.L. Gould, and D. McCollum. 2008. The SIN kinase Sid2 regulates cytoplasmic retention of the S. pombe Cdc14-like phosphatase Clp1. *Curr Biol*. 18:1594-1599.

Chen, J.S., J.R. Beckley, N.A. McDonald, L. Ren, M. Mangione, S.J. Jang, Z.C. Elmore, N. Rachfall, A. Feoktistova, C.M. Jones, A.H. Willet, R. Guillen, D.A. Bitton, J. Bahler, M.A. Jensen, N. Rhind, and K.L. Gould. 2015. Identification of new players in cell division, DNA damage response, and morphogenesis through construction of Schizosaccharomyces pombe deletion strains. *G3*. 5:361-370.

Chen, J.S., M.R. Broadus, J.R. McLean, A. Feoktistova, L. Ren, and K.L. Gould. 2013. Comprehensive proteomics analysis reveals new substrates and regulators of the fission yeast clp1/cdc14 phosphatase. *Mol Cell Proteomics*. 12:1074-1086.

Choi, K.Y., B. Satterberg, D.M. Lyons, and E.A. Elion. 1994. Ste5 tethers multiple protein kinases in the MAP kinase cascade required for mating in S. cerevisiae. *Cell*. 78:499-512.

Cipak, L., C. Zhang, I. Kovacikova, C. Rumpf, E. Miadokova, K.M. Shokat, and J. Gregan. 2011. Generation of a set of conditional analog-sensitive alleles of essential protein kinases in the fission yeast Schizosaccharomyces pombe. *Cell Cycle*. 10:3527-3532.

Clifford, D.M., B.A. Wolfe, R.H. Roberts-Galbraith, W.H. McDonald, J.R. Yates, 3rd, and K.L. Gould. 2008. The Clp1/Cdc14 phosphatase contributes to the robustness of cytokinesis by association with anillin-related Mid1. *J Cell Biol*. 181:79-88.

Cobb, M.H., and O.M. Rosen. 1983. Description of a protein kinase derived from insulin-treated 3T3-L1 cells that catalyzes the phosphorylation of ribosomal protein S6 and casein. *J Biol Chem*. 258:12472-12481.

Dahlberg, C.L., E.Z. Nguyen, D. Goodlett, and D. Kimelman. 2009. Interactions between Casein kinase Iepsilon (CKIepsilon) and two substrates from disparate signaling pathways reveal mechanisms for substrate-kinase specificity. *PLoS One*. 4:e4766.

Deshaies, R.J., and C.A. Joazeiro. 2009. RING domain E3 ubiquitin ligases. *Annu Rev Biochem*. 78:399-434.

Desjardins, P.R., P.F. Lue, C.C. Liew, and A.G. Gornall. 1972. Purification and properties of rat liver nuclear protein kinases. *Can J Biochem*. 50:1249-1259.

Dhillon, N., and M.F. Hoekstra. 1994. Characterization of two protein kinases from Schizosaccharomyces pombe involved in the regulation of DNA repair. *EMBO J*. 13:2777-2788.

Elias, L., A.P. Li, and J. Longmire. 1981. Cyclic adenosine 3':5'-monophosphate-dependent and -independent protein kinase in acute myeloblastic leukemia. *Cancer Res*. 41:2182-2188.

Elledge, S.J. 1996. Cell cycle checkpoints: preventing an identity crisis. *Science*. 274:1664-1672.

Feoktistova, A., J. Morrell-Falvey, J.S. Chen, N.S. Singh, M.K. Balasubramanian, and K.L. Gould. 2012. The fission yeast septation initiation network (SIN) kinase, Sid2, is required for SIN asymmetry and regulates the SIN scaffold, Cdc11. *Mol Biol Cell*. 23:1636-1645.

Ferrarese, A., O. Marin, V.H. Bustos, A. Venerando, M. Antonelli, J.E. Allende, and L.A. Pinna. 2007. Chemical dissection of the APC Repeat 3 multistep phosphorylation by the concerted action of protein kinases CK1 and GSK3. *Biochemistry*. 46:11902-11910.

Flotow, H., P.R. Graves, A.Q. Wang, C.J. Fiol, R.W. Roeske, and P.J. Roach. 1990. Phosphate groups as substrate determinants for casein kinase I action. *J Biol Chem*. 265:14264-14269.

Flotow, H., and P.J. Roach. 1991. Role of acidic residues as substrate determinants for casein kinase I. *J Biol Chem*. 266:3724-3727.

Furge, K.A., K. Wong, J. Armstrong, M. Balasubramanian, and C.F. Albright. 1998. Byr4 and Cdc16 form a two-component GTPase-activating protein for the Spg1 GTPase that controls septation in fission yeast. *Curr Biol*. 8:947-954.

Gardner, R.D., and D.J. Burke. 2000. The spindle checkpoint: two transitions, two pathways. *Trends Cell Biol*. 10:154-158.

Ghalei, H., F.X. Schaub, J.R. Doherty, Y. Noguchi, W.R. Roush, J.L. Cleveland, M.E. Stroupe, and K. Karbstein. 2015. Hrr25/CK1delta-directed release of Ltv1 from pre-40S ribosomes is necessary for ribosome assembly and cell growth. *The Journal of cell biology*. 208:745-759.

Gietzen, K.F., and D.M. Virshup. 1999. Identification of inhibitory autophosphorylation sites in casein kinase I epsilon. *The Journal of biological chemistry*. 274:32063-32070.

Glinsky, G.V. 2006. Genomic models of metastatic cancer: functional analysis of death-from-cancer signature genes reveals aneuploid, anoikis-resistant, metastasis-enabling phenotype with altered cell cycle control and activated Polycomb Group (PcG) protein chromatin silencing pathway. *Cell Cycle*. 5:1208-1216.

Glotzer, M., A.W. Murray, and M.W. Kirschner. 1991. Cyclin is degraded by the ubiquitin pathway. *Nature*. 349:132-138.

Good, M.C., J.G. Zalatan, and W.A. Lim. 2011. Scaffold proteins: hubs for controlling the flow of cellular information. *Science*. 332:680-686.

Gordon, C., G. McGurk, P. Dillon, C. Rosen, and N.D. Hastie. 1993. Defective mitosis due to a mutation in the gene for a fission yeast 26S protease subunit. *Nature*. 366:355-357.

Gordon, C., G. McGurk, M. Wallace, and N.D. Hastie. 1996. A conditional lethal mutant in the fission yeast 26 S protease subunit mts3+ is defective in metaphase to anaphase transition. *J Biol Chem*. 271:5704-5711.

Gould, K.L., S. Moreno, D.J. Owen, S. Sazer, and P. Nurse. 1991. Phosphorylation at Thr167 is required for Schizosaccharomyces pombe p34cdc2 function. *EMBO J*. 10:3297-3309.

Goyal, A., M. Takaine, V. Simanis, and K. Nakano. 2011. Dividing the spoils of growth and the cell cycle: The fission yeast as a model for the study of cytokinesis. *Cytoskeleton (Hoboken)*. 68:69-88.

Grant, P.A., D. Schieltz, M.G. Pray-Grant, D.J. Steger, J.C. Reese, J.R. Yates, 3rd, and J.L. Workman. 1998. A subset of TAF(II)s are integral components of the SAGA

complex required for nucleosome acetylation and transcriptional stimulation. *Cell*. 94:45-53.

Graves, P.R., D.W. Haas, C.H. Hagedorn, A.A. DePaoli-Roach, and P.J. Roach. 1993. Molecular cloning, expression, and characterization of a 49-kilodalton casein kinase I isoform from rat testis. *J Biol Chem*. 268:6394-6401.

Graves, P.R., and P.J. Roach. 1995. Role of COOH-terminal phosphorylation in the regulation of casein kinase I delta. *J Biol Chem*. 270:21689-21694.

Greer, Y.E., and J.S. Rubin. 2011. Casein kinase 1 delta functions at the centrosome to mediate Wnt-3a-dependent neurite outgrowth. *J Cell Biol*. 192:993-1004.

Greer, Y.E., C.J. Westlake, B. Gao, K. Bharti, Y. Shiba, C.P. Xavier, G.J. Pazour, Y. Yang, and J.S. Rubin. 2014. Casein kinase 1delta functions at the centrosome and Golgi to promote ciliogenesis. *Mol Biol Cell*. 25:1629-1640.

Gregan, J., C. Zhang, C. Rumpf, L. Cipak, Z. Li, P. Uluocak, K. Nasmyth, and K.M. Shokat. 2007. Construction of conditional analog-sensitive kinase alleles in the fission yeast Schizosaccharomyces pombe. *Nat Protoc*. 2:2996-3000.

Guertin, D.A., L. Chang, F. Irshad, K.L. Gould, and D. McCollum. 2000. The role of the sid1p kinase and cdc14p in regulating the onset of cytokinesis in fission yeast. *EMBO J*. 19:1803-1815.

Guertin, D.A., S. Venkatram, K.L. Gould, and D. McCollum. 2002a. Dma1 prevents mitotic exit and cytokinesis by inhibiting the septation initiation network (SIN). *Dev Cell*. 3:779-790.

Guertin, D.A., S. Venkatram, K.L. Gould, and D. McCollum. 2002b. Dma1 prevents mitotic exit and cytokinesis by inhibiting the septation initiation network (SIN). *Dev Cell*. 3:779-790.

Gupta, S., and D. McCollum. 2011. Crosstalk between NDR kinase pathways coordinates cell cycle dependent actin rearrangements. *Cell division*. 6:19.

Hathaway, G.M., and J.A. Traugh. 1979. Cyclic nucleotide-independent protein kinases from rabbit reticulocytes. Purification of casein kinases. *J Biol Chem*. 254:762-768.

He, X., M.H. Jones, M. Winey, and S. Sazer. 1998. Mph1, a member of the Mps1-like family of dual specificity protein kinases, is required for the spindle checkpoint in S. pombe. *J Cell Sci*. 111 (Pt 12):1635-1647.

He, X., T.E. Patterson, and S. Sazer. 1997. The Schizosaccharomyces pombe spindle checkpoint protein mad2p blocks anaphase and genetically interacts with the anaphase-promoting complex. *Proc Natl Acad Sci U S A*. 94:7965-7970.

Helmlinger, D. 2012. New insights into the SAGA complex from studies of the Tra1 subunit in budding and fission yeast. *Transcription*. 3:13-18.

Helmlinger, D., S. Marguerat, J. Villen, D.L. Swaney, S.P. Gygi, J. Bahler, and F. Winston. 2011. Tra1 has specific regulatory roles, rather than global functions, within the SAGA co-activator complex. *EMBO J*. 30:2843-2852.

Hergovich, A., and B.A. Hemmings. 2012. Hippo signalling in the G2/M cell cycle phase: lessons learned from the yeast MEN and SIN pathways. *Semin Cell Dev Biol*. 23:794-802.

Heride, C., S. Urbe, and M.J. Clague. 2014. Ubiquitin code assembly and disassembly. *Current biology : CB*. 24:R215-220.

Hershko, A., and A. Ciechanover. 1998. The ubiquitin system. *Annu Rev Biochem*. 67:425-479.

Hindley, J., G. Phear, M. Stein, and D. Beach. 1987. Sucl+ encodes a predicted 13-kilodalton protein that is essential for cell viability and is directly involved in the division cycle of Schizosaccharomyces pombe. *Mol Cell Biol*. 7:504-511.

Hoekstra, M.F., N. Dhillon, G. Carmel, A.J. DeMaggio, R.A. Lindberg, T. Hunter, and J. Kuret. 1994. Budding and fission yeast casein kinase I isoforms have dual-specificity protein kinase activity. *Mol Biol Cell*. 5:877-886.

Hutchins, J.R., Y. Toyoda, B. Hegemann, I. Poser, J.K. Heriche, M.M. Sykora, M. Augsburg, O. Hudecz, B.A. Buschhorn, J. Bulkescher, C. Conrad, D. Comartin, A. Schleiffer, M. Sarov, A. Pozniakovsky, M.M. Slabicki, S. Schloissnig, I. Steinmacher, M. Leuschner, A. Ssykor, S. Lawo, L. Pelletier, H. Stark, K. Nasmyth, J. Ellenberg, R. Durbin, F. Buchholz, K. Mechtler, A.A. Hyman, and

J.M. Peters. 2010. Systematic analysis of human protein complexes identifies chromosome segregation proteins. *Science*. 328:593-599.

Ianes, C., P. Xu, N. Werz, Z. Meng, D. Henne-Bruns, J. Bischof, and U. Knippschild. 2015. CK1delta activity is modulated by CDK2/E- and CDK5/p35-mediated phosphorylation. *Amino Acids*.

Ingvarsdottir, K., N.J. Krogan, N.C.T. Emre, A. Wyce, N.J. Thompson, A. Emili, T.R. Hughes, J.F. Greenblatt, and S.L. Berger. 2005. H2B Ubiquitin Protease Ubp8 and Sgf11 Constitute a Discrete Functional Module within the Saccharomyces cerevisiae SAGA Complex. *Molecular and Cellular Biology*. 25:1162-1172.

Iwaki, T., M. Onishi, M. Ikeuchi, A. Kita, R. Sugiura, Y. Giga-Hama, Y. Fukui, and K. Takegawa. 2007. Essential roles of class E Vps proteins for sorting into multivesicular bodies in Schizosaccharomyces pombe. *Microbiology*. 153:2753-2764.

Jia, L., S. Kim, and H. Yu. 2013. Tracking spindle checkpoint signals from kinetochores to APC/C. *Trends Biochem Sci*. 38:302-311.

Johnson, A.E., J.S. Chen, and K.L. Gould. 2013. CK1 is required for a mitotic checkpoint that delays cytokinesis. *Curr Biol*. 23:1920-1926.

Johnson, A.E., and K.L. Gould. 2011a. Dma1 ubiquitinates the SIN scaffold, Sid4, to impede the mitotic localization of Plo1 kinase. *EMBO J*. 30:341-354.

Johnson, A.E., and K.L. Gould. 2011b. Dma1 ubiquitinates the SIN scaffold, Sid4, to impede the mitotic localization of Plo1 kinase. *The EMBO journal*. 30:341-354.

Johnson, A.E., D. McCollum, and K.L. Gould. 2012. Polar opposites: Fine-tuning cytokinesis through SIN asymmetry. *Cytoskeleton (Hoboken)*. 69:686-699.

Johnson, D.G., and C.L. Walker. 1999. Cyclins and cell cycle checkpoints. *Annu Rev Pharmacol Toxicol*. 39:295-312.

Keeney, J.B., and J.D. Boeke. 1994. Efficient targeted integration at leu1-32 and ura4-294 in Schizosaccharomyces pombe. *Genetics*. 136:849-856.

Kelley, L.A., S. Mezulis, C.M. Yates, M.N. Wass, and M.J. Sternberg. 2015. The Phyre2 web portal for protein modeling, prediction and analysis. *Nature protocols*. 10:845-858.

Kholodenko, B.N., J.F. Hancock, and W. Kolch. 2010. Signalling ballet in space and time. *Nat Rev Mol Cell Biol*. 11:414-426.

Kim, D.U., J. Hayles, D. Kim, V. Wood, H.O. Park, M. Won, H.S. Yoo, T. Duhig, M. Nam, G. Palmer, S. Han, L. Jeffery, S.T. Baek, H. Lee, Y.S. Shim, M. Lee, L. Kim, K.S. Heo, E.J. Noh, A.R. Lee, Y.J. Jang, K.S. Chung, S.J. Choi, J.Y. Park, Y. Park, H.M. Kim, S.K. Park, H.J. Park, E.J. Kang, H.B. Kim, H.S. Kang, H.M. Park, K. Kim, K. Song, K.B. Song, P. Nurse, and K.L. Hoe. 2010. Analysis of a genome-wide set of gene deletions in the fission yeast Schizosaccharomyces pombe. *Nat Biotechnol*. 28:617-623.

Knippschild, U., A. Gocht, S. Wolff, N. Huber, J. Lohler, and M. Stoter. 2005. The casein kinase 1 family: participation in multiple cellular processes in eukaryotes. *Cell Signal*. 17:675-689.

Knippschild, U., M. Kruger, J. Richter, P. Xu, B. Garcia-Reyes, C. Peifer, J. Halekotte, V. Bakulev, and J. Bischof. 2014. The CK1 Family: Contribution to Cellular Stress Response and Its Role in Carcinogenesis. *Frontiers in oncology*. 4:96.

Kohler, A., E. Zimmerman, M. Schneider, E. Hurt, and N. Zheng. 2010. Structural basis for assembly and activation of the heterotetrameric SAGA histone H2B deubiquitinase module. *Cell*. 141:606-617.

Komander, D., M.J. Clague, and S. Urbe. 2009. Breaking the chains: structure and function of the deubiquitinases. *Nat Rev Mol Cell Biol*. 10:550-563.

Komander, D., and M. Rape. 2012. The ubiquitin code. *Annu Rev Biochem*. 81:203-229.

Kouranti, I., J.R. McLean, A. Feoktistova, P. Liang, A.E. Johnson, R.H. Roberts-Galbraith, and K.L. Gould. 2010. A global census of fission yeast deubiquitinating enzyme localization and interaction networks reveals distinct compartmentalization profiles and overlapping functions in endocytosis and polarity. *PLoS Biol*. 8.

Koutelou, E., C.L. Hirsch, and S.Y. Dent. 2010. Multiple faces of the SAGA complex. *Curr Opin Cell Biol*. 22:374-382.

Krapp, A., M.P. Gulli, and V. Simanis. 2004. SIN and the art of splitting the fission yeast cell. *Curr Biol*. 14:R722-730.

Lang, G., J. Bonnet, D. Umlauf, K. Karmodiya, J. Koffler, M. Stierle, D. Devys, and L. Tora. 2011. The tightly controlled deubiquitination activity of the human SAGA complex differentially modifies distinct gene regulatory elements. *Mol Cell Biol*. 31:3734-3744.

Lee, K.K., L. Florens, S.K. Swanson, M.P. Washburn, and J.L. Workman. 2005. The deubiquitylation activity of Ubp8 is dependent upon Sgf11 and its association with the SAGA complex. *Mol Cell Biol*. 25:1173-1182.

Li, C., K.A. Furge, Q.C. Cheng, and C.F. Albright. 2000. Byr4 localizes to spindle-pole bodies in a cell cycle-regulated manner to control Cdc7 localization and septation in fission yeast. *J Biol Chem*. 275:14381-14387.

Liu, Y.L., Y.M. Yang, H. Xu, and X.S. Dong. 2010. Increased expression of ubiquitin-specific protease 22 can promote cancer progression and predict therapy failure in human colorectal cancer. *J Gastroenterol Hepatol*. 25:1800-1805.

Locasale, J.W., A.S. Shaw, and A.K. Chakraborty. 2007. Scaffold proteins confer diverse regulatory properties to protein kinase cascades. *Proc Natl Acad Sci U S A*. 104:13307-13312.

Longenecker, K.L., P.J. Roach, and T.D. Hurley. 1996. Three-dimensional structure of mammalian casein kinase I: molecular basis for phosphate recognition. *Journal of molecular biology*. 257:618-631.

Longenecker, K.L., P.J. Roach, and T.D. Hurley. 1998. Crystallographic studies of casein kinase I delta toward a structural understanding of auto-inhibition. *Acta Crystallogr D Biol Crystallogr*. 54:473-475.

Mana-Capelli, S., J.R. McLean, C.T. Chen, K.L. Gould, and D. McCollum. 2012. The kinesin-14 Klp2 is negatively regulated by the SIN for proper spindle elongation and telophase nuclear positioning. *Molecular biology of the cell*. 23:4592-4600.

Marguerat, S., A. Schmidt, S. Codlin, W. Chen, R. Aebersold, and J. Bahler. 2012. Quantitative analysis of fission yeast transcriptomes and proteomes in proliferating and quiescent cells. *Cell*. 151:671-683.

Marin, O., V. Burzio, M. Boschetti, F. Meggio, C.C. Allende, J.E. Allende, and L.A. Pinna. 2002. Structural features underlying the multisite phosphorylation of the A domain of the NF-AT4 transcription factor by protein kinase CK1. *Biochemistry*. 41:618-627.

Marin, O., V.H. Bustos, L. Cesaro, F. Meggio, M.A. Pagano, M. Antonelli, C.C. Allende, L.A. Pinna, and J.E. Allende. 2003. A noncanonical sequence phosphorylated by casein kinase 1 in beta-catenin may play a role in casein kinase 1 targeting of important signaling proteins. *Proc Natl Acad Sci U S A*. 100:10193-10200.

Maruyama, T., T. Nakamura, T. Hayashi, and M. Yanagida. 2006. Histone H2B mutations in inner region affect ubiquitination, centromere function, silencing and chromosome segregation. *EMBO J*. 25:2420-2431.

Matsumoto, T. 1997. A fission yeast homolog of CDC20/p55CDC/Fizzy is required for recovery from DNA damage and genetically interacts with p34cdc2. *Mol Cell Biol*. 17:742-750.

Matsumura, S., and M. Takeda. 1972. Phosphoprotein kinases from rat liver cytosol. *Biochim Biophys Acta*. 289:237-241.

Matsuyama, A., R. Arai, Y. Yashiroda, A. Shirai, A. Kamata, S. Sekido, Y. Kobayashi, A. Hashimoto, M. Hamamoto, Y. Hiraoka, S. Horinouchi, and M. Yoshida. 2006. ORFeome cloning and global analysis of protein localization in the fission yeast Schizosaccharomyces pombe. *Nature biotechnology*. 24:841-847.

Maundrell, K. 1993. Thiamine-repressible expression vectors pREP and pRIP for fission yeast. *Gene*. 123:127-130.

McLean, J.R., D. Chaix, M.D. Ohi, and K.L. Gould. 2011. State of the APC/C: organization, function, and structure. *Crit Rev Biochem Mol Biol*. 46:118-136.

Meggio, F., J.W. Perich, O. Marin, and L.A. Pinna. 1992. The comparative efficiencies of the Ser(P)-, Thr(P)- and Tyr(P)-residues as specificity determinants for casein kinase-1. *Biochem Biophys Res Commun*. 182:1460-1465.

Meggio, F., J.W. Perich, E.C. Reynolds, and L.A. Pinna. 1991. A synthetic beta-casein phosphopeptide and analogues as model substrates for casein kinase-1, a ubiquitous, phosphate directed protein kinase. *FEBS Lett*. 283:303-306.

Mehta, S., and K.L. Gould. 2006. Identification of functional domains within the septation initiation network kinase, Cdc7. *J Biol Chem*. 281:9935-9941.

Meng, Z., J. Bischof, C. Ianes, D. Henne-Bruns, P. Xu, and U. Knippschild. 2016. CK1delta kinase activity is modulated by protein kinase C alpha (PKCalpha)-mediated site-specific phosphorylation. *Amino Acids*. 48:1185-1197.

Milne, D.M., P. Looby, and D.W. Meek. 2001. Catalytic activity of protein kinase CK1 delta (casein kinase 1delta) is essential for its normal subcellular localization. *Exp Cell Res*. 263:43-54.

Mishra, M., J. Karagiannis, M. Sevugan, P. Singh, and M.K. Balasubramanian. 2005. The 14-3-3 protein rad24p modulates function of the cdc14p family phosphatase clp1p/flp1p in fission yeast. *Curr Biol*. 15:1376-1383.

Mitchison, J.M., and P. Nurse. 1985. Growth in cell length in the fission yeast Schizosaccharomyces pombe. *J Cell Sci*. 75:357-376.

Mocciaro, A., and M. Rape. 2012. Emerging regulatory mechanisms in ubiquitin-dependent cell cycle control. *J Cell Sci*. 125:255-263.

Mohan, R.D., G. Dialynas, V.M. Weake, J. Liu, S. Martin-Brown, L. Florens, M.P. Washburn, J.L. Workman, and S.M. Abmayr. 2014. Loss of Drosophila Ataxin-7, a SAGA subunit, reduces H2B ubiquitination and leads to neural and retinal degeneration. *Genes Dev*. 28:259-272.

Moreno, S., A. Klar, and P. Nurse. 1991. Molecular genetic analysis of fission yeast Schizosaccharomyces pombe. *Methods Enzymol*. 194:795-823.

Morrell, J.L., G.C. Tomlin, S. Rajagopalan, S. Venkatram, A.S. Feoktistova, J.J. Tasto, S. Mehta, J.L. Jennings, A. Link, M.K. Balasubramanian, and K.L. Gould. 2004. Sid4p-Cdc11p assembles the septation initiation network and its regulators at the S. pombe SPB. *Curr Biol*. 14:579-584.

Mulvihill, D.P., J. Petersen, H. Ohkura, D.M. Glover, and I.M. Hagan. 1999. Plo1 kinase recruitment to the spindle pole body and its role in cell division in *Schizosaccharomyces pombe*. *Mol Biol Cell*. 10:2771-2785.

Murone, M., and V. Simanis. 1996. The fission yeast dma1 gene is a component of the spindle assembly checkpoint, required to prevent septum formation and premature exit from mitosis if spindle function is compromised. *EMBO J*. 15:6605-6616.

Musacchio, A. 2011. Spindle assembly checkpoint: the third decade. *Philos Trans R Soc Lond B Biol Sci*. 366:3595-3604.

Musacchio, A. 2015. The Molecular Biology of Spindle Assembly Checkpoint Signaling Dynamics. *Curr Biol*. 25:R1002-1018.

Nabetani, A., T. Koujin, C. Tsutsumi, T. Haraguchi, and Y. Hiraoka. 2001. A conserved protein, Nuf2, is implicated in connecting the centromere to the spindle during chromosome segregation: a link between the kinetochore function and the spindle checkpoint. *Chromosoma*. 110:322-334.

Nakatogawa, H. 2015. Hrr25: an emerging major player in selective autophagy regulation in Saccharomyces cerevisiae. *Autophagy*. 11:432-433.

Nijman, S.M., M.P. Luna-Vargas, A. Velds, T.R. Brummelkamp, A.M. Dirac, T.K. Sixma, and R. Bernards. 2005. A genomic and functional inventory of deubiquitinating enzymes. *Cell*. 123:773-786.

Nurse, P. 2000. A long twentieth century of the cell cycle and beyond. *Cell*. 100:71-78.

Ohi, M.D., A. Feoktistova, L. Ren, C. Yip, Y. Cheng, J.S. Chen, H.J. Yoon, J.S. Wall, Z. Huang, P.A. Penczek, K.L. Gould, and T. Walz. 2007. Structural organization of the anaphase-promoting complex bound to the mitotic activator Slp1. *Mol Cell*. 28:871-885.

Ohkura, H., I.M. Hagan, and D.M. Glover. 1995. The conserved *Schizosaccharomyces pombe* kinase plo1, required to form a bipolar spindle, the actin ring, and septum, can drive septum formation in G1 and G2 cells. *Genes Dev*. 9:1059-1073.

Ozkan, E., H. Yu, and J. Deisenhofer. 2005. Mechanistic insight into the allosteric activation of a ubiquitin-conjugating enzyme by RING-type ubiquitin ligases. *Proc Natl Acad Sci U S A*. 102:18890-18895.

Peng, Y., A. Grassart, R. Lu, C.C. Wong, J. Yates, 3rd, G. Barnes, and D.G. Drubin. 2015a. Casein kinase 1 promotes initiation of clathrin-mediated endocytosis. *Dev Cell*. 32:231-240.

Peng, Y., M. Moritz, X. Han, T.H. Giddings, A. Lyon, J. Kollman, M. Winey, J. Yates, 3rd, D.A. Agard, D.G. Drubin, and G. Barnes. 2015b. Interaction of CK1delta with gammaTuSC ensures proper microtubule assembly and spindle positioning. *Mol Biol Cell*. 26:2505-2518.

Penney, M., C. Wilkinson, M. Wallace, J.P. Javerzat, K. Ferrell, M. Seeger, W. Dubiel, S. McKay, R. Allshire, and C. Gordon. 1998. The Pad1+ gene encodes a subunit of the 26 S proteasome in fission yeast. *J Biol Chem*. 273:23938-23945.

Petronczki, M., J. Matos, S. Mori, J. Gregan, A. Bogdanova, M. Schwickart, K. Mechtler, K. Shirahige, W. Zachariae, and K. Nasmyth. 2006. Monopolar attachment of sister kinetochores at meiosis I requires casein kinase 1. *Cell*. 126:1049-1064.

Pickart, C.M. 2004. Back to the future with ubiquitin. *Cell*. 116:181-190.

Primorac, I., and A. Musacchio. 2013. Panta rhei: the APC/C at steady state. *J Cell Biol*. 201:177-189.

Qi, S.T., Z.B. Wang, L. Huang, L.F. Liang, Y.X. Xian, Y.C. Ouyang, Y. Hou, Q.Y. Sun, and W.H. Wang. 2015. Casein kinase 1 (alpha, delta and epsilon) localize at the spindle poles, but may not be essential for mammalian oocyte meiotic progression. *Cell cycle*. 14:1675-1685.

Rachfall, N., A.E. Johnson, S. Mehta, J.S. Chen, and K.L. Gould. 2014. Cdk1 promotes cytokinesis in fission yeast through activation of the septation initiation network. *Mol Biol Cell*. 25:2250-2259.

Reyes-Turcu, F.E., K.H. Ventii, and K.D. Wilkinson. 2009. Regulation and cellular roles of ubiquitin-specific deubiquitinating enzymes. *Annu Rev Biochem*. 78:363-397.

Rivers, A., K.F. Gietzen, E. Vielhaber, and D.M. Virshup. 1998. Regulation of casein kinase I epsilon and casein kinase I delta by an in vivo futile phosphorylation cycle. *J Biol Chem*. 273:15980-15984.

Roberts-Galbraith, R.H., M.D. Ohi, B.A. Ballif, J.S. Chen, I. McLeod, W.H. McDonald, S.P. Gygi, J.R. Yates, 3rd, and K.L. Gould. 2010. Dephosphorylation of F-BAR protein Cdc15 modulates its conformation and stimulates its scaffolding activity at the cell division site. *Mol Cell*. 39:86-99.

Rosenberg, J.A., G.C. Tomlin, W.H. McDonald, B.E. Snydsman, E.G. Muller, J.R. Yates, 3rd, and K.L. Gould. 2006a. Ppc89 links multiple proteins, including the septation initiation network, to the core of the fission yeast spindle-pole body. *Mol Biol Cell*. 17:3793-3805.

Rosenberg, J.A., G.C. Tomlin, W.H. McDonald, B.E. Snydsman, E.G. Muller, J.R. Yates, 3rd, and K.L. Gould. 2006b. Ppc89 links multiple proteins, including the septation initiation network, to the core of the fission yeast spindle-pole body. *Mol Biol Cell*. 17:3793-3805.

Rotin, D., and S. Kumar. 2009. Physiological functions of the HECT family of ubiquitin ligases. *Nat Rev Mol Cell Biol*. 10:398-409.

Sadeghi, L., L. Siggens, J.P. Svensson, and K. Ekwall. 2014. Centromeric histone H2B monoubiquitination promotes noncoding transcription and chromatin integrity. *Nat Struct Mol Biol*. 21:236-243.

Sakuno, T., and Y. Watanabe. 2015. Phosphorylation of cohesin Rec11/SA3 by casein kinase 1 promotes homologous recombination by assembling the meiotic chromosome axis. *Developmental cell*. 32:220-230.

Samara, N.L., A.B. Datta, C.E. Berndsen, X. Zhang, T. Yao, R.E. Cohen, and C. Wolberger. 2010. Structural insights into the assembly and function of the SAGA deubiquitinating module. *Science*. 328:1025-1029.

Samara, N.L., A.E. Ringel, and C. Wolberger. 2012. A role for intersubunit interactions in maintaining SAGA deubiquitinating module structure and activity. *Structure*. 20:1414-1424.

Samara, N.L., and C. Wolberger. 2011. A new chapter in the transcription SAGA. *Curr Opin Struct Biol*. 21:767-774.

Samejima, I., and M. Yanagida. 1994. Bypassing anaphase by fission yeast cut9 mutation: requirement of cut9+ to initiate anaphase. *J Cell Biol*. 127:1655-1670.

Santos, J.A., E. Logarinho, C. Tapia, C.C. Allende, J.E. Allende, and C.E. Sunkel. 1996. The casein kinase 1 alpha gene of Drosophila melanogaster is developmentally regulated and the kinase activity of the protein induced by DNA damage. *J Cell Sci*. 109 (Pt 7):1847-1856.

Schittek, B., and T. Sinnberg. 2014. Biological functions of casein kinase 1 isoforms and putative roles in tumorigenesis. *Mol Cancer*. 13:231.

Schmidt, S., M. Sohrmann, K. Hofmann, A. Woollard, and V. Simanis. 1997. The Spg1p GTPase is an essential, dosage-dependent inducer of septum formation in Schizosaccharomyces pombe. *Genes Dev*. 11:1519-1534.

Schwartz, M.A., and H.D. Madhani. 2004. Principles of MAP kinase signaling specificity in Saccharomyces cerevisiae. *Annu Rev Genet*. 38:725-748.

Sczaniecka, M., A. Feoktistova, K.M. May, J.S. Chen, J. Blyth, K.L. Gould, and K.G. Hardwick. 2008. The spindle checkpoint functions of Mad3 and Mad2 depend on a Mad3 KEN box-mediated interaction with Cdc20-anaphase-promoting complex (APC/C). *J Biol Chem*. 283:23039-23047.

Seeger, M., C. Gordon, K. Ferrell, and W. Dubiel. 1996. Characteristics of 26 S proteases from fission yeast mutants, which arrest in mitosis. *J Mol Biol*. 263:423-431.

Shaner, N.C., G.G. Lambert, A. Chammas, Y. Ni, P.J. Cranfill, M.A. Baird, B.R. Sell, J.R. Allen, R.N. Day, M. Israelsson, M.W. Davidson, and J. Wang. 2013. A bright monomeric green fluorescent protein derived from Branchiostoma lanceolatum. *Nat Methods*. 10:407-409.

Shimanuki, M., Y. Saka, M. Yanagida, and T. Toda. 1995. A novel essential fission yeast gene pad1+ positively regulates pap1(+)-dependent transcription and

is implicated in the maintenance of chromosome structure. *J Cell Sci*. 108 (Pt 2):569-579.

Sillibourne, J.E., D.M. Milne, M. Takahashi, Y. Ono, and D.W. Meek. 2002. Centrosomal anchoring of the protein kinase CK1delta mediated by attachment to the large, coiled-coil scaffolding protein CG-NAP/AKAP450. *J Mol Biol*. 322:785-797.

Simanis, V. 2015. Pombe's thirteen - control of fission yeast cell division by the septation initiation network. *J Cell Sci*. 128:1465-1474.

Stegmeier, F., M. Rape, V.M. Draviam, G. Nalepa, M.E. Sowa, X.L. Ang, E.R. McDonald, 3rd, M.Z. Li, G.J. Hannon, P.K. Sorger, M.W. Kirschner, J.W. Harper, and S.J. Elledge. 2007. Anaphase initiation is regulated by antagonistic ubiquitination and deubiquitination activities. *Nature*. 446:876-881.

Stone, M., R. Hartmann-Petersen, M. Seeger, D. Bech-Otschir, M. Wallace, and C. Gordon. 2004. Uch2/Uch37 is the major deubiquitinating enzyme associated with the 26S proteasome in fission yeast. *J Mol Biol*. 344:697-706.

Sun, B., L. Chen, W. Cao, A.F. Roth, and N.G. Davis. 2004. The yeast casein kinase Yck3p is palmitoylated, then sorted to the vacuolar membrane with AP-3-dependent recognition of a YXXPhi adaptin sorting signal. *Mol Biol Cell*. 15:1397-1406.

Tagwerker, C., K. Flick, M. Cui, C. Guerrero, Y. Dou, B. Auer, P. Baldi, L. Huang, and P. Kaiser. 2006. A tandem affinity tag for two-step purification under fully denaturing conditions: application in ubiquitin profiling and protein complex identification combined with in vivocross-linking. *Mol Cell Proteomics*. 5:737-748.

Tanaka, K., J. Petersen, F. MacIver, D.P. Mulvihill, D.M. Glover, and I.M. Hagan. 2001. The role of Plo1 kinase in mitotic commitment and septation in *Schizosaccharomyces pombe*. *Embo J*. 20:1259-1270.

Tanny, J.C., H. Erdjument-Bromage, P. Tempst, and C.D. Allis. 2007. Ubiquitylation of histone H2B controls RNA polymerase II transcription elongation independently of histone H3 methylation. *Genes Dev*. 21:835-847.

Tasto, J.J., R.H. Carnahan, W.H. McDonald, and K.L. Gould. 2001. Vectors and gene targeting modules for tandem affinity purification in Schizosaccharomyces pombe. *Yeast*. 18:657-662.

Teixeira, L.K., and S.I. Reed. 2013. Ubiquitin ligases and cell cycle control. *Annu Rev Biochem*. 82:387-414.

Toda, T., K. Umesono, A. Hirata, and M. Yanagida. 1983. Cold-sensitive nuclear division arrest mutants of the fission yeast Schizosaccharomyces pombe. *J Mol Biol*. 168:251-270.

Tomko, R.J., Jr., and M. Hochstrasser. 2013. Molecular architecture and assembly of the eukaryotic proteasome. *Annu Rev Biochem*. 82:415-445.

Trautmann, S., B.A. Wolfe, P. Jorgensen, M. Tyers, K.L. Gould, and D. McCollum. 2001. Fission yeast Clp1p phosphatase regulates G2/M transition and coordination of cytokinesis with cell cycle progression. *Curr Biol*. 11:931-940.

Tuazon, P.T., and J.A. Traugh. 1991. Casein kinase I and II--multipotential serine protein kinases: structure, function, and regulation. *Adv Second Messenger Phosphoprotein Res*. 23:123-164.

Vancura, A., A. Sessler, B. Leichus, and J. Kuret. 1994. A prenylation motif is required for plasma membrane localization and biochemical function of casein kinase I in budding yeast. *J Biol Chem*. 269:19271-19278.

Venerando, A., O. Marin, G. Cozza, V.H. Bustos, S. Sarno, and L.A. Pinna. 2010. Isoform specific phosphorylation of p53 by protein kinase CK1. *Cell Mol Life Sci*. 67:1105-1118.

Verma, R., L. Aravind, R. Oania, W.H. McDonald, J.R. Yates, 3rd, E.V. Koonin, and R.J. Deshaies. 2002. Role of Rpn11 metalloprotease in deubiquitination and degradation by the 26S proteasome. *Science*. 298:611-615.

Vo, T.V., J. Das, M.J. Meyer, N.A. Cordero, N. Akturk, X. Wei, B.J. Fair, A.G. Degatano, R. Fragoza, L.G. Liu, A. Matsuyama, M. Trickey, S. Horibata, A. Grimson, H. Yamano, M. Yoshida, F.P. Roth, J.A. Pleiss, Y. Xia, and H. Yu. 2016. A Proteome-wide Fission Yeast Interactome Reveals Network Evolution Principles from Yeasts to Human. *Cell*. 164:310-323.

Wang, P.C., A. Vancura, T.G. Mitcheson, and J. Kuret. 1992. Two genes in Saccharomyces cerevisiae encode a membrane-bound form of casein kinase-1. *Molecular biology of the cell*. 3:275-286.

Wang, Y., W.Z. Li, A.E. Johnson, Z.Q. Luo, X.L. Sun, A. Feoktistova, W.H. McDonald, I. McLeod, J.R. Yates, 3rd, K.L. Gould, D. McCollum, and Q.W. Jin. 2012. Dnt1 acts as a mitotic inhibitor of the spindle checkpoint protein dma1 in fission yeast. *Mol Biol Cell*. 23:3348-3356.

Weake, V.M., and J.L. Workman. 2008. Histone ubiquitination: triggering gene activity. *Mol Cell*. 29:653-663.

Wickliffe, K., A. Williamson, L. Jin, and M. Rape. 2009. The multiple layers of ubiquitin-dependent cell cycle control. *Chem Rev*. 109:1537-1548.

Willet, A.H., N.A. McDonald, K.A. Bohnert, M.A. Baird, J.R. Allen, M.W. Davidson, and K.L. Gould. 2015. The F-BAR Cdc15 promotes contractile ring formation through the direct recruitment of the formin Cdc12. *J Cell Biol*. 208:391-399.

Wixon, J. 2002. Featured organism: Schizosaccharomyces pombe, the fission yeast. *Comp Funct Genomics*. 3:194-204.

Xu, R.M., G. Carmel, R.M. Sweet, J. Kuret, and X. Cheng. 1995. Crystal structure of casein kinase-1, a phosphate-directed protein kinase. *EMBO J*. 14:1015-1023.

Yamashita, Y.M., Y. Nakaseko, I. Samejima, K. Kumada, H. Yamada, D. Michaelson, and M. Yanagida. 1996. 20S cyclosome complex formation and proteolytic activity inhibited by the cAMP/PKA pathway. *Nature*. 384:276-279.

Ye, Q., S.N. Ur, T.Y. Su, and K.D. Corbett. 2016. Structure of the Saccharomyces cerevisiae Hrr25:Mam1 monopolin subcomplex reveals a novel kinase regulator. *The EMBO journal*. 35:2139-2151.

Zhao, B., K. Tumaneng, and K.L. Guan. 2011. The Hippo pathway in organ size control, tissue regeneration and stem cell self-renewal. *Nat Cell Biol*. 13:877-883.

Zhao, Y., G. Lang, S. Ito, J. Bonnet, E. Metzger, S. Sawatsubashi, E. Suzuki, X. Le Guezennec, H.G. Stunnenberg, A. Krasnov, S.G. Georgieva, R. Schule, K.

Takeyama, S. Kato, L. Tora, and D. Devys. 2008. A TFTC/STAGA module mediates histone H2A and H2B deubiquitination, coactivates nuclear receptors, and counteracts heterochromatin silencing. *Mol Cell*. 29:92-101.

Zhou, C., S. Wee, E. Rhee, M. Naumann, W. Dubiel, and D.A. Wolf. 2003. Fission yeast COP9/signalosome suppresses cullin activity through recruitment of the deubiquitylating enzyme Ubp12p. *Mol Cell*. 11:927-938.

Zofall, M., and S.I. Grewal. 2007. HULC, a histone H2B ubiquitinating complex, modulates heterochromatin independent of histone methylation in fission yeast. *J Biol Chem*. 282:14065-14072.